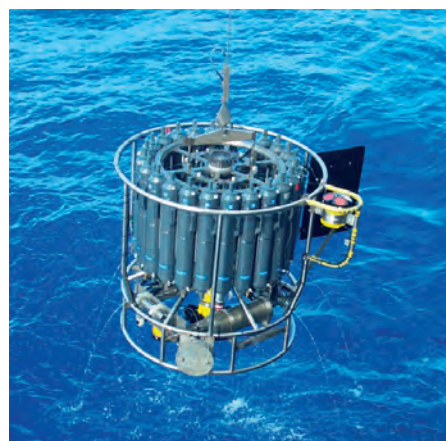




The influence of phosphorus cycling and
temperature acclimation of
photosynthesis
on the land carbon cycle

Daniel Sebastian Goll



Hinweis

Die Berichte zur Erdsystemforschung werden vom Max-Planck-Institut für Meteorologie in Hamburg in unregelmäßiger Abfolge herausgegeben.

Sie enthalten wissenschaftliche und technische Beiträge, inklusive Dissertationen.

Die Beiträge geben nicht notwendigerweise die Auffassung des Instituts wieder.

Die "Berichte zur Erdsystemforschung" führen die vorherigen Reihen "Reports" und "Examensarbeiten" weiter.



Notice

The Reports on Earth System Science are published by the Max Planck Institute for Meteorology in Hamburg. They appear in irregular intervals.

They contain scientific and technical contributions, including Ph. D. theses.

The Reports do not necessarily reflect the opinion of the Institute.

The "Reports on Earth System Science" continue the former "Reports" and "Examensarbeiten" of the Max Planck Institute.

Anschrift / Address

Max-Planck-Institut für Meteorologie
Bundesstrasse 53
20146 Hamburg
Deutschland

Tel.: +49-(0)40-4 11 73-0
Fax: +49-(0)40-4 11 73-298
Web: www.mpimet.mpg.de

Layout:

Bettina Diallo, PR & Grafik

Titelfotos:

vorne:

Christian Klepp - Jochem Marotzke - Christian Klepp

hinten:

Clotilde Dubois - Christian Klepp - Katsumasa Tanaka

The influence of phosphorus cycling and
temperature acclimation of
photosynthesis
on the land carbon cycle

Daniel Sebastian Goll

aus Bietigheim-Bissingen

Hamburg 2013

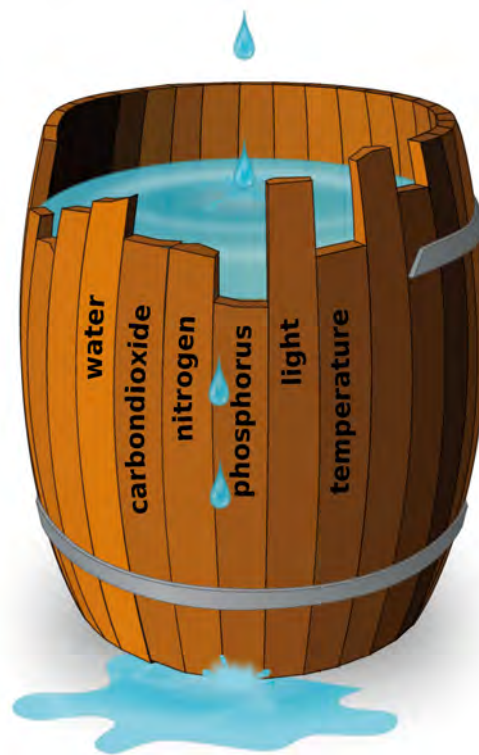
Daniel Sebastian Goll
Max-Planck-Institut für Meteorologie
Bundesstrasse 53
20146 Hamburg

Als Dissertation angenommen
vom Department Geowissenschaften der Universität Hamburg

auf Grund der Gutachten von
Dr. Victor Brovkin
und
Dr. Christian H. Reick

Hamburg, den 21. Dezember 2012
Prof. Dr. Jürgen Oßenbrügge
Leiter des Departments für Geowissenschaften

The influence of phosphorus cycling and
temperature acclimation of
photosynthesis
on the land carbon cycle



Daniel Sebastian Goll

Hamburg 2013

Science has increased man's control over nature, and might therefore be supposed likely to increase his happiness and well-being. This would be the case if men were rational, but in fact they are bundles of passions and instincts.

Bertrand Russel, "Icarus, Or The Future of Science", 1924

Abstract

Terrestrial carbon (C) cycle models applied for climate projections simulate a strong increase in net primary productivity (NPP) due to elevated atmospheric CO₂ concentration during the 21st century. These models usually neglect the limited availability of nitrogen (N) and phosphorus (P), nutrients that commonly limit plant growth and soil carbon turnover. In addition, these models treat the temperature dependence of photosynthesis rigidly, although warming experiments illustrate a high variability in the temperature response of photosynthesis due to acclimation (adjustments by an individual plant in response to an environmental stimulus). Both aspects, nutrient limitation and temperature acclimation, are discussed as major uncertainties in projecting future land C uptake. To investigate how the projected C sequestration and global productivity is altered when nutrient limitation or temperature acclimation of photosynthesis are considered, I incorporated representations for P cycling and for temperature acclimation into the Max Planck Earth System model (MPI-ESM).

In direct comparison with simulations which do not consider nutrient cycles, the accumulated land C uptake between 1860 and 2100 (SRES A1B scenario) is 13 % and 16 % lower in simulations with N and P cycling, respectively. The combined effect of both nutrients reduces land C uptake by 25 % compared to simulations without N or P cycling. Nutrient limitation in general may be biased by the model simplicity, but the ranking of limitations is robust against the parameterization and the inflexibility of stoichiometry. After 2100, increased temperature and high CO₂ concentration cause a shift from N to P limitation at high latitudes, while nutrient limitation in the tropics declines. The increase in P limitation at high-latitudes is induced by a strong increase in NPP and the low P sorption capacity of soils, while a decline in tropical NPP due to high autotrophic respiration rates alleviates N and P limitations. The quantification of P limitation remains challenging. The poorly constrained processes of soil P sorption and biochemical mineralization are identified as the main uncertainties in the strength of P limitation, while changes in P release rate by chemical weathering may become of importance on multi-centennial time scale.

In contrast, acclimation of photosynthesis has only a minor effect on global productivity. Temperature acclimation slightly increases extra-tropical productivity under present climatic conditions by 5% and under future climatic conditions by 7%. The effect of temperature acclimation on tropical ecosystems is elusive. On the one hand, it is under debate if tropical trees do acclimate to temperature at all, as temperatures at low latitudes do not vary much during the growing season. On the other hand, if they acclimate, the sign of their response to warming depends on how the temperature response of the ratio between rubisco activity limited and electron transport limited photosynthesis is treated in the model. More experimental research is needed to evaluate whether this ratio is influenced by temperature or not.

My findings indicate that global land C uptake in the 21st century is likely overestimated in models that neglect P and N limitations. In the long-term, insufficient P availability might become an important constraint on C cycling at high latitudes. Temperature acclimation is of minor importance for assessing the response of the global C cycle to warming, unlike previously suggested. Accordingly, I argue that the P cycle must be included in global models used for C cycle projections, but I recommend to wait with the implementation of temperature acclimation until a better process understanding has been achieved.

Contents

Abstract	iii
List of Figures	ix
List of Tables	xi
List of Abbreviations	xiv
1 Introduction	1
1.1 The terrestrial sink	2
1.2 Earth system models	4
1.3 Nutrient limitation	5
1.4 Temperature acclimation of photosynthesis	7
1.5 Formal remarks	8
2 Nutrient limitation reduces land C uptake for centuries.	9
2.1 Introduction	9
2.2 Methods	11
2.2.1 Model	11
2.2.1.1 The C cycle	13
2.2.1.2 The N cycle	13
2.2.1.3 The P model	14
2.2.1.4 Nutrient demands	17
2.2.1.5 Parameter estimates	18
2.2.2 Experimental setup	20
2.3 Results and discussion	21
2.3.1 Present day: comparison with observations	21
2.3.2 Land C sink until 2100	26
2.3.3 Land C sink after 2100	29
2.4 Conclusions	32
2.5 Acknowledgements	33
3 Changes of P release by chemical weathering can be higher than expected.	35

CONTENTS

3.1	Introduction	35
3.2	Methods	37
3.2.1	Model of P release	37
3.2.2	Climatic forcing	37
3.2.3	Simulations	38
3.3	Results & Discussion	39
3.3.1	Present day	39
3.3.2	Future	41
3.3.3	Implications of the strong increase in P weathering	41
3.3.4	Limitations of the modelling approach	44
3.4	Conclusions	45
3.5	Acknowledgements	46
4	Temperature acclimation of photosynthesis has a minor impact on present and future productivity.	47
4.1	Introduction	47
4.2	Model & experiments	49
4.2.1	Model description	50
4.2.1.1	General photosynthesis	50
4.2.1.2	Standard temperature dependence of V_{max} and J_{max} (Knorr, 2000)	51
4.2.1.3	New formulation (Kattge and Knorr, 2007)	51
4.2.1.4	Parameterization of frost inhibition	52
4.2.2	Simulation setup	52
4.2.2.1	Site scale simulations using FLUXNET data	53
4.2.2.2	Simulations with prescribed SSTs	53
4.2.2.3	4×CO ₂ simulations	54
4.3	Results & Discussion	55
4.3.1	Site scale simulations	55
4.3.2	Simulations with prescribed SSTs	56
4.3.3	4×CO ₂	60
4.4	Conclusions	63
4.5	Acknowledgements	63
5	Summary & Conclusions	65
5.1	Summary of findings	65
5.1.1	Nutrient limitation	65
5.1.1.1	How much and where is N and P availability limiting land C uptake in this century?	65
5.1.1.2	What is the long-term (multi-centennial) evolution of N and P limitation?	65

5.1.1.3	What are the main uncertainties in projecting terrestrial P availability?	65
5.1.1.4	How much and where is the P release by chemical weathering altered due to climate change?	66
5.1.1.5	To what extent do changes in temperature and runoff contribute to the overall change in P release?	66
5.1.1.6	To what extent could land C uptake be affected by the expected changes in P release?	66
5.1.2	Temperature acclimation of photosynthesis	66
5.1.2.1	How much and where is present productivity and productivity in a warmer climate affected by temperature acclimation? . . .	66
5.1.2.2	How does this effect relate to changes in productivity due to other factors constraining the temperature response of photosynthesis?	67
5.1.2.3	What are the main uncertainties in the quantification of the effect of temperature acclimation on productivity?	67
5.2	Conclusions	67
5.3	Implications for further model developments	68
5.4	Implications for studies on past climate and marine systems	69
	Bibliography	71
	A Appendix of Chapter 2	91
A.1	Derivation of equations for labile P dynamics	91
A.2	Respiration fluxes	92
A.3	Sensitivity simulations on stoichiometry	92
A.4	Additional figure and tables	95
	B Acknowledgements	97

List of Figures

2.1	Schematic representation of pools and fluxes in JSBACH.	12
2.2	Simulated organic P stocks and annual uptake rates.	23
2.3	Land C uptake in simulations with and without nutrients cycles.	27
2.4	Geographic distribution of N and P limitation during the 21st century.	28
2.5	Reduction in NPP due to nutrient limitation.	31
3.1	The simulated P release rates using forcings from 4 different ESMs (1850–2100).	40
3.2	Present day P release using forcings from 4 different ESMs.	42
3.3	Maps of the increase in P release due to climate change.	43
3.4	Potential C uptake from 1850 to 2100 due to increasing P release.	44
4.1	Photosynthesis on leaf level using differing temperature dependences.	48
4.2	The simulated and measured daily cycle of GPP for 6 FLUXNET sites.	56
4.3	The simulated and measured annual cycle of GPP for 6 FLUXNET sites.	58
4.4	The effect of temperature acclimation on present GPP.	59
4.5	The effect of the choice of the instantaneous temperature dependency on present GPP.	60
4.6	Map of temperature increases due to quaddrupling of CO ₂	61
A.1	Reduction in NPP due to nutrient limitation in simulation with PFT-specific stoichiometry.	92
A.2	Land C uptake in simulations with flexible stoichiometry.	93
A.3	Land C uptake in simulations with perturbed stoichiometric parameterization.	94
A.4	The changes in global vegetation and soil carbon stocks.	96

List of Tables

2.1	Variables of the CNP model.	14
2.2	Parameters used in the P model.	19
2.3	List of experiments performed.	20
2.4	Simulated decadal land C uptake: the effect of nutrients and comparison with published estimates.	22
2.5	Simulated inorganic P stocks.	24
2.6	Simulated stock of labile P in comparison with measurements.	24
2.7	PFT-specific P fluxes for present day.	25
3.1	Variables of the P release model.	37
3.2	List of ESM used in this study.	38
3.3	Simulations specifications. For both forcing variables, q and T , the respective time period used during the whole simulation duration (249 yr) is given and also the values used for the parameter E_a	39
4.1	Overview: simulations and model versions used.	53
4.2	Description of FLUXNET sites.	54
4.3	Global fluxes in simulations with prescribed SSTs.	58
4.4	Statistical significance of changes in GPP (prescribed SSTs).	60
4.5	Regional fluxes in simulations with prescribed SSTs.	61
4.6	Global fluxes in simulations with $4\times\text{CO}_2$	62
4.7	Statistical significance of changes in GPP ($4\times\text{CO}_2$).	62
4.8	Regional fluxes in simulations with $4\times\text{CO}_2$	62
A.1	Ranges used to constrain the probability functions of the stoichiometric parameters in the LHS.	93
A.2	PFT specific values of model parameters.	95
A.3	Soil order specific values of model parameters.	95

List of Abbreviations

AMIP	project: Atmospheric Model Intercomparison Project
BNL	background nutrient limitation
C	carbon
C model	model of carbon cycling
C4MIP	project: Coupled Climate Carbon Cycle Model Intercomparison Project
CCSM4	Community Earth System Model 4.0; National Center for Atmospheric Research
CMIP5	project: Coupled Model Intercomparison Project Phase 5
CN model	model of combined carbon and nitrogen cycling
CNL	CO ₂ -induced nutrient limitation
CNP model	model of combined carbon, nitrogen and phosphorus cycling
CO ₂	carbon dioxide
ECHAM5	atmosphere model of the MPI-ESM
ENSEMBLES	project: Ensemble-based Predictions of Climate Change and their Impacts
ESM	earth system model
FLUXNET	network to coordinate regional and global analysis of observations from micrometeorological tower sites
GPP	gross primary productivity
IPSL-CM5A	French earth system model; Institut Pierre-Simon Laplace
JSBACH	land surface scheme of the MPI-ESM
LAI	leaf area index
LHS	latin hypercube sampling
MAT	mean annual temperature
MIROC-ESM	Japanese earth system model; Japan Agency for Marine-Earth Science and Technology, Atmosphere and Ocean Research Institute (The University of Tokyo), and National Institute for Environmental Studies
MPI-ESM	Max Planck Institute Earth System Model
MPI-OM	ocean model of the MPI-ESM
N	nitrogen
NPP	net primary productivity
O ₂	oxygen in its molecular form
P	phosphorus
PFT	plant functional type
RCP	Representative concentration pathways; scenarios used in CMIP5
Rubisco	Ribulose-1,5-bisphosphat-carboxylase/-oxygenase

LIST OF ABBREVIATIONS

SAR	sum of annual runoff and drainage
SRES	Special Report on Emission Scenarios, scenarios used in C4MIP
SST	sea surface temperature
TRY	plant trait data base
USDA	U. S. Department of Agriculture

Chapter 1

Introduction

Currently we experience atmospheric CO₂ concentrations, which are unprecedented during the last 2 millions years (Luethi et al., 2008; Hoenisch et al., 2009) and projected to increase at a rate unseen in the geological past (Denman et al., 2007). Within the last century, the global mean surface temperature increased by 0.6 °C, and will likely continue to increase by 1.4–6.4 °C during this century (Denman et al., 2007). The increasing CO₂ concentrations are the primary cause for the warming trend during the last 50 years and is attributed to human activities, namely combustion of fossil fuels, cement production and deforestation (Denman et al., 2007). Not all of the CO₂ emitted by human activities accumulates in the atmosphere. About two third of the emissions are taken up in equal parts by the ocean and by terrestrial ecosystems (Sabine et al., 2004). The CO₂ uptake capacity of terrestrial systems (sink strength) and the future development of the terrestrial sink are considered major uncertainties in assessing future climate change (Denman et al., 2007; Friedlingstein et al., 2006). The size of the currently observed terrestrial sink is the result of an imbalance between several sink and source processes. As all processes act simultaneously their respective contributions to the net sink and their dynamics are hard to quantify.

Not only is the terrestrial sink affecting atmospheric CO₂ concentrations and therefore affecting climate, but the resulting changes in atmospheric CO₂ concentrations and climate affect the sink processes in return (feedback). Several vegetation-atmosphere feedbacks exist, some of them are damping (negative feedback), some are amplifying (positive feedback) the initial change. It is therefore crucial for projections of future climate and reconstructions of past climate to understand the processes underlying the terrestrial sink and to represent them as accurately as possible in global models. This thesis aims to improve the understanding of nutrient limitation and temperature acclimation of photosynthesis and to provide a quantification of these two important aspects of the terrestrial sink, both of which are considered to evoke major uncertainties in models used to for the reconstruction of past climate, future projections, and the linkage of causes and effects in climate change.

In the following I explain in more detail (1) the nature of the terrestrial sink, (2) the models used for projecting future sink dynamics, and the uncertainties emerging in these projections from the omission of (3) nutrient limitation of ecosystem productivity and (4) temperature acclimation of photosynthesis.

1.1 The terrestrial sink

Strong evidence exists that terrestrial ecosystems have acted as a net C sink over the last three decades (Sabine et al., 2004; Canadell et al., 2007; Friedlingstein et al., 2010). The sink strength is highly variable from year to year ranging from 0.3 to 5.0 Pg C yr⁻¹; an amount comparable to the anthropogenic emissions of 7 Pg C yr⁻¹ (Denman et al., 2007). There is a sparse understanding of the many processes responsible for the terrestrial sink and their future dynamics. But such information is crucial to predict the future sink strength and therefore the pace at which atmospheric CO₂ will rise.

The processes contributing to the terrestrial sink are: (i) CO₂ fertilization, (ii) nitrogen (N) deposition, (iii) temperature (and precipitation) effects on plant productivity and heterotrophic respiration, and (iv) processes driven by land-use change or land management (deforestation, forest regrowth, woody encroachment, forest thickening due to fire suppression, afforestation and reforestation, and changes in soil carbon (C) under cultivation and grazing) (Canadell et al., 2007). Subsequent changes in the competitive strength of vegetation types may occur which can result in a redistribution of ecosystems and their species composition. Despite the diversity of the listed processes there is one single aspect which is common for all: photosynthesis and plant growth. Therefore a short explanation of photosynthesis and growth is appropriate at this point before I introduce the sink processes in detail.

Photosynthesis, the capturing of energy from sun light and its storage in form of carbohydrates, is the key process in the biosphere. Since the origin of photosynthesis more than 2.5 billion years ago (Lenton and Watson, 2011), tremendous amounts of bound energy and C have accumulated in terrestrial ecosystems and geological formations. Without photosynthesis, the energy which drives human activities today, fossil fuels, would not exist. Not only would there be no fossil fuels, but also complex life would be impossible, as (oxygenic) photosynthesis is the only known natural process known which can sustain the high energy demand of complex organisms (Catling et al., 2005). Only a fraction of the C fixed by photosynthesis is used in the built-up of organic matter. The rest is released back to the atmosphere when organisms (photosynthetic active ones [autotrophs] as well as organisms which feed on them or their remainings [heterotrophs]) utilize the energy bound in the carbohydrates (respiration). When photosynthesis exceeds respiration plant biomass starts to increase. On the ecosystem level, the balance between photosynthesis and ecosystem respiration (respiration by autotrophs and heterotrophs) defines the net C balance.

The theory behind *plant growth* was revolutionized by Carl Sprengel. In 1828 he developed the “Law of the Minimum” (Sprengel, 1838), which was later popularized by Justus von Liebig. The principle states that growth is not controlled by the total amount of resources available, but by the scarcest resource. This simple rule is a cornerstone of modern agriculture and ecological theory. It does not only apply to plants but to all organism, as each biomolecule, the building blocks of life, has a distinct chemical composition. Therefore every organism needs, in addition to energy (the only perfect limiting factor), essential elements (nutrients) to synthesize the bio-

chemical compounds they consist of: nucleic acids, proteins, carbohydrates and lipids. Besides the main constituents of biomolecules, C, hydrogen and oxygen, the following elements occur in organism: N, phosphorus (P), sulfur, iron, magnesium, potassium, sodium and calcium. Several other elements occur in traces. The degree to which organisms maintain a constant chemical composition (stoichiometric homeostasis) in the face of variations in their environment is highly diverse. While heterotrophs have a strict stoichiometric (Redfield, 1934; Cleveland and Liptzin, 2007), autotrophs are more flexible (McGroddy et al., 2004; Kattge et al., 2011).

The *CO₂ fertilization effect* is an example of how growth is enhanced by an increase in a resource. CO₂ is a substrate for photosynthesis and for the majority of (C₃) plant species CO₂ concentrations will remain below saturation levels of photosynthesis even at twice-current concentrations (Canadell et al., 2007). Thus the rate of leaf level photosynthesis increases as atmospheric CO₂ concentration rise, which means an increase in a growth-relevant resource. In addition to the direct physiological effect, increasing atmospheric CO₂ concentration improve the water use efficiency of plants. Stomata, the valves controlling the exchange of gas between air and the leaf interior (where photosynthesis takes place), act in a way to minimize water losses *and* keep CO₂ concentrations inside the leaf high. When atmospheric CO₂ rises the probability that such a valve is open decreases; thereby water losses are reduced and the water use efficiency increases. As a result, the growth resource water becomes more abundant. This is an example how the availability of a certain resource can affect the availability on another one.

The *N deposition effect* is of the same kind. Many terrestrial ecosystems experience higher N inputs from dry and wet deposition as the atmospheric load of NO_x has increased through fossil fuel and biomass combustion (Galloway et al., 2004). Thomas et al. (2009) estimated by extrapolating the response of 11 North-American tree species to current N deposition during the 1980s and 1990s to the globe, that N deposition could increase tree carbon storage by 0.31 Pg C yr⁻¹.

Changes in *temperature* are likely to have profound effects on the functioning of ecosystems (Rustad and Norby, 2002). Temperature is one of the fundamental regulators of all chemical and biological processes, such as respiration, litter decomposition, mineralization, denitrification, CH₄ emission, photosynthesis, plant growth, plant nutrient uptake, and phenology (Canadell et al., 2007). Despite the extensive literature in this field, the long-term responses of ecosystems and terrestrial C cycling to warming remain elusive (Rustad and Norby, 2002; Canadell et al., 2007; Denman et al., 2007; Friedlingstein et al., 2006; Raddatz et al., 2007).

The contribution of processes driven by land-use change or land management are not directly considered in this study, as the focus lies on the response of natural ecosystem to climate change and increasing CO₂. Since these processes are of global significance (Denman et al., 2007), the implication of their omission in my study are discussed in each chapter and also summarized in chapter 5.

Temperature and CO₂ are closely linked and predictions of the terrestrial C cycle based solely on changes in a single factor are likely to be misleading. Thus comprehensive models of the earth

systems are used to make future projections, and to link causes and effects in climate change. In the following section, I describe how photosynthesis is represented in these models and its respective implications.

1.2 Earth system models

Earth system models (ESMs) are the current generation of models formerly known as coupled general circulation models (of CGCMs). CGCMs incorporate submodels for the atmospheric and ocean circulation, while Earth system models also account for the dynamics of the biosphere and human activities (Claussen et al., 2002). The submodels are coupled through the exchange of energy, momentum, water and important trace gases, like CO₂. The aim of ESMs is to represent all processes and their interactions relevant for the climate. To do so progressively additional processes are incorporated that are thought to be relevant. However, being limited by poor understanding and the slow processes of model development, they still represent a only partial set of relevant processes. This limits the ability to produce robust projections of the pace with which atmospheric CO₂ is presently increasing and will increase in the future.

The initial (seconds to minutes) CO₂ response curve of photosynthesis (see CO₂ fertilization) is a cornerstone of modeling the biosphere response to CO₂ in these models. Due to the strong responsiveness of photosynthesis to elevated CO₂ concentrations and the omission of growth resources other than light, temperature, water and C, the majority of these models project a strong increase in productivity during the 21st century (Denman et al., 2007). However, during the 1990s, more than 4000 publications testing the hypothesis that the CO₂ fertilization effect will enhance plant growth, showed that the leaf level response of photosynthesis to increases in CO₂ is a rather unreliable predictor of plant growth (Körner, 2000) and therefore of net C uptake.

The temperature dependence of photosynthesis is described by an optimum curve in these models, given that in most plants, the light-saturated rates of photosynthesis are low at extreme low and high temperatures and have an optimum temperature at intermediate temperature. The negative effect of high temperature on photosynthesis is poorly quantified from data (Kattge and Knorr, 2007). Therefore models differ in the projected response of vegetation to warming (Raddatz et al., 2007). Recent warming experiments reveal a high variability of the photosynthetic response to elevated temperature (see references in (Lin et al., 2012)), indicating that the temperature dependence of photosynthesis is treated in models in a too rigid way (Kattge and Knorr, 2007; Raddatz et al., 2007).

In the next section I present evidence that the omission of nutrients may be responsible for a significant overestimation of the terrestrial sink in such kind of models. Afterwards, I present evidence that the temperature dependence of photosynthesis is responsible for part of the large uncertainty in the response of the terrestrial sink to warming.

1.3 Nutrient limitation

In the ecological community, it is well established that the CO₂ fertilization effect can be prevented by nutrient limitation (Luo et al., 2004; Reich et al., 2006; Norby et al., 2010). Based on remote sensing data, Fisher et al. (2012) recently estimated a reduction of present day productivity by nutrients (in general) between 16-28%. A compilation of fertilizer experiments showed that N and P limitation of plant growth is widespread (Elser et al., 2007). Bearing the Law of Minimum in mind, it becomes clear that the omission of globally important resources, namely N and P, is problematic when quantifying the effect of increasing CO₂ availability.

Ten years ago, Hungate et al. (2003) showed by simple back-of-the-envelope calculations that the amount of C projected to be sequestered during the 21st century by global models is not in line with the availability of nitrogen (N), namely that these models overestimate C uptake. The missing representation of nutrients is considered the largest source of error in C cycle projections (Friedlingstein et al., 2006; Denman et al., 2007). As a result, during the last decade several models which account for N cycling were developed (Thornton et al., 2007; Wang et al., 2007; Sokolov et al., 2008; Xu-Ri and Prentice, 2008; Jain et al., 2009; Fisher et al., 2010; Gerber et al., 2010; Zaehle et al., 2010b; Esser et al., 2011; Parida, 2010). All but one of these models (Esser et al., 2011) showed a reduction of terrestrial carbon uptake during the 21st century between 7% (Zaehle et al., 2010b) to 64% (Thornton et al., 2007). Although, P limitation is considered to affect plant growth with a similar strength as N (Elser et al., 2007), to date only a single global model incorporates a P cycle (Wang et al., 2010), which has yet not been applied in projections.

Thus the aim of chapter 2 is to fill this knowledge gap and improve the understanding on how strong land C uptake could be limited by P. In particular, the following research question are investigated:

1. How much and where is N and P availability limiting land C uptake in this century?
2. What is the long-term (multi-centennial) evolution of N and P limitation?
3. What are the main uncertainties in projecting terrestrial P availability?

The global P cycle is strongly enhanced by the mining of P and its application on agricultural land (Smil, 2000). The mining of P is two orders of magnitude larger than the natural rate of P release from rocks: 161 Tg P yr^{-1} (Gilbert, 2009) compared to 1.6 Tg P yr^{-1} (Hartmann and Moosdorf, 2011). The current annual demand of P fertilizer is estimated to be 42 Tg P yr^{-1} in a recent FAO report (FAO, 2012). In spite of the enormous amount of P fertilizer applied on agricultural land, the P balance of the great majority of natural terrestrial ecosystems is still constrained by P inputs from weathering. Recently, the first global model of P release by chemical weathering was developed (Hartmann and Moosdorf, 2011). The P release is controlled mainly by the P content of the minerals, runoff and temperature. Due to the warming projected for this century the rate at which P enters ecosystems is likely to change.

Yet, a quantification of the changes in P release and the resulting changes in land C uptake during the next century is lacking. Filling this gap is the aim of chapter 3, with the following research questions being investigated:

1. How much and where is the P release by chemical weathering altered due to climate change?
2. To what extent do changes in temperature and runoff contribute to the overall change in P release?
3. To what extent could land C uptake be affected by the expected changes in P release?

1.4 Temperature acclimation of photosynthesis

Changes in temperature affect fundamental processes and their interactions in ecosystems. Models which incorporate our best understanding of all the modes of action of the individual factors will also capture many of the major interactions regarding temperature. In projections for the 21st century, the response of tropical ecosystems to warming dominates the dynamics of the terrestrial sink (Raddatz et al., 2007). It is the tropical ecosystems where temperatures are most likely to exceed the optimum for photosynthesis in a warming climate.

There is considerable controversy about the vulnerability of tropical trees to a future warming (Clark, 2004; Feeley et al., 2007; Lloyd and Farquhar, 2008). In particular, the limited understanding of the extent to which ecosystems adjust to gradual changes in temperature (temperature acclimation) (Medlyn et al., 2002; June et al., 2004; Lin et al., 2012) hampers our ability to constrain ecosystem responses to global warming (Lloyd and Farquhar, 2008; Booth et al., 2012). Booth et al. (2012) identified with a systematic parameter disturbance method the relationship between photosynthesis and temperature as the largest uncertainty in interactions between climate/warming and the C cycle. Kattge and Knorr (2007) developed a new formulation of the temperature dependence of photosynthesis which accounts for acclimation. This formulation has not been applied in a global model yet.

Thus it exists a gap of knowledge on the global significance of temperature acclimation of photosynthesis and its influence on land C cycling for present day and the future. Filling this gap is the aim of chapter 4. The particular research questions are:

1. How much and where is present productivity and productivity in a warmer climate affected by temperature acclimation?
2. How does this effect relate to changes in productivity due to other factors constraining the temperature response of photosynthesis?
3. What are the main uncertainties in the quantification of the effect of temperature acclimation on productivity?

1.5 Formal remarks

Each of the next three chapters constituting my dissertation corresponds to an either already realised or planned publication in a peer-review journal. Chapter 2 deals with the effect of nutrient limitation on the present and future terrestrial sink and has already been accepted in the journal *Biogeosciences* (Goll et al., 2012). Chapter 3 is on the effect of climate change on P release rates and how the expected changes in P release affect the terrestrial sink and chapter 4 addresses the influence of temperature acclimation on productivity. The latter two chapters form the basis of a second and third publication that will soon be submitted to an appropriate journal.

The main part of the thesis focus on projections of the land C balance into the future, but the scope of a mechanistic model of combined C, N, and P cycling is broader. For example it can also facilitate more comprehensive studies on understanding past climate changes or provide dynamic boundary conditions regarding nutrients for marine studies. Such implications are discussed in chapter 5.

I conducted the studies under supervision and guidance of Dr. Victor Brovkin and support from others regarding data and technical solutions. In contrast to this introduction and the summary and conclusions, the next three chapters are therefore written in the first person plural. I kindly ask the reader to be indulgent with this kind of imperfection.

Chapter 2

Nutrient limitation reduces land C uptake for centuries.

2.1 Introduction

The neglect of nutrient limitation in carbon (C) cycle models has been criticized for being unjustified from an ecological point of view (Reich et al., 2006) and for overestimating terrestrial C sequestration in the future (Hungate et al., 2003; Thornton et al., 2007). The incorporation of a nitrogen (N) cycle into the biogeochemical components of Earth System Models (ESM) generally reduces the CO₂ fertilization effect and C losses due to soil warming (Zaehle and Dalmonech, 2011). It even may change the sign of the feedback between climate and the terrestrial C cycle from positive to negative (Thornton et al., 2007; Sokolov et al., 2008). However, this is not generally the case (Zaehle et al., 2010a). In the current generation of coupled terrestrial carbon and nitrogen (CN) models, N limits productivity mainly in high latitude ecosystems (Sokolov et al., 2008; Thornton et al., 2007; Zaehle et al., 2010b), whereas the low latitude ecosystems, which are the most productive ones (Lieth, 1972; Field et al., 1998; Pan et al., 2011), are less N-limited. Low latitude systems are expected to show the highest direct CO₂ response of NPP (Hickler et al., 2008) and in climate change projections they are responsible for a substantial positive feedback between climate and the C cycle (Friedlingstein et al., 2006; Raddatz et al., 2007). At the same time, low latitude ecosystems are expected to be more P-limited (Townsend et al., 2011). Therefore, an inclusion of the terrestrial P cycle into global C cycle models seems essential to appropriately determine land C uptake.

Globally, in addition to N, P is the nutrient most commonly limiting plant growth and soil C cycling (Vitousek and Howarth, 1991; Aerts and Chapin, 2000). Theoretical (Walker and Syers, 1976) and observational (Reich and Oleksyn, 2004) studies suggest that at present, productivity of tropical forests and savannahs is generally constrained by P, while N constrains the productivity in temperate and boreal regions. The geographical patterns of N and P limitations are commonly explained by the age of the soils (Walker and Syers, 1976; Vitousek et al., 2010). Young soils tend to have a high P availability, but low N availability, because N is nearly absent in the parental material and accumulates over time from the atmosphere by biological N fixation. P enters the ecosystem

by weathering of primary minerals. As soils age, the parental material can become P-depleted and P gets progressively occluded in secondary minerals. Therefore, old highly-weathered soils tend to have low P availability. As glaciation has periodically reset soil development at high latitudes, these soils tend to be much younger than the ones at low latitudes, where glaciation was absent for hundreds of millions of years.

Additional mechanisms, operating on timescales of years to centuries (Vitousek et al., 2010), may cause the occurrence of nutrient limitation. Mechanisms limiting the availability of N include constraints on biological N fixation (Houlton et al., 2008) and losses by leaching and volatilization, which may even occur to some extent in N deficient ecosystems (Davidson et al., 2007). As soil P is less mobile than N, losses are of minor importance for the occurrence of P limitation. A mechanism that affects both N and P limitation is the sequestration of N or P in an accumulating pool (Vitousek et al., 2010); in particular, the sequestration of nutrients in long-lived but non-photosynthetic pools of organic matter (Luo et al., 2004). Additionally, an enhanced supply of nutrients other than P, for example N (Perring et al., 2008), can cause P limitation. As the P cycle has a much slower turnover rate than the N cycle such limitation can remain for centuries. Because mechanisms underlying N and P limitation differ from each other, the responses of N and P limitation to changes in atmospheric CO₂, climate, and land use change likely differ, too (Davidson et al., 2007; Vitousek et al., 2010; Gruber and Galloway, 2008).

Despite evidence of widespread phosphorus limitation on plant productivity from fertilizer experiments (Elser et al., 2007) and modelling (Wang et al., 2010; Zhang et al., 2011), to our knowledge, so far no study has assessed to what extent land C uptake projected by C only models can be realized when stoichiometric constraints of N and P on the build-up of organic matter are accounted for. Results from Zhang et al. (2011) suggest that during the 20th century the global C balance can be fully quantified with just N, while at continental scale the P cycle is also of importance for the C balance. However, the uncertainties in simulating P cycling are large (Wang et al., 2010; Zhang et al., 2011). So far, a detailed analysis of whether and how P limitation may develop in future has not been done.

As it is yet not clear where and how strong N and P constrain today's plant productivity and soil C turnover (Elser et al., 2007; Zaehle and Dalmonech, 2011; Townsend et al., 2011), we developed a new modelling concept of nutrient limitation to avoid prescribing nutrient limitation in the initial model state. We assume that during thousands of years of stable Holocene climate and relatively low atmospheric CO₂ concentration, plants have adapted to their environment such that their growth is limited by multiple resources (Field et al., 1992; Townsend et al., 2011). We thus hypothesize that for present day, ecosystems are co-limited by the availability of N and P, which is in broad terms consistent with a meta analysis of N and P manipulation experiments across global biomes (Elser et al., 2007). As nutrients are needed for the build-up of organic compounds (C sink) from carbohydrates, nutrient uptake and C fixation (C source) have to be adjusted, such that C sinks and sources are in balance. The adaptation of photosynthesis to nutrient availability is to some part represented in photosynthesis models, as the parameters of these models are specific

for each plant functional type (PFT). Based on global data compilations, Kattge et al. (2009) concluded that the maximal rate of carboxylation ($V_{c_{max}}$) is affected by N and P availability. Reich et al. (2009) showed that leaf P, an indicator of P availability, modulates the N dependence of photosynthesis. The nutrient limitation hidden in the parameterization of photosynthesis is called background nutrient limitation (BNL).

Today's atmospheric CO₂ concentration is unprecedented in the last 2 million years (Luethi et al., 2008; Hoenisch et al., 2009) and it is projected to increase further with a rate unseen in the geological past. In C only models, photosynthesis is independent from the actual need of carbohydrates and therefore the projected increase in plant productivity is invalid if the carbohydrate sink can not grow as fast as photosynthesis increases. To account for such a possible imbalance, plant productivity must be adjusted to the actual need of carbohydrates, which can be derived from the stoichiometry of plant tissue. The difference between the potentially possible productivity under elevated CO₂ and the sink corrected productivity is defined as the effect of CO₂-induced nutrient limitation (CNL). CNL is per definition absent in the pre-industrial state. In aggregate, the modeling approach taken herein does not attempt to quantify the overall background nutrient limitation, and instead, estimates how much less C can be stored on land when changes in N and P supply are simulated; our approach is distinct from one which would quantify total N and P limitation, as is done with fertilizer experiments (Elser et al., 2007) or in terrestrial ecosystem models (Sokolov et al., 2008; Thornton et al., 2007; Zaehle et al., 2010b; Wang et al., 2010; Zhang et al., 2011).

In this paper we aim to quantify how much of the land C uptake projected by a C model can be sustained when accounting for stoichiometric constraints on C storage in organic matter. Further, we aim to identify the processes responsible for the occurrence of P limitation. To do so, we implemented a P cycle into the biogeochemical cycle model (Parida, 2010) of JSBACH (Raddatz et al., 2007), which includes C and N cycling. The model was applied under the SRES A1B scenario with and without N and/or P cycles to allow a separation of the effects of N and P limitation on land C cycling. In addition, a set of sensitivity experiments was performed to identify the main drivers of nutrient limitation.

2.2 Methods

2.2.1 Model

JSBACH describes the processes for land hydrology, phenology, biogeochemical cycling (Fig. 2.1). The submodel for the biogeochemical cycles of JSBACH is driven by net primary productivity (NPP), leaf area index (LAI) and climate variables (soil temperature, soil moisture, runoff) obtained from full climate simulations with the Max Planck Institute Earth System Model (MPI-ESM) (Roeckner et al., 2011). By driving the submodel for biogeochemical cycling with NPP and LAI, we omit effects of CO₂-induced changes in N or P availability on these properties because, so far, it is unclear whether we can generalize about how elevated CO₂ affects the interactions

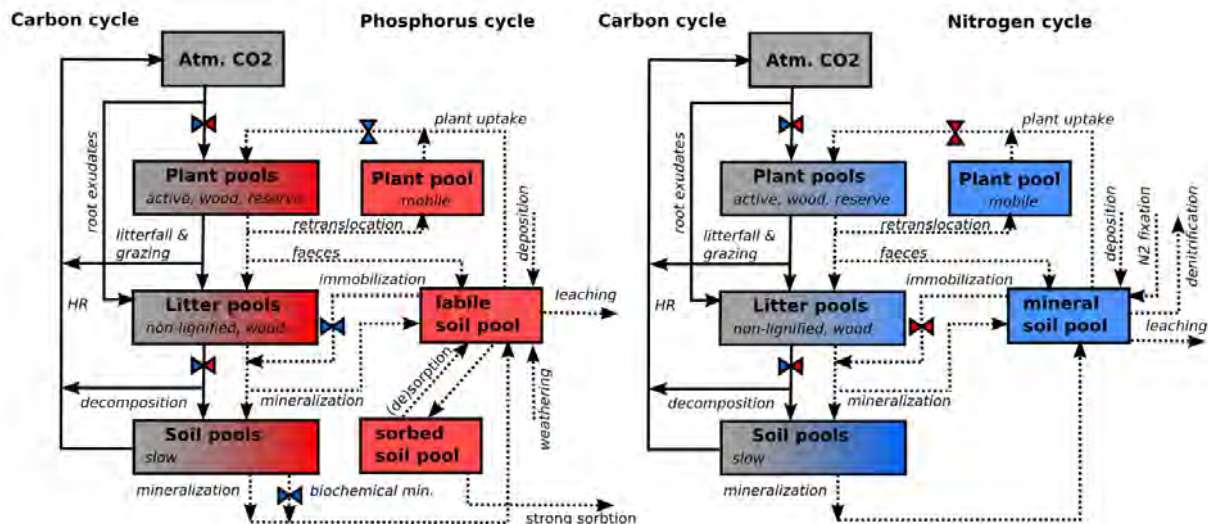


Figure 2.1: Schematic representation of pools and fluxes in JSBACH. Solid arrows indicate carbon fluxes and dashed arrows nutrient fluxes. The plant compartment consists of the three C pools: active (leaves and non-lignified tissue), wood (stem and branches) and reserve (sugar and starches). The litter compartment consists of non-lignified litter, woody litter (lignified litter and fast-decomposing soil organic matter). The soil compartment consists of one pool (slow) representing slow-decomposing organic matter. All carbon pools except the reserve pool have a corresponding nutrient pool with variable C:N:P ratio (slow, non-lignified litter) or fixed C:N:P ratio (rest). There is one mobile plant pool representing mobile nutrient stored internal plants. Soil mineral nitrogen is represented by a single pool (soil mineral pool), while mineral P is represented by labile (available) pool and sorbed pool. The opposing triangles indicated that the flux is controlled by phosphorus (red triangles), nitrogen (blue triangles) or both (mixed triangles).

between nutrients and leaf level photosynthesis (Reich et al., 2006).

Background nutrient limitation (BNL) is indirectly considered in the model as part of the PFT-specific parameterization of the C cycle, which is based on measurements in present day ecosystems and therefore reflects the mean of present day nutrient conditions for a single PFT (Knorr, 2000). However, the range of different soil environments on which a single PFT can grow, may lead to a variability of BNL within a PFT, which is not captured by our approach. The additional nutrient limitation caused by the increase in atmospheric CO_2 (CNL) is computed dynamically in the model assuming globally-uniform constant C:N:P stoichiometry for the different biosphere compartments, such as active and woody biomass and soil organic matter. The model further employs a supply-demand-approach, in which plant nutrient demand is derived from the ratio of potential C-allocation to the plant's C:nutrient-ratios, while nutrient demand by soil microorganisms is derived from the potential immobilization fluxes. Subsequently, the total nutrient demand by plants and soil microorganisms are compared against the supply. If the supply is insufficient to meet the demand, the demand is diminished. These strong simplifications allow us to simulate the N and P cycles with a minimum number of parameters. The merit of our approach is that it avoids the introduction of additional parameters which are hard to quantify, unlike more mechanistically oriented C-N models (Xu-Ri and Prentice, 2008; Jain et al., 2009; Zaehle and Friend, 2010; Esser

et al., 2011) and thereby reduces its dependence on model parameters which are difficult to constrain by available ecosystem observations. The assumption of stoichiometric inflexibility is a strong simplification and may lead to an overestimation of CNL, but we argue it is an appropriate first-order approach given the limited process understanding and data to quantify the full nutrient dynamics including adaptation at plant and ecosystem level (Reich et al., 2006). The implications of these assumptions on nutrient limitation are discussed in detail in Parida (2010).

2.2.1.1 The C cycle

The C cycle in the biogeochemical cycling part of JSBACH is driven by NPP derived from the photosynthesis scheme, following Farquhar et al. (1980) for C₃ and Collatz et al. (1992) for C₄ plants including an explicit dependence of productivity on atmospheric CO₂ concentration (Knorr, 2000). NPP is allocated in fixed fractions to root exudates and the three plant pools: a wood pool representing lignified plant tissue, a active pool for active plant tissue (leaves, fine roots, etc.), and a reserve pool containing C stored as sugars and starch. Upon leaf shedding, C is transferred from the active pool and the reserve pool to the non-lignified litter pool. The wood pool has a fixed turn-over time and C is transferred to a woody litter pool, which differs from the non-lignified litter pool in its turn-over time. Microbial activity mediates the transfer of C from the litter pools to the atmosphere and to the slow soil pool. The latter pool represents slowly decomposing organic matter and is depleted by heterotrophic respiration. The respiration rates depend on soil moisture, nutrient availability, and exponentially on soil temperature.

2.2.1.2 The N cycle

The N cycle is described in detail in Parida (2010). N is taken up by vegetation from a single soil mineral N pool and allocated to the woody and active plant tissue according to the N:C ratios of the these pools. Prior to leaf shedding a certain fraction of N is retranslocated to the mobile N pool, representing internal N storage. Upon leaf shedding, the remaining N is transferred to the non-lignified litter pool. The wood pool has a fixed turn-over time and N is transferred to a woody litter pool. Microbial activity mediates the transfer of N from the litter pools to the slow soil pool. As the N:C ratio of the slow soil pool is larger than the N:C ratios of the litter pools, additional N from the soil mineral N pool is transferred (immobilization). The slow soil pool represents slowly decomposing organic matter and is depleted by biological mineralization. Biological N fixation, the flux of N from the atmosphere to the soil mineral N pool, is a function of NPP, comparable to the approach by Thornton et al. (2007). In this case, we use potential NPP to account for the positive effects of increases in N demand and carbohydrate supply on N fixation (Vitousek et al., 2002). We account for the effect of P limitation on N fixation (Reich et al., 2006) by scaling the fixation rate using the P limitation factor (Eq. (2.2)). Denitrification, the loss flux to the atmosphere, is simulated as a function of the soil mineral N pool (Meixner and Bales, 2003). N losses by leaching are described analogously to P leaching using the approach of Meixner and

Table 2.1: Model variables (Fig. 2.1). For the C cycle, the indexes i and j are: A (atmosphere), a (active), w (wood), r (reserve), la (non-lignified litter), lw (litter wood), s (slow). For the P cycle, the indexes i and j are: a (active), w (wood), m (mobile), la (non-lignified litter), lw (litter wood), s (slow), l (labile), and sr (sorbed). The index e stands for the element (N or P).

Symbol	Description	units
C_i	C in pool i	[mol (C) m ⁻² (canopy)]
P_i	P in pool i	[mol (P) m ⁻² (canopy)]
$F_{i \rightarrow j}^e$	potential flux of element e from pool i to pool j ; $e \in \{N, P\}$	[mol (E) m ⁻² (canopy)]
D_k	P demand of vegetation ($k = \text{veg}$) or microbes ($k = \text{micr}$)	[mol (P) m ⁻² (canopy) s ⁻¹]
F_{BC}	biochemical mineralization flux	[mol (P) m ⁻² (canopy) s ⁻¹]
F_D	P deposited via atmospheric transport	[mol (P) m ⁻² (canopy) s ⁻¹]
F_M	sum of all biological P mineralization fluxes	[mol (P) m ⁻² (canopy) s ⁻¹]
d_i	decomposition rate of pool i	[s ⁻¹]
f_{limit}^e	limitation factor of element e ; $e \in \{N, P\}$	[]

Bales (2003).

2.2.1.3 The P model

The P cycle in JSBACH is designed to diagnose the P distribution on land and to adjust C fluxes for P availability. To include the cycling of P the same methodology as for N is employed (Parida, 2010). Assuming that the C allocation is not affected by nutrients, potential C allocation and heterotrophic respiration are computed. We refer to these fluxes as potential C fluxes. In combination with the stoichiometry of the involved pools we use the potential C fluxes to derive diagnostic P fluxes

$$F_{i \rightarrow j}^P = (r_j - r_i)F_{i \rightarrow j}^C \quad (2.1)$$

where $F_{i \rightarrow j}^C$ is the potential C flux from pool i to pool j , $F_{i \rightarrow j}^P$ the corresponding diagnostic P flux, and r_i and r_j the P:C ratios of the pools i and j , respectively. P is released if $r_i > r_j$ or sequestered if $r_i < r_j$. The latter case may only be realized to the extent that additional P is supplied. Therefore we introduced the following rule: If the diagnosed demand is larger than the supply, P fluxes are diminished according to the available P supply. The supply is given by the labile P (P) and the demand is given by the sum of plant demand (D_{veg}) and microbial demand (D_{micr}). Based on the assumption that vegetation and soil organisms are equally strong in their competition for P, we use a single limitation factor to diminish plant and microbial demand. The amount of potential NPP which cannot be allocated due to P limitation is interpreted as an increase in autotrophic respiration. This reflects the high cost of nutrient foraging in a nutrient limited system (Hogberg et al., 2003). This is supported by a large-scale fertilization experiment in a N-limited boreal forest (Olsson et al., 2005), where fertilization reduces autotrophic respiration, while aboveground

productivity increases. We define the P limitation factor ($f_{\text{limit}}^{\text{P}}$) as

$$f_{\text{limit}}^{\text{P}} = \begin{cases} [\frac{dP}{dt}]^{\text{max}} / (D_{\text{veg}} + D_{\text{micr}}) & \text{for } (D_{\text{veg}} + D_{\text{micr}}) > [\frac{dP}{dt}]^{\text{max}} \\ 1 & \text{otherwise} \end{cases} \quad (2.2)$$

where the term in square bracket is the maximum rate at which the labile P pool can supply P. Note that in the discretized formulation the labile pool can at most be depleted during a single model time step (Δt). We thus set this maximum rate to $\frac{P_l}{\Delta t}$. If the N cycle is active in addition to the P cycle, the limitation factor of the more limiting nutrient is taken to correct potential C fluxes and their corresponding diagnostic nutrient fluxes.

$$f_{\text{limit}} = \min(f_{\text{limit}}^{\text{P}}, f_{\text{limit}}^{\text{N}}) \quad (2.3)$$

where $f_{\text{limit}}^{\text{N}}$ is calculated analogously to $f_{\text{limit}}^{\text{P}}$ (Parida, 2010). This is the only modification in the structure of the C cycle in comparison to Parida et al. (2011).

The P cycle consists of nine pools (P_i ; see Fig. 2.1 and Table 2.1). P enters the terrestrial ecosystems by the weathering of P-bearing minerals. Weathered P enters the labile P pool (P_l), which is available to plants and microbes. Labile P is rapidly adsorbed onto soil particles. The associated pool for sorbed P is denoted by P_{sr} . There are three pools representing P in vegetation. One pool is for P in active tissue (P_a), one pool is for P in woody tissue (P_w) and one pool represents mobile P, which acts as a internal buffer of plant P (P_m). Plants and microbes take up P from the labile P pool (P_l). Upon litterfall, P enters the litter pool for woody litter (P_{lw}) and the pool for non-lignified litter and fast-decomposing (life time ≈ 1.5 yr) soil organic matter (P_{la}). P in slow-decomposing organic matter (life time ≈ 100 yr) is represented by one single pool (P_{slow}). Three P pools have constant P:C ratios (r_i), namely the active pool ($i = a$), wood pool ($i = w$), and woody litter pool ($i = \text{lw}$). P pools with a constant r_i can be derived from the corresponding C pools (C_i) by

$$P_i = r_i C_i \quad (2.4)$$

The other P pools have a constant r_i for the incoming flux but not for the pool itself ($P_{\text{la}}, P_{\text{s}}$), or have no corresponding C pool and thus no r_i (P_l, P_m, P_{sr}).

The mobile P pool (P_m) is a short term P storage internal to plants. It is filled by P retranslocated prior to litterfall and is depleted by P used to allocate as much of the potential NPP ($\text{NPP}_i^{\text{pot}}$) to C_w and C_a as possible.

$$\frac{dP_m}{dt} = (r_a - r_{\text{la}}) F_{\text{a>la}}^{\text{C}} - (r_a \text{NPP}_a^{\text{dir}} + r_w \text{NPP}_w^{\text{dir}}) \quad (2.5)$$

The fraction of $\text{NPP}_i^{\text{pot}}$ which is directly allocated by use of P_m is named $\text{NPP}_i^{\text{dir}}$. $\text{NPP}_w^{\text{dir}}$ and

NPP_a^{dir} are given by

$$NPP_i^{\text{dir}} = \frac{NPP_i^{\text{pot}}}{(r_w NPP_w^{\text{pot}} + r_a NPP_a^{\text{pot}})} \left[\frac{dP_m}{dt} \right]_{\text{max}} \quad (2.6)$$

Litterfall and wood shedding connect plant pools with the litter pools. Green litter is made of fast decomposing organic matter and leaves. The dynamics of the non-lignified litter P pool (P_a) are

$$\frac{dP_a}{dt} = r_{la} F_{a>la}^C + (1 - \beta_l) \epsilon P_a - f_{\text{limit}} \frac{P_a}{C_{la}} \alpha_{la} F_{la>s}^C \quad (2.7)$$

where the first term describes the P influx from litter fall, the second term describes the flux of P from herbivores' excrements which is not directly available to biota, and the third term arises from the P released by biological mineralization of litter. We assume that active plant material (P_a) is consumed by herbivores at a constant rate (ϵ) and immediately excreted (Parida, 2010). We separate the excrement into labile (β_l) and fast decomposing ($1 - \beta_l$) P compounds, which enters the non-lignified litter pool (P_a). The decomposition flux $F_{la>s}^C$ is a demand flux ($r_{la} < r_s$) therefore it is multiplied with f_{limit} . α_i indicates the fraction of decomposed non-lignified litter which enters the atmosphere by respiration. The P of the respired fraction of $F_{la>s}^C$ is mineralized and enters the P_a .

The change in the P content of slow-decomposing soil organic matter (P_s) is given by the net of immobilization and mineralization fluxes

$$\frac{dP_s}{dt} = f_{\text{limit}} r_s ((1 - \alpha_{la}) F_{la>s}^C + (1 - \alpha_{lw}) F_{lw>s}^C) - d_s P_s - F_{BC} \quad (2.8)$$

The first two terms describe P immobilization due to decomposition of non-lignified litter and woody litter. Mineralization occurs as biological mineralization ($d_s P_s$) and the phosphatases-mediated biochemical mineralization (F_{BC}). The decomposition rate d_s is computed by a Q_{10} model as described in the Appendix. Biochemical mineralization is modeled using a rate constant M_{min} if P limitation is absent ($f_{\text{limit}}^P = 1$), but increases under P limitation until a maximum mineralization rate (M_{max}) with a lag time of 30 days. There is no observational evidence to support 30 days, but the results of this study are insensitive to the time lag. If P limitation occurs we use a 30 day mean of f_{limit}^P ($\overline{f_{\text{limit}}^P}$) to increase the rate until the maximal mineralization rate is reached.

$$F_{BC} = \max(M_{\text{max}}(1 - e^{\eta(1 - \overline{f_{\text{limit}}^P})}), M_{\text{min}}) \quad (2.9)$$

This formulation base on the concept of McGill and Cole (1981) that biochemical mineralization is P demand driven. The biochemical mineralization flux, which is mediated by N-rich enzymes (Phosphatases), depend on the availability of N. If the N cycle is active in addition to the P cycle, we use the 30 day mean of the difference between f_{limit}^P and f_{limit}^N (f_{limit}^Δ) instead of $\overline{f_{\text{limit}}^P}$ in eq. (2.9).

$$f_{\text{limit}}^\Delta = \begin{cases} 0 & \text{if } f_{\text{limit}}^P > f_{\text{limit}}^N \\ f_{\text{limit}}^N - f_{\text{limit}}^P & \text{if } f_{\text{limit}}^P < f_{\text{limit}}^N \end{cases} \quad (2.10)$$

Thereby we account for a decreased stimulation of biochemical mineralization in cases when N is limiting in addition to P. If N is limiting more strongly than P a stimulation of F_{BC} is inhibited. If N is limiting, but less than P, the stimulation is less pronounced.

The equations governing the dynamics of labile and sorbed P (P_l and P_{sr}) are adopted from Wang et al. (2010). It is assumed that the labile P pool and the sorbed P pool are in equilibrium on a daily time step. The relationship between the amount of labile P and sorbed P is describe using the Langmuir equation (Barrow, 1978) in its differential form:

$$\frac{dP_{sr}}{dt} = \frac{S_{max}K_s}{(K_s + P_l)^2} \frac{dP_l}{dt} \quad (2.11)$$

where S_{max} is the maximum amount of sorbed phosphorus in the soil and K_s is an empirical constant.

Under these assumption the dynamics of the labile P pool can be described by (see Appendix for derivation)

$$\begin{aligned} \frac{dP_l}{dt} = & \frac{1}{1 + \frac{S_{max}K_s}{(P_l + K_s)^2}} (F_M + F_D + F_W + F_{BC} + \varepsilon\beta_1 P_a) \\ & - \gamma_s P_l R - \frac{1}{\tau_{sr}} P_{sr} - f_{limit}(D_{veg} + D_{micr}) \end{aligned} \quad (2.12)$$

The inputs to the labile P pool are biological P mineralization (F_M), biochemical P mineralization (F_{BC}), dust deposition (F_D), P weathering (F_W), and directly-available P in excrement of herbivores ($\varepsilon\beta_1 P_a$). Losses are leaching, strong sorption, and demand fluxes ($f_{limit}(D_{veg} + D_{micr})$). The loss rate of sorbed P to strongly sorbed and occluded P forms is assumed to be proportional to the amount of sorbed P in the soil ($\frac{1}{\tau_{sr}} P_{sr}$) (Wang et al., 2010). The flux of leached P is a function of runoff (R) and the amount of P_l dissolved in solution (γP_l). Biological P mineralization (F_M) is the sum of the mineralization flux from the slow pool and P leached from freshly shedded wood:

$$F_M = d_s P_s + (r_w - r_{lw}) F_{w>lw}^C \quad (2.13)$$

2.2.1.4 Nutrient demands

The P demand of vegetation (D_{veg}) is given by the amount of labile P needed for the allocation of the potential NPP to the vegetation compartments wood (NPP_w^{pot}) and active (NPP_a^{pot}).

$$D_{veg} = r_w (NPP_w^{pot} - NPP_w^{dir}) + r_a (NPP_a^{pot} - NPP_a^{dir}) \quad (2.14)$$

The microbial P demand is the sum of all potential P immobilization fluxes, which are the fluxes from litter pools, (non-lignified litter and woody litter) to the slow pool. When litter is decomposed a certain fraction of its C is respired to the atmosphere and the remaining C becomes slowly-decomposing organic matter. Denoting the respired fraction by (α_i), the microbial P demand

becomes:

$$D_{\text{micr}} = \left(r_s - \frac{P_{\text{la}}}{C_{\text{la}}}\right)F_{\text{la}\triangleright\text{s}}^{\text{C}} + (r_s - r_{\text{lw}})F_{\text{lw}\triangleright\text{s}}^{\text{C}} - \frac{P_{\text{la}}}{C_{\text{la}}}F_{\text{la}\triangleright\text{a}}^{\text{C}} - r_{\text{lw}}F_{\text{lw}\triangleright\text{a}}^{\text{C}} \quad (2.15)$$

By respiration some P becomes available, which is subsequently immobilized by microbes and therefore is subtracted from the microbial demand. The non-lignified litter pool does not have a fixed r_i , instead the term $\frac{P_{\text{la}}}{C_{\text{la}}}$ is used in the above equations. The decomposition fluxes are

$$F_{i\triangleright\text{s}}^{\text{C}} = d_i(1 - \alpha_i)C_i \quad (2.16)$$

and

$$F_{i\triangleright\text{a}}^{\text{C}} = d_i\alpha_iC_i \quad (2.17)$$

where i can be lw or la. d_i is the decomposition rate of litter pool i and its calculation is described in the Appendix.

2.2.1.5 Parameter estimates

The parameters of the P model are globally uniform, except for the biochemical mineralization rates which depend on soil order, and their values are shown in Table 2.2. We use information from the global data set of plant traits TRY (Kattge et al., 2011) to compute the N:P ratios for the active and wood pools, as well as the flux from the active pool to the non-lignified litter pool. From these N:P ratios P:C ratios are derived using the N:C ratios from Parida (2010). The P:C ratio of the woody litter is set to a value within the range of spread of P:C of bark (Kattge et al., 2011), as data for heartwood is scarce. The initial P:C ratio for the slow decomposing organic matter is taken from Smil (2000).

Leaching is calibrated so that first of all the global leaching flux compares well with estimates from empirical modelling (Seitzinger et al., 2005) and in addition, according to our concept of limitation, that CNL by P is absent under pre-industrial conditions.

The biochemical mineralization flux is calibrated such that the N:P ratio of soil organic matter is close to the estimates by Yang and Post (2011). The outcomes of this study are insensitive to parameter values for the adjustment intensity (η) (not shown) of the biochemical mineralization flux in eq. (2.9), which is set arbitrarily due to a lack of data. The dynamics of the labile and sorbed P are parameterized based on measurements on US soils using the USDA soil classification (Wang et al., 2010), because there is no more comprehensive data. Therefore, the history and the characteristics (soil texture, redox potential, etc.) of the different soil types reflect global patterns to the extent that US soil types are representative for the global diversity of soils.

Table 2.2: Parameters of the P model. The soil order specific and the PFT specific values of parameters are listed in the appendix. In the case of Kattge et al. (2011), plant trait data have been made available via the TRY database. These data are related to the following original references: Bakker et al. (2005, 2006); Baker et al. (2009); Cornelissen (1996); Cornelissen et al. (1996, 2003, 2004); Craine et al. (2005, 2009); Diaz et al. (2004); Fortunel et al. (2005, 2009); Fyllas et al. (2009); Garnier et al. (2007); Han et al. (2005); He et al. (2006, 2008); Kazakou et al. (2006); Laughlin et al. (2010); Meziane and Shipley (1999); Niinemets (1999, 2001); Ogaya and Penuelas (2003, 2006, 2007, 2008); Ordóñez et al. (2010b,a); Patino et al. (2009); Pakeman et al. (2008, 2009); Quested et al. (2003); Reich et al. (2008); Sardans et al. (2008a,b); Shipley and Lechowicz (2000); Swaine (2007); Willis et al. (2010); Wright et al. (2004, 2006)

Symbol	Parameter	Units	Value	Source
Δt	time step	day	1	
τ_{sr}	life time of P in the sorbed pool	year	100	Wang et al. (2010)
α_{fa}	the fraction of decomposed C from non-lignified litter which is respired	[]	depends on PFT	Parida (2010)
α_{fw}	the fraction of decomposed C from woody litter which is respired	[]	0.2	
β_1	fraction of P in excrements which is directly available to biota	[]	$\frac{r_i}{r_i+r_{fa}}$	
r_a	P to C ratio of P_a	[mol (P) mol ⁻¹ (C)]	$\frac{1}{1440}$	Kattge et al. (2011)
r_w	P to C ratio of P_w	[mol (P) mol ⁻¹ (C)]	$\frac{1}{7690}$	Kattge et al. (2011)
r_{fa}	P to C ratio of P_{fa}	[mol (P) mol ⁻¹ (C)]	$\frac{10000}{10000}$	Kattge et al. (2011) (assumed)
r_{fw}	P to C ratio of P_{fw}	[mol (P) mol ⁻¹ (C)]	$\frac{1}{3650}$	Smil (2000)
r_s	P to C ratio of P_s	[mol (P) mol ⁻¹ (C)]	$\frac{1}{465}$	Wang et al. (2010)
S_{max}	maximal amount of sorbed P	[mol (P) m ⁻²]	depends on soil order	Wang et al. (2010)
K_s	empirical parameter describing sorption	[mol (P) m ⁻²]	depends on soil order	Wang et al. (2010) (calibrated)
$\%_f$	fraction of labile P which is dissolved in soil solution	[]	.0001	Wang et al. (2010)
F_w	P released from primary minerals by weathering	[mol (P) m ⁻² s ⁻¹]	depends on soil order	Wang et al. (2010) (calibrated)
M_{min}	minimal (background) biochemical mineralization rate	[mol (P) m ⁻² s ⁻¹]	depend on soil order	(calibrated)
M_{max}	maximal biochemical mineralization rate	[mol (P) m ⁻² s ⁻¹]	depend on soil order	(calibrated)
η	scaling factor for biochemical mineralization	[]	-5	(calibrated)
ϵ	fraction of C_g removed by herbivores	[]	depend on PFT	Parida (2010)

Table 2.3: List of experiments performed. The climatic forcing is for all simulations the same. See Appendix C for further simulations regarding the stoichiometric parameterization.”

Experiment	N cycle	P cycle	Modification
C-only	off	off	
CN	on	off	
CP	off	on	
CNP	on	on	
CP _{ox}	off	on	soils have high sorption capacity
CP _{mo}	off	on	soils have low sorption capacity
CP _{bc}	off	on	rigid biochemical mineralization
CN _{dp}	on	off	N deposition constant
CP _{pft}	off	on	PFT-specific C:P ratios
CN _{pft}	on	off	PFT-specific C:N ratios

2.2.2 Experimental setup

The simulation setup is adopted from the CN simulations performed by Parida (2010). We run the submodel of JSBACH for the biogeochemical cycles independently from the rest of JSBACH driven by net primary productivity (NPP), leaf area index, soil temperature, soil moisture and surface runoff. The forcing variables are extracted from simulations performed with the MPI-ESM (Roeckner et al., 2011) under the framework of the ENSEMBLES project. The MPI-ESM consists of the atmosphere model ECHAM5 (Roeckner et al., 2003) and its land surface scheme JSBACH (Raddatz et al., 2007) coupled to the ocean model MPI-OM (Marsland et al., 2003). The simulations by Roeckner et al. (2011) were performed at horizontal resolution T31 (approx. 400×400 km) and 19 vertical atmospheric layers, driven by prescribed atmospheric CO₂ concentration (SRES A1B scenario 1860–2100) prescribing anthropogenic land cover changes. Accordingly, our JSBACH stand-alone simulations are conducted at T31 resolution, but without land cover changes using a map of potential vegetation. Output variables of the MPI-ESM are provided for every PFT at every grid independent of the prescribed vegetation cover. Therefore the initial distribution of PFTs in simulations with the stand-alone model can be different from the one used in the forcing simulation. To investigate the long-term evolution of nutrient limitation, we performed an additional simulation with the full MPI-ESM to derive forcing data where we prolonged the original ESM simulation for additional 400 yr keeping the atmospheric CO₂ concentration fixed at the level of 2100. In this period, climate slowly approaches a new equilibrium.

Using the submodel of JSBACH for the biogeochemical cycles, we brought the element cycles into equilibrium (less than 1 % change in the 30-yr mean of global pools) using a repeated 30-yr cycle of the forcing data from the coupled simulation (1860–1889). We equilibrated the element cycle consecutively in three steps. Firstly, we run the model in the C only mode reaching equilibrium after 5000 yr. Secondly, we prolonged this simulation switching on the N cycle for additional 5000 yr. Thirdly, the P cycle was brought into equilibrium after prolonging the CN equilibrium

simulation for additional 8000 yr in the CNP mode. We made sure that this sequential spin up procedure did not result in a different equilibrium state than a simultaneous spin up. During the spin up, N and P deposition were kept constant at the level of 1860 and present day, respectively, as the human impact on P deposition is marginal (Mahowald et al., 2008).

We conducted several transient simulations with the submodel: without nutrients (C-only), with N (CN), with P (CP), and with N and P (CNP) (Table 2.3). Land use, land use change, and fertilizer application are not accounted for. N deposition is read in from maps (Galloway et al., 2004; Dentener et al., 2006) which are interpolated in time proportionally to the increases of atmospheric CO₂ concentrations of the forcing simulation until 2030 and afterwards extrapolated also using CO₂ of the forcing simulation, following Wang and Houlton (2009). Present day P deposition maps (Mahowald et al., 2008) are used for the whole simulation period.

To test the robustness of our results, we conducted several sensitivity simulations (Table 2.3). A set of simulations was performed with PFT-specific C:N:P ratios from Wang et al. (2010) and McGroddy et al. (2004) (CN_{pft}, CP_{pft}). As a redistribution of P from unavailable pools to available ones can affect nutrient limitation, we varied parameters controlling the size of redistributable P, namely sorbed P, (CP_{mo}, CP_{ox}) and modified the adaptive strength of biochemical mineralization (CP_{bc}). In another simulation (CN_{dp}), we kept N deposition constant at the present level to test for the effect of increasing N deposition rates. Furthermore, we performed simulations with flexible stoichiometry, as well as a set of simulations with perturbed stoichiometric parameters. The latter simulations are described in detail in the Appendix C.

2.3 Results and discussion

2.3.1 Present day: comparison with observations

For present day, the model simulates a terrestrial C stock of 2881 Gt(C), 24 % of it stored in vegetation (682 Gt(C)), 8 % in litter and fast decomposing soil organic matter (229 Gt(C)), and 69 % in slow-decomposing soil organic matter (1970 Gt(C)). When N and P cycling are taken into account (CN, CP, CNP) the present day C stocks are only slightly reduced (<1 %). The simulated vegetation C storage is slightly above the higher end of inventory based estimates that range from 560 to 652 Gt(C) (Saugier and Roy, 2001). This relatively high vegetation C stock can be attributed to the land cover prescribed in our simulation, which differs from the real world as crop land is replaced with potential vegetation, which stores more C than crops. The simulated soil C stock is in the range of observation-based estimates that range from 1500 to 2300 Gt(C) (Post et al., 1982; Batjes, 1996) depending on the considered soil depth.

The decadal means of the net land to atmosphere fluxes for the 1980s, 1990s, and 2000s (Table 2.4) are between 2.2 and 3.7 Gt(C) yr⁻¹ when nutrients are not considered. When N and P are considered, the fluxes are reduced up to 10 %. The simulated fluxes are higher but of the same magnitude as the ones by Friedlingstein et al. (2010). Note that we do not account for land use in

Table 2.4: Simulated decadal land C uptake [Gt(C) yr^{-1}] with and without accounting for nutrients compared to published estimates of the natural terrestrial sink from the Global Carbon Project (GCP) (Friedlingstein et al., 2010). Note that we omit land use (change) in our simulations.

period	C-only	CN	CP	CNP	GCP
1980s	-2.2	-2.1	-2.0	-1.9	-1.5
1990s	-2.8	-2.7	-2.5	-2.4	-2.5
2000s	-3.7	-3.5	-3.3	-3.1	-2.4

our simulation, in contrast to Friedlingstein et al. (2010). When land use and land cover change is explicitly accounted for, the land C uptake is reduced by 20 % to 30 % (Parida, 2010). The inclusion of the P cycle into JSBACH only slightly changes present day C cycling because CNL by P is mostly absent between 1860 and 2000 and reduces present day NPP by less than 3 % (not shown). Overall, the model performs well in simulating C cycling given the large uncertainties in quantifying present day C cycling (Friedlingstein et al., 2010). For a detailed discussion of the C and N cycle see Parida (2010).

The current state of the terrestrial P cycle is even less constrained by observations than the C and N cycle. Estimates of total terrestrial soil P range from 40 Gt(P) (Smil, 2000) to 200 Gt(P) (Jahnke, 1992). P stocks are often derived from C or N stocks using assumptions about the stoichiometry (Smil, 2000). Soil P is mostly measured in agricultural soils (Johnson et al., 2003), which are heavily influenced by fertilizer and manure application (Smil, 2000). Measurements of the fraction of soil P which is available to biota are prone to high uncertainties (Johnson et al., 2003). The mean sizes of the simulated P pools (CNP) for present day are summarized in Table 2.5 and the spatial distribution is shown in Fig. 2.2. When compared to modelling and empirical estimates, the simulated P storages are at the lower end of estimates. The upper ends of the estimates for P in soils of 200 Gt(P) (Jahnke, 1992) and in vegetation of 3 Gt(P) are criticized for being unrealistic (Smil, 2000; Wang et al., 2010). Our study supports these findings unless we have overestimated C:N ratios. However, the C:N ratios used in JSBACH are relatively low (Parida, 2010). The N:P ratios for the vegetation compartments are derived from a comprehensive stoichiometric dataset for plants (Kattge et al., 2011), which is an improvement to earlier studies based on more restricted data sets.

The model seems to underestimate the amount of labile P in highly weathered soils when compared to a recent data compilation (Table 2.6) (Yang and Post, 2011). The compilation by Yang and Post (2011) includes the data which were used to calibrate the sorption model (Wang et al., 2010). Two aspects make the estimation of plant available P difficult. First, the interpretation of P measurements is not straightforward, as the measured fractions cannot be linked directly to physiological ones, like plant available P (Johnson et al., 2003; Yang and Post, 2011). Second, the area based estimates by Yang and Post (2011) depend on assumptions about the bulk density of soils, which is highly variable within one class of soil. However, in the next section, we will show that the amount of labile P in the initial model state is of relative small importance for the

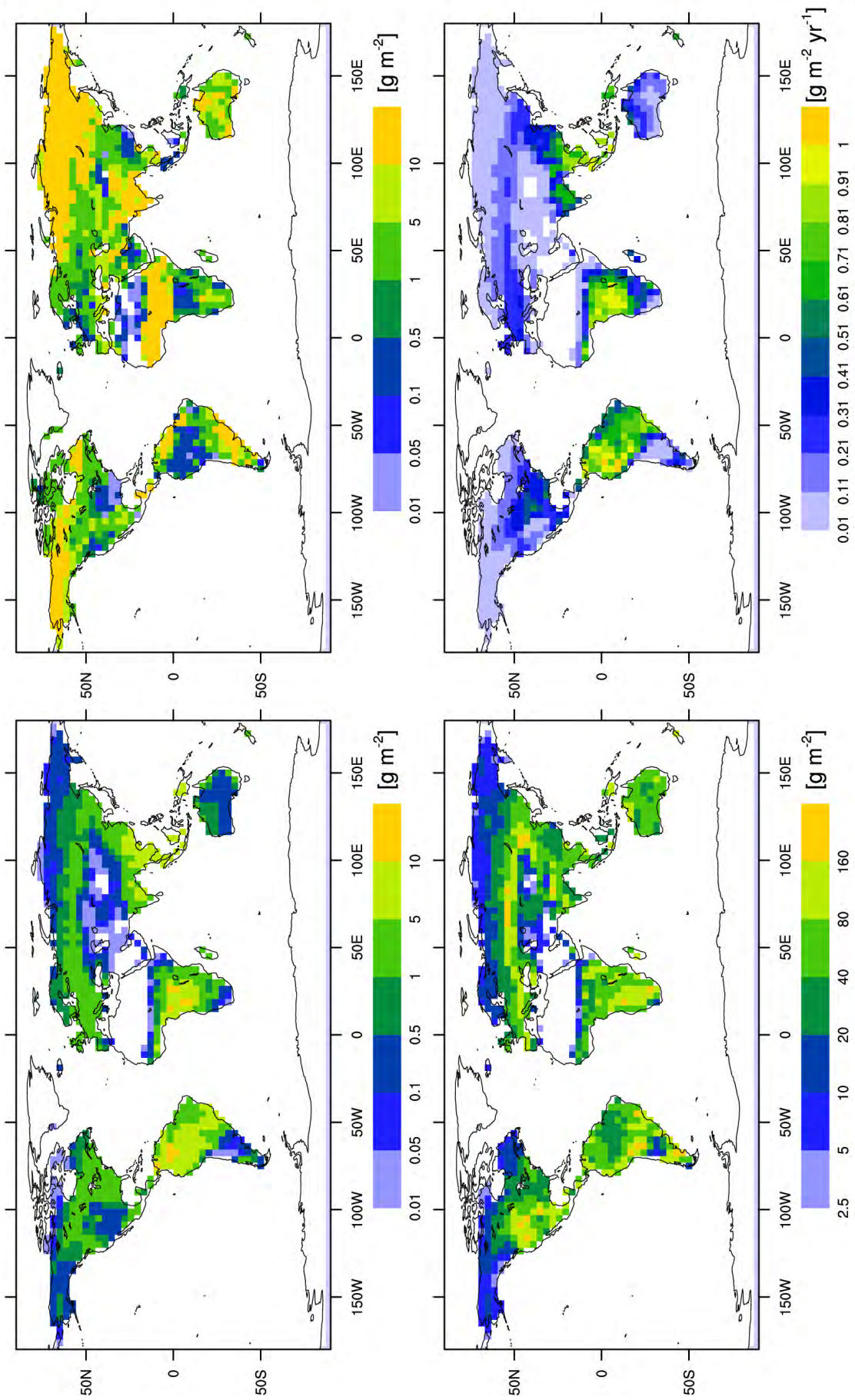


Figure 2.2: The simulated P in vegetation (top left), sorbed P (top right), P in soil organic matter and litter (bottom left), and the annual P uptake by vegetation (bottom right) for present day.

Table 2.5: Simulated P stocks [Gt(P)] from the simulation CNP compared with published estimates. The simulated stock sizes are means of the years 1970–1999. The litter pool contains leaf litter and fast decomposing soil organic matter.

Pool	JSBACH	other
Vegetation	0.23	0.39–3 (Wang et al., 2010; Jahnke, 1992)
Litter	0.08	0.04 (Wang et al., 2010)
Soil organic	5.74	5–10 (Smil, 2000)
Labile P	0.98	1.5 (Wang et al., 2010)
Sorbed P	1.25	1.7 (Wang et al., 2010)

Table 2.6: Mean (\pm standard deviation) for simulated labile P [$\text{g(P)}\text{m}^{-2}$] that typically support forests compared to measurements (Yang and Post, 2011). The stocks, which are averaged over a 30 yr period (1970–1999), are from simulations with present day soils (CP), uniform low sorption soils (CP_{mo}), and uniform high sorption soils (CP_{ox}).

Soil	<i>n</i>	CP	CP_{mo}	CP_{ox}	(Yang and Post, 2011)
Entisols	91	9.352 \pm 13.022	2.573 \pm 4.387	1.681 \pm 1.634	8.082 \pm 5.317
Inceptisols	199	8.571 \pm 10.508	1.967 \pm 3.599	1.485 \pm 1.569	8.728 \pm 5.204
Alfisols	110	6.014 \pm 8.563	6.083 \pm 8.906	3.578 \pm 3.051	4.125 \pm 2.983
Oxisols	67	0.946 \pm 0.432	0.939 \pm 0.435	0.948 \pm 0.431	1.972 \pm 1.918
Spodosols	42	1.564 \pm 3.873	2.229 \pm 4.800	2.417 \pm 2.614	5.939 \pm 1.438
Ultisols	63	1.010 \pm 1.804	1.723 \pm 4.586	1.545 \pm 2.220	2.334 \pm 1.858

occurrence of P limitation.

The annual P uptake by vegetation is shown in Fig. 2.2 and Table 2.7. From measurements, the annual P uptake can be estimated as the sum of P required to replace P in litterfall, P in wood increment, and P required for root growth, assuming equilibrium. Johnson et al. (2003) estimated the mean annual P requirement of temperate forests to be $0.52 \pm 0.38 \text{ g(P)}\text{m}^{-2}\text{a}^{-1}$. For temperate broadleaf forests we simulate a mean (\pm standard deviation) uptake rate of $0.52 \pm 0.23 \text{ g(P)}\text{m}^{-2}\text{a}^{-1}$. For tropical evergreen forests, P lost by litterfall, which makes up the largest part (approx. 60%) of the P uptake in temperate forests (Yanai, 1992; Johnson et al., 2003; Yang and Post, 2011), is in the range of 0.2 to $0.4 \text{ g(P)}\text{m}^{-2}\text{a}^{-1}$ (Vitousek, 1984; Valdespino et al., 2009; Yang and Post, 2011). Yang and Post (2011) report a higher mean loss rate of $0.6 \text{ g(P)}\text{m}^{-2}\text{a}^{-1}$ using a litterfall database. The simulated mean P uptake of evergreen tropical forests is $0.68 \pm 0.32 \text{ g(P)}\text{m}^{-2}\text{a}^{-1}$. Thus, despite spatially uniform CNP ratios the model is able to simulate reasonable P uptake rates for forests. However, it may underestimate P uptake in grasslands. In the budget of two semiarid grasslands given by Cole et al. (1977), plant uptake was 0.53 and $1.2 \text{ g(P)}\text{m}^{-2}\text{a}^{-1}$, respectively. We simulate lower uptake rates of 0.24 ± 0.22 and $0.31 \pm 0.28 \text{ g(P)}\text{m}^{-2}\text{a}^{-1}$ for C_3 and C_4 grasslands, respectively. The low uptake rates are mainly caused by a low NPP of 340 and $420 \text{ g(C)}\text{m}^{-2}\text{a}^{-1}$ for C_3 and C_4 grasslands. Observation-based estimates of grassland NPP range from 200–2000 $\text{g(C)}\text{m}^{-2}\text{a}^{-1}$, but may be even higher (Scurlock et al., 2002). For the 20th century, we can rule out an influence of low P availability on P uptakes rates via P limitation,

Table 2.7: Simulated P fluxes as means of PFT [$\text{g(P) m}^{-2} \text{a}^{-1}$]. The fluxes are averaged over the years 1970–1999.

PFT	plant uptake	immobilization	biological min.	biochemical min.
Tropical evergreen trees	0.68	2.01	1.24	1.26
Tropical deciduous trees	0.71	2.41	1.69	1.25
Temperate broadleaf evergreen trees	0.52	1.33	0.72	0.87
Temperate broadleaf deciduous trees	0.18	0.52	0.30	0.36
Coniferous evergreen trees	0.20	0.56	0.36	0.35
Coniferous deciduous trees	0.08	0.22	0.11	0.18
Raingreen shrubs	0.15	0.34	0.21	0.25
Deciduous shrubs	0.06	0.17	0.10	0.11
C ₃ grass	0.24	0.67	0.49	0.32
C ₄ grass	0.31	0.78	0.53	0.48
Tundra	0.02	0.12	0.05	0.08

as present day NPP is reduced by P limitation by less than 3 % in the model. In the sensitivity simulation with PFT-specific C:P ratios, P uptake by vegetation is reduced in tropical PFTs by 10–20 %, but increased in temperate PFTs by 40–50 %. Overall, the mean uptake rates do not improve using a PFT-specific set of C:P ratios. As the uptake is strongly controlled by the P demand of vegetation, the differences in P uptake rates between PFTs are dominated by the differences in NPP.

Immobilization of P by microbes is generally larger than the uptake by plants (Yang and Post, 2011). In a budget of two grassland sites the immobilization fluxes exceeded the uptake by vegetation by factors of 2.6 and 4.7, respectively (Cole et al., 1977). In our simulation, the immobilization fluxes of grasslands are globally 2.8 and 2.5 times larger than plant uptake for C₃ and C₄ grasslands, respectively. In the case of N, the immobilization flux is 1.7 times larger than plant uptake. The more dominant role of microbes in P immobilization compared to N, is supported by the finding of Aponte et al. (2010) that 8.8 % of total P is immobilized by microbes compared to 4.7 % in the case of N.

The mineralization of P from slowly-decomposing soil organic matter can occur by biological and biochemical mineralization (McGill and Cole, 1981). Biochemical mineralization is mediated by extracellular enzymes which specifically cleave out P from organic matter, thus it is controlled by the P demand of biota (Stewart and Tiessen, 1987). In contrast, biological mineralization is driven by the energy demand of microorganisms, as it is coupled to heterotrophic respiration. Although phosphatase activity, which is a qualitative measure for biochemical mineralization, is common in soils (Stewart and Tiessen, 1987), the quantification of the mineralization rates in the field is not yet possible. The simulated biochemical mineralization fluxes are in the same order of magnitude as the biological mineralization flux (Table 2.7). In a simulation without biochemical mineralization, the amount of P in soil organic matter was 16.2 Gt(P)), which is 3.13 times more than in the standard simulations. The increased amount of P in soil organic matter in the simulation without biochemical mineralization is comparable in magnitude with the results of Wang et al. (2010) about the effect of biochemical mineralization on soil P.

Biochemical mineralization partly decouples P mineralization from decomposition of soil organic matter, namely N mineralization. Therefore the N:P ratio of the slowly-decomposing soil organic matter can vary in the model and we used it to calibrate the strength of biochemical mineralization. The lower end of the N:P ratio is given by a prescribed C:N:P ratio, while the higher end depends on the strength of biochemical mineralization. The simulated N:P ratios of slowly-decomposing soil organic matter of 20.3, 26.8, and 37.7 for slightly, intermediate, and highly weathered soil compare well with data compiled by Yang and Post (2011). The agreement of simulated and observed N:P ratios indicates that in the model the biochemical mineralization is in a reasonable order of magnitude, unless the C:P ratio of newly-formed organic matter used in the model is wrong.

2.3.2 Land C sink until 2100

In the C-only simulation, land accumulates 550 Gt(C) from 1860 to 2100. The uptake is in the range of land C uptake simulated by different C cycle models (Friedlingstein et al., 2006). As in Friedlingstein et al. (2006), we do not account for land use change, which would reduce the land C uptake. The C sequestered on land is stored in vegetation (+315 Gt(C)), soil (+195 Gt(C)) and litter and fast-decomposing soil organic matter (+40 Gt(C)) (Fig. 2.3). When considering nutrient limitation, the projected land C uptake for the period 1860–2100 is reduced by 13 %, 16 % or 25 % due to limitation by nitrogen (CN), by phosphorus (CP) or by both (CNP), respectively (Fig. 2.3c). The strengths of nutrient limitations in the given model setup are not affected by the assumption of stoichiometric inflexibility (see Appendix C). Parameter perturbation simulations reveal that the strength of N and P limitation depends to some extent on the parameterization of stoichiometry, but the ranking of limitations is not affected (Appendix C). P limitation reduces the amount of C stored in vegetation more strongly than N (Fig. 2.3d). This is explained by the geographic occurrence of N and P limitation (Fig. 2.4). P limits C uptake mainly at low latitudes, where the C taken up is predominately stored in vegetation (see Fig. A.4 in the Appendix). At high latitudes the soil sink dominates.

The partly additive nature of N and P limitation on land C uptake can be attributed to their distinct geographic occurrence (Fig. 2.4). In addition, in the model, N limits mainly grasslands while P limitation is nearly absent in grasslands (not shown). Hence N and P limitation are to a large degree additive, despite their geographical co-occurrence in some regions. The lack of synergetic effects between the nutrient cycles can be attributed to the simple representation of N-P interactions in our model and may not reflect the actual effects. For example, N fixation is represented by an empirical function, which cannot account for all pathways of N-P interactions underlying N fixation. To rule out that the pattern of nutrient limitations is a result of the globally uniform C:N:P ratios, we performed additional sensitivity simulations with a PFT-specific set of C:N:P ratios from Wang et al. (2010). In these simulations the pattern of limitations is not changed, although the strength of N and P limitation is slightly reduced (see Fig. A.1 in Appendix).

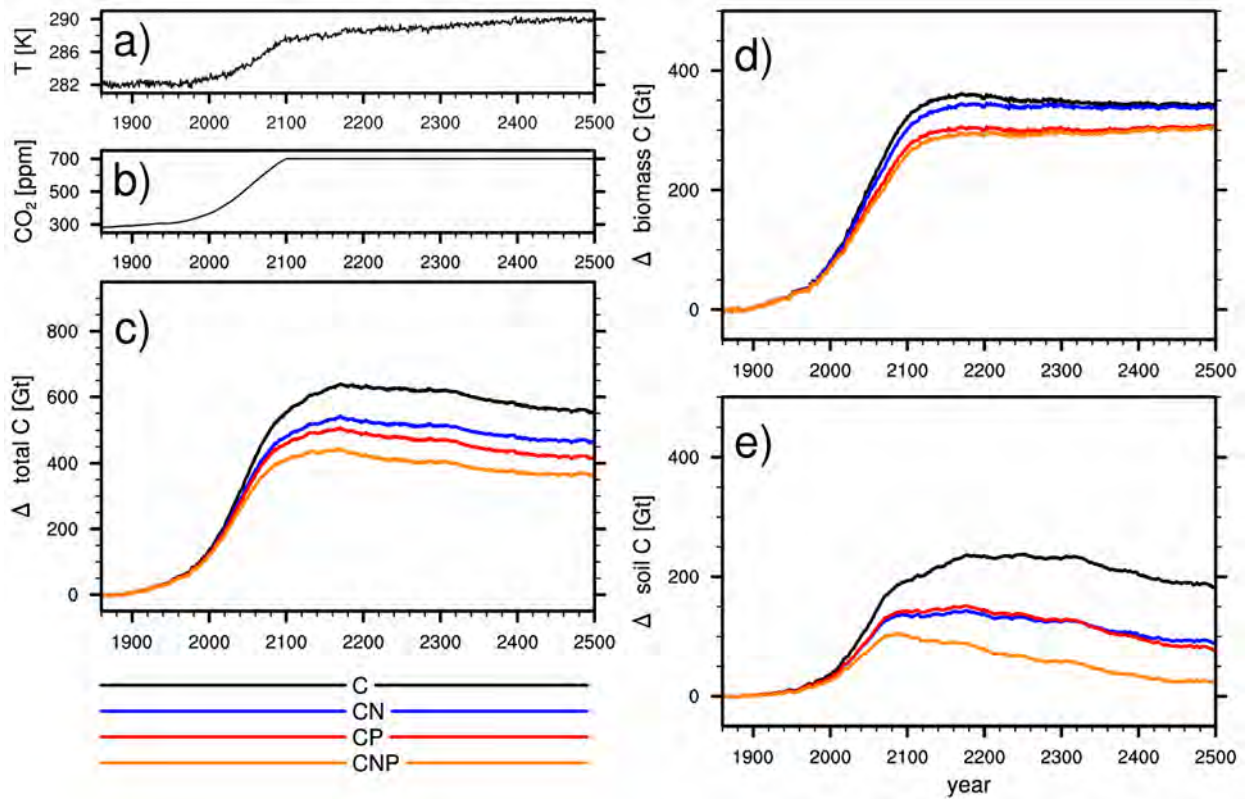


Figure 2.3: The simulated change in land carbon storage under the SRES A1B scenario. Shown are the 10 yr mean of soil temperature (a), the CO₂ concentration as used in the forcing simulation (b), the resulting change in total land C storage (c), and the changes in the two main land compartments vegetation (d) and soil (e).

To test the influence of soil P sorption capacities on P limitation, we performed simulations with globally uniform parameters for the dynamics of labile and adsorbed P. The parameter for the sorption capacity (S_{\max}) constrains the amount of adsorbed P in the initial state. As sorbed P is a buffer for labile P, the extent to which increased P demands can be sustained by a redistribution of adsorbed P to labile P is constrained by S_{\max} . The typical tropical soils, Oxisols and Ultisols, have the highest sorption capacities and the fertile soils of temperate regions, Alfisols or Molisols, have lower capacities. Therefore, as expected, an artificial exchange of all soils with Molisols (CP_{mo}) does not alleviate but increase P limitation drastically during the 21st century (Fig. 2.4). CNL by P becomes even larger than CNL by N at high latitudes. The low sorption capacities of soils in central Europe and eastern North America make these regions vulnerable to CO₂-induced P limitation. An exchange with Oxisols reduces P limitation in our simulations due to the high sorption capacity. The accumulated land C uptake between 1860 and 2100 in CP_{mo} and CP_{ox} simulations is reduced by 19% and 4% respectively compared to the C-only simulation. When compared to the simulation CP, the land C uptake is less limited by P in the CP_{ox} , despite the stocks of labile P are smaller (Table 2.6). This shows that the stocks of labile P do not necessarily correlate with P limitation. It is difficult to assess how realistic such a redistribution of adsorbed P to labile forms is. Evidence from short-term CO₂ enrichment studies suggest that a redistri-

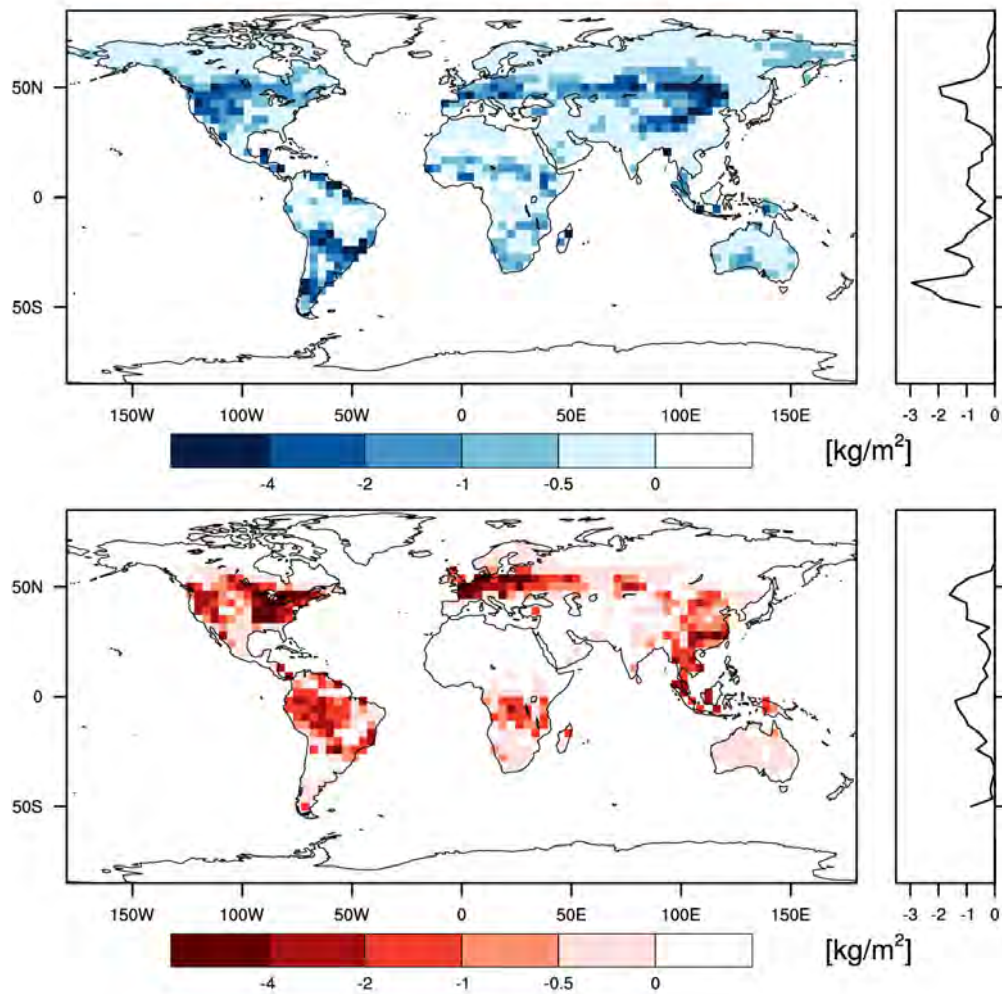


Figure 2.4: The reduction in C storage [kg m^{-2}] by nutrient limitation at the end of the 21st century. Shown is the difference in the mean C storage (2070–2099) between the CN simulation and the C-only simulation (upper panel) or between the CP simulation and the C-only simulation (lower panel). The latitudinal means over land points are shown on the right side.

bution of P from unavailable to available forms does occur under elevated CO_2 (Johnson et al., 2004; Khan et al., 2008). However, it is unclear which processes are responsible for the observed redistribution and how these results from short-term experiments translate to natural ecosystems affected by a steady increase in CO_2 over centuries.

Biochemical mineralization is an additional mechanism that can shift P from unavailable to available forms. We assume that biochemical mineralization is highly adaptive to P limitation. In the CP simulation, biochemical mineralization rates increase by 37% by the end of the 21st century. This is higher than an increase in biochemical mineralization by 18% caused by doubling of CO_2 in the simulations by Wang et al. (2007). As the biochemical mineralization rates so far cannot be quantified from measurements, we conducted a sensitivity simulation (CP_{bc}) in which we kept the biochemical mineralization rates constant at the pre-industrial level. This results in a reduction of land C uptake by CNL by P of 39% for the period 1860–2100, while the geographic

pattern is only affected marginally (not shown). This sensitivity test shows, in addition to the sensitivity simulations CP_{ox} and CP_{mo} , the importance of adaptive processes which shift nutrients from unavailable forms to available forms for projecting nutrient limitation in a transient state.

High inputs by N deposition can shift ecosystems from N-limited to P-limited by increasing the P demand due to N-stimulated productivity and by acidifying soils which increase P sorption. In JSBACH, the effect of increasing N deposition rates on the geographic pattern of N and P limitation is marginal, as the differences in the latitudinal means of CNL between the simulation with increasing N deposition and the one with constant N deposition (CN_{dp}) is small (Fig. 2.4). In general, the effect of N deposition on the land C uptake during the 21st century is small in JSBACH owing to our concept of CNL (Parida, 2010). In addition, the P sorption characteristics are prescribed in the model. Hence we may underestimate the effects of N deposition. While the simulations show high uncertainties in the quantification of nutrient limitation, a robust outcome of the simulations is the occurrence of CNL by P in low latitude and high latitude ecosystems during the 21st century and the nearly additive nature of P and N limitation. The geographical pattern of CNL by P and N is comparable to the pattern of total nutrient limitation in simulations by Wang et al. (2010). This pattern is to a large extent robust against the assumptions about biochemical mineralization and soil sorption and it is not a result of a special calibration procedures; this pattern automatically emerges in the simulation when atmospheric CO_2 concentration increases.

2.3.3 Land C sink after 2100

The global mean annual temperature over land increases in our simulations by more than 5 K during the 21st century (Fig. 2.3a), which is comparable to other models (Friedlingstein et al., 2006). Temperature is a main driver of the biogeochemical cycles. Under ongoing climate change the cycling of elements gradually changes, leading to an imbalance between the C and the nutrient cycles. After stabilization of temperature and climate at the new level, biogeochemical cycles are slowly approaching a new equilibrium. To analyze nutrient limitation in the new climate state, we prolonged the simulation for 400 yr keeping CO_2 concentration constant at the level of 2100, but letting climate evolve.

Warming has two counteractive effects on the land C cycling in JSBACH. On the one hand, C losses by autotrophic and heterotrophic respiration increase. However, adaptive and acclimative responses that might limit such respiration losses (Wythers et al., 2005; Atkin and Tjoelker, 2003; Reich, 2010) are not considered in the model. Concepts for their representation in models are currently under investigation. On the other hand, temperatures at high latitudes become more suitable for plant growth and the growing seasons extend and therefore NPP increases. Overall, land becomes a source of C in JSBACH as the losses outweigh the sinks (Fig. 2.3c). Increasing temperature also directly influences the N and P cycling by enhancing mineralization in many parts of the world. The increase in mineralization of N and P by 35 % globally at the end of the 2100 is comparable to the enhancement of N mineralization by 45 % measured in a 7-yr soil warming experiment

with a comparable increase in temperature (+5 K) (Melillo et al., 2011). However, as temperature effects on N and P mineralization will strongly depend on interactions between temperature and soil water, such comparisons must be made with considerable caution. A decrease in tropical NPP at mean land temperatures warmer by as much as 7 K compared to today due to climate change is a feature of several coupled climate-carbon cycle simulations, although the amplitude of the drop in NPP varies considerably among models (Raddatz et al., 2007). A negative effect of increasing temperature on tropical productivity is supported by observational evidence (Clark, 2004). An increase in the NPP of temperate and boreal systems due to warming is projected in all simulations analyzed Friedlingstein et al. (2006) (T. Raddatz, personal communication, 2011). Part of this increase can be attributed to an advancement of leaf unfolding. In JSBACH, leaf unfolding of temperate broadleaf forests appears 17 days earlier at end of the 21st century than present day. The reported changes in late 20th century tree phenology correspond to an advancement of leaf unfolding of 16–24 days per K of warming, assuming that the average warming over the last five decades was about 0.6 K (Solomon et al., 2007). This relationship may not apply to the future, as a decline in freezing events may delay the breaking of dormancy and therefore the effect of warming may be much smaller and could be even reversed (Morin et al., 2009). The phenology model of JSBACH accounts for this inhibitory effect and the more moderate advancement of leaf unfolding is closer to the simulations by Morin et al. (2009), which project an advancement by 5 to 10 days during the 21st century under the SRES scenarios A2 (+3.2 K) and B2 (+1 K).

As a result of the increase in NPP, the N and P demands increase at high latitudes. In the tropics and subtropics, however, nutrient demands decrease as NPP declines with increasing temperatures. In JSBACH the increases in autotrophic respiration, may be overestimated as the model does not account for temperature acclimatization of autotrophic respiration (Wythers et al., 2005; Tjoelker et al., 2009) nor adjust for complexities of the instantaneous temperature response curve of respiration (Tjoelker et al., 2001). Therefore the nutrient demand may be higher than our simulations suggest. In addition, we can not rule out that we may have underestimated tropical N limitation due to the simplistic representation of N fixation in the model, which does not account for possible negative effects of warming on N fixation in the tropics (Wang and Houlton, 2009). The stocks of soil organic matter decrease at low latitudes releasing nutrients, while at high latitudes the stocks of soil organic matter increase and nutrients get progressively sequestered (see Fig. A.4 in the Appendix). Together, the changes in demand and sequestration of nutrients result in an increase of CO₂-induced nutrient limitation at high latitudes, and a decline in CNL at low latitudes (Fig. 2.5). As a consequence of the decline in tropical CNL, the land C stocks of these regions are nearly the same for all simulations (C, CN, CP, CNP) at the end of our simulations.

At high latitudes, N limitation declines while P limitation stagnates (Fig. 2.5). This shift from N to P limitation is more pronounced in the simulation with PFT-specific C:N:P ratios (CNP_{pft}) (see Fig. A.1 in Appendix), as P demands are higher for temperate and boreal forests due to lower C:P ratios. However it is not known whether these lower C:P ratios merely reflect luxury consumption at present (Agren, 2008); if so the PFT-specific simulations would not differ by so much. Changes

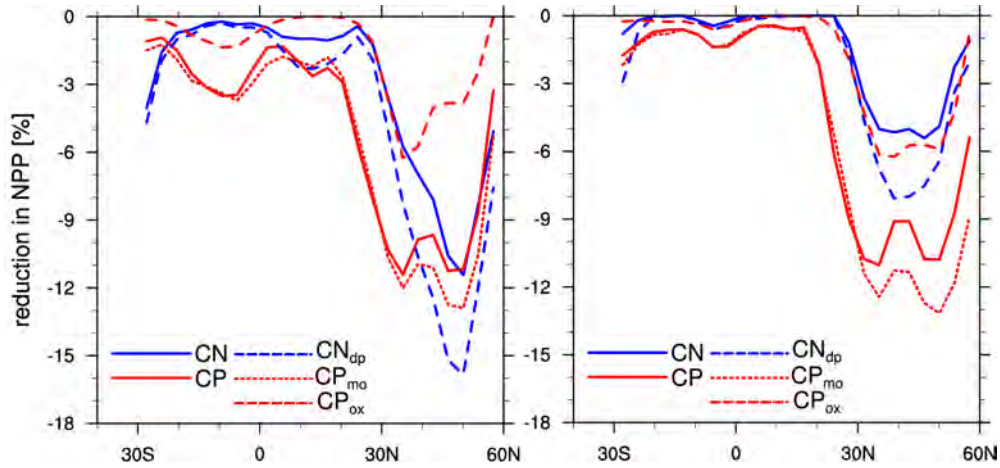


Figure 2.5: Mean reduction of NPP [%] due to CNL (N or P) averaged over 30 yr (2070–2099 (left) and 2320–2349 (right)) as latitudinal means. Solid line are results from the CN and the CP simulation for N and P limitation, respectively. The dashed lines are results from the sensitivity experiments CP_{ox} , CP_{mo} , and CN_{dp} .

in species composition to more P efficient plants, which are not account in our simulations, could also alleviate the increase in P demand. In general, the mechanisms underlying stoichiometric flexibility on all levels (leaf, single plant, ecosystem) are not yet fully understood to account for such flexibility in a comprehensive manner.

In the model, the predominance of P limitation is caused by the low P sorption capacity of temperate and boreal soils. This can be seen in the simulation where all soils have high sorption capacities (CP_{ox}). In this simulation P limitation is comparable in strength to N limitation (Fig. 2.5). The shift is also robust against the assumption of increasing N deposition rates in the future. When N deposition rates are maintained at the present day level during the whole simulation (CN_{dp}), N limitation is still less than P limitation in the CP simulation (Fig. 2.5). We do not account for the increase in substrate availability for mineralization due to the thawing of boreal soils (Anisimov et al., 1997). This may partly counteract a shortage of nutrients at latitudes above 50° N.

In summary, our findings suggest that high latitude ecosystems could become significantly more limited by both N and P in the future as growing seasons expand and soil stocks increase. From a theoretical point of view, a shift from N to P limitation is plausible as the buffer of available P, P adsorbed, gets depleted. However, it is still uncertain how soil C stocks will be affected by climate change, as the temperature dependence of heterotrophic respiration, which is also the main control of nutrient mineralization in JSBACH, is still a major uncertainty in simulating the C and nutrient cycles (Raddatz et al., 2007; Reich, 2010).

2.4 Conclusions

The quantification of P limitation remains challenging because of limited data and process understanding. Our simplistic approach does not account for all synergies between the element cycles. Using data from 34 separate fertilization studies, Marklein and Houlton (2012) found that an increase in N availability may accelerate P cycling via a stimulation of biochemical mineralization. Since the effect has not yet been quantified and the responses varied between plant and microbial mediated mineralization rates, the incorporation of such an interaction in a global model is not feasible at the moment. Moreover, it is commonly assumed that N fixation may be controlled by P availability (Cleveland et al., 1999; Wang et al., 2010). We use an empirical N fixation model which does not represent effects of changing P availability on N fixation, because the regulation mechanisms of N fixation are elusive and recent findings from a long term fertilization experiment reveal that N fixation in an intact tropical forest responded to molybdenum but not to P addition (Barron et al., 2008). Recently, Morford et al. (2011) raised the possibility that bedrock N input, which is omitted in the model, may present an important component of the N cycle. However, it is yet unclear whether this finding can be generalized from two forest sites to global scale ecosystems. Due to our limitation concept, additional nutrients in general increase productivity just in case of CO₂-induced nutrient limitation which is relatively minor at present conditions. Overall, our model may tend to maximize nutrient limitation and actual nutrient limitation may be less than projected.

We identified two processes which critically determine the strength and, to a lesser extent, the global distribution of P limitation: biochemical mineralization and the sorption capacity of soils. Both processes control the shift of P from unavailable forms (P adsorbed and in soil organic matter) to available ones (labile P) and therefore counteract a scarcity of P resulting from an accumulation of P in vegetation and soil organic matter. As both processes are poorly constrained by measurements (Coss and Schlesinger, 1995; Johnson et al., 2003) and changes in soil properties like maximum sorption capacity can not be captured by the empirical sorption model, more basic research on these soil processes is needed to better constrain P cycling.

Even so, our results suggest that models that do not account for P limitation overestimate the land C uptake during the 21st century. The geographic pattern of N and P limitation is to a large extent robust against the assumptions about soil P sorption, biochemical mineralization, CNP ratios, and N deposition. The reduction of tropical NPP by P limitation is in all cases larger than the reduction by N, while a shift from N to P limitation may occur with warming at higher latitudes. The low soil P sorption capacity of temperate soils is responsible for this shift in limitations.

A reduction in the response of NPP to increasing atmospheric CO₂ concentration due to P limitation is expected to weaken the land carbon sink. As a consequence the climate-C cycle feedback (Friedlingstein et al., 2006) increases, leading to a more pronounced warming than projected by C only models. As most climate C cycle models do not account for P limitation, they most probably overestimate tropical C storage potential. This is problematic because tropical regions dominate

the exchange of C between land and atmosphere in observation (Pan et al., 2011) as well as in model projections for the 21st century (Raddatz et al., 2007; Hickler et al., 2008). Therefore, it is important to include the P cycle into global models used for C cycle projections.

2.5 Acknowledgements

We thank Thomas Raddatz, Veronica Gayler and Reiner Schnur for their technical support with JSBACH, Maren Göhler for the short term support regarding latin hypercube sampling, and Soenke Zaehle for his detailed comments on the manuscript. We are also grateful to two anonymous reviewers for their constructive and helpful comments.

Chapter 3

Changes of P release by chemical weathering can be higher than expected.

3.1 Introduction

The release of phosphorus (P) from soil minerals by chemical weathering constrains P availability for biota on a geological time scale. On this time scale the productivity of terrestrial ecosystems is assumed to be limited by the availability of P, as carbon (C) and nitrogen (N) are taken up at much higher rates from the large atmospheric reservoirs than P is released by weathering (Walker and Syers, 1976). P weathering, in general, affects the chemical compositions of ground water, river and lake water, and ultimately, of oceans. It is unclear how P release rates have changed in the past and how these rates may change in the near future.

Presently, terrestrial P availability spans several orders of magnitude (see Figure 2.2). This can be attributed in a first approximation to the weathering state of soils (Walker and Syers, 1976). As soil ages, the P content of the bedrock progressively declines and the soil becomes deeper which can result in a separation of the biological active zone from the bedrock (shielding) (Stallard and Edmond, 1983). Therefore the P availability in young shallow soils is much higher than in old, highly weathered soils. As glaciation periodically resets soil development, P limited ecosystems are commonly found in tropics where low land glaciations were absent for millions of years. In general, thick soils develop where chemical erosion exceeds physical erosion. Other than glaciations, low tectonic uplift and thus low physical erosion favors deep soils, for example at the Amazon basin (Buendía et al., 2010). For instance Raymo et al. (1988) hypothesized a control of mountain uplift on chemical weathering rates in general. In addition to the absence of glaciations and low uplift rates, aging of soils is intensified at low latitudes, because weathering is the more intense the wetter the environment. This is attributed to a rate limitation of the weathering reaction itself by the removal of weathering products via water flow.

Besides lithology, runoff and physical erosion, key factors controlling chemical weathering are: temperature, morphology, soil, ecosystem, land use as well as plate tectonics (see references in Hartmann and Moosdorf (2011)). Temperature is an important factor controlling weathering rates in laboratory experiments (e. g. Brady and Carroll, 1994; White et al., 1999). The tempera-

ture control may also hold true for the total available reaction volume of a catchment (Hartmann and Moosdorf, 2011), but measurements on the temperature control in the field are scarce. The standard tools to quantify the environmental constraints on weathering at catchment scale are regression models. Regression models, in general, are not designed to investigate the mechanisms underlying a certain process, but to reliably predict the dynamics of the process using correlations with observed quantities. As temperature correlates with other factors (e.g. runoff), the temperature control on weathering is difficult to be investigated using such models. For the same reasoning, the biological control of weathering is uncertain. Biological activity acts indirectly on weathering rates via its effect on physical erosion, and the physical and chemical soil environment (for example acidity, porosity, hydration, perturbation, etc) (Drever, 1994), as well as direct via targeted root growth and the mining of elements by soil microbes (Banfield et al., 1999). It is clear that biological processes can enhance weathering (Banfield et al., 1999), but to what extent weathering is controlled by biological activity is under debate. As all energy used in biological processes originates in the first place from photosynthesis, changes in plant productivity are likely to have an influence on weathering rates. Feedbacks between terrestrial productivity and weathering are used to explain the resilience of concentrations of atmospheric CO₂ (Pagani et al., 2009) and O₂ (Lenton, 2001) of the geological past.

Besides terrestrial productivity, the productivity of aquatic and marine systems is constrained by P release too (Elser et al., 2007). Although present P cycling is greatly enhanced by P mining/fertilizer application (Smil, 2000), natural weathering rates are still of great importance in determining coastal export of dissolved inorganic P (DIP), especially in tropical and high latitude regions (Harrison, 2005). Only a small fraction of P enters the ocean as DIP (1.5 Mt yr⁻¹ as DIP (including human sources) compared to 20 Mt yr⁻¹ as total P (Meybeck, 1982)). However, whereas all of the DIP is generally thought of being available to biota, significant portions of organic and particulate P are not available to biota (Bradford and Peters, 1987).

Currently, we experience a time when CO₂ concentrations are unprecedented during the last 2 millions years and projected to increase at a rate unseen in the geological past. Significant changes in temperature and the hydrological cycle are observed and these changes are expected to continue at an even faster rate. Terrestrial productivity is expected to increase due to the increasing CO₂ concentrations resulting in an increasing demand of P which may result in a shortage of P (see chapter 2). There is a complete lack of information on how P release rates may change in the next 100 years. Recently, Hartmann and Moosdorf (2011) developed a model of P release which accounts for lithology, runoff and temperature as controls of P release. To give a first approximation of future P release we apply an enhanced version of the P weathering model by Hartmann and Moosdorf (2011) driven by climate projections performed under the framework of CMIP5 (Hurrell and Visbeck, 2011).

3.2 Methods

3.2.1 Model of P release

We used an empirical model of P release by (Hartmann and Moosdorf, 2011; Hartmann et al., 2012) which is based on a silicate weathering model assuming that P is released at the same rate as the bulk of minerals is dissolved. The P released by chemical weathering (P_r) is calculated as

$$P_r = \alpha f(T)qs \quad (3.1)$$

where q is the sum of surface runoff and drainage, α the weathering factor, s the factor for soil shielding, and $f(T)$ a term to describe the Arrhenius type temperature dependence of P release.

$$f(T) = e^{\frac{E_a}{R}(\frac{1}{T_{ref}} - \frac{1}{T})} \quad (3.2)$$

where E_a is the activation energy, R the gas constant, T_{ref} the reference temperature and T the 2 m air temperature. The parameter α depends on the site-specific lithological composition and was originally calibrated and validated by Hartmann and Moosdorf (2011) using observational data on runoff and temperature as well as lithological maps. The here used version of the P weathering model was recalibrated as described in Hartmann et al. (2012) using more comprehensive data on geochemical composition and a refined classification of soil types. The soil shielding factor s was introduced to reduce the model data mismatch for deeply weathered soils. E_a is derived from a compilation of data from several publications on the dependence of chemical weathering on temperature under field conditions (Hartmann and Moosdorf, 2011). The parameters α , E_a and s are read in from global maps to allow a spatial-explicit application of the model.

Table 3.1: Variables of the P release model.

Acronym	Description	units
P_r	P released by chemical weathering	[g (P) m ⁻² yr ⁻¹]
q	surface runoff and drainage	[10 ³ g (H ₂ O) m ⁻² yr ⁻¹]
T_{ref}	reference temperature	[K]
T	annual mean 2m air temperature	[K]
E_a	activation energy	[J mol ⁻¹]
α	weathering factor	[g (P) 10 ³ g ⁻¹ (H ₂ O)]
s	soil shielding factor	[]
R	gas constant	[J K ⁻¹ mol ⁻¹]

3.2.2 Climatic forcing

The empirical model of P release is driven by the annual sum of surface runoff and drainage (SAR) and the annual mean 2 m air temperature (MAT). We derived the climatic forcing from existing

ESM simulations which have been performed under the framework of CMIP5 (Hurrell and Visbeck, 2011). These simulations span the historical period (1850–2005) as well as a projection period (2006–2099). According to the CMIP5 protocol, the ESMs had been forced with observed CO₂ concentrations for the historical period and afterwards with concentrations projected for a given representative concentration pathway (RCP) (in this study: RCP8.5). For our study we selected simulations from the following ESMs: CCSM4, MIROC-ESM, IPSL-CM5A-LR, and MPI-ESM-LR (Table 3.2). For each model, except the MIROC-ESM, a set of three simulations (ensemble) exists for the whole time period. In the case of the MIROC-ESM, only a single simulation had been performed for the future (2005–2099). As the different ESM simulations have been done in different resolutions, we reprojected them all on a T63 grid, which corresponds to a grid spacing of approximately 140×120 km at mid latitudes. It was assured that the land area is in all ESM simulation the same.

Table 3.2: List of ESM used in this study. The data is provided by the CMIP5 project.

Model	Group
MPI-ESM-LR	Max Planck Institute for Meteorology
IPSL-CM5A-LR	Institut Pierre-Simon Laplace
MIROC-ESM	Japan Agency for Marine-Earth Science and Technology, Atmosphere and Ocean Research Institute (The University of Tokyo), and National Institute for Environmental Studies
CCSM4	National Center for Atmospheric Research

3.2.3 Simulations

Using each of the climate forcings we derived 4×3 time series of P release. To disentangle the effect of warming on P release from the effect of runoff changes, we performed additional calculations in which we kept T fixed on the preindustrial level. We account for climate variability by using a repeating loop of the years 1850–1879 for the whole time period. As the calibration of the activation energy E_a of the temperature response function is uncertain, we performed also simulations in which we varied E_a by $\pm 20,000 \text{ J mol}^{-1}$ to quantify the uncertainty of the temperature dependence. This range is about twice as wide as the range of E_a identified from a compilation of weathering studies on catchment scale (Hartmann, personal communication). We use a wider range as observed as the field data is rather restricted and laboratory experiments indicate an average range of E_a between 50,000–80,000 J mol^{-1} (White et al., 1999). The specifications of the four sets of simulations are given in Table 3.3.

Table 3.3: Simulations specifications. For both forcing variables, q and T , the respective time period used during the whole simulation duration (249 yr) is given and also the values used for the parameter E_a .

Simulation	q	T	E_a
1	1850–2099	1850–2099	std (Hartmann and Moosdorf, 2011)
2	1850–2099	1850–1879	std (Hartmann and Moosdorf, 2011)
3	1850–2099	1850–2099	– 20 kJ mol ⁻¹
4	1850–2099	1850–2099	+ 20 kJ mol ⁻¹

3.3 Results & Discussion

3.3.1 Present day

The climatic forcing shows a strong variability. Simulated MAT over land and global SAR vary strongly among the four ESMs (Figure 3.1) and deviate significantly from observation based estimates. Based on a recent compilation of 16 preexisting data archives, present day MAT over land is estimated 9.760 ± 0.041 °C (2000–2009) (Berkeley Earth). Except of the MIROC-ESM, the models underestimate present day land temperature (up to 1.5 °C in the case of the IPSL-ESM-LR). Based on a global compilation of river discharge data, present day global SAR is estimated $38,320 \text{ km}^3 \text{ yr}^{-1}$ (Fekete, 2002). The simulated global SARs range from 29,500 to 41,500 $\text{km}^3 \text{ yr}^{-1}$.

Due to significant differences in the climatic forcings, the P release rates for present day differ, too (Figure 3.1). The P release is for all ESM simulations about 50% less than the 1.6 Mt yr^{-1} estimated by Hartmann and Moosdorf (2011) using the same P release model but with observational data and on a much higher resolution. The consistent underestimation of the P release in our simulations may be attributed to the loss of regions of extremely high weathering (hotspots) due to the low resolution. The importance of weathering hotspots regarding the quantification of the silicate weathering was stressed by Hartmann et al. (2009). They reported that 3.5% (9%) of the total exorheic area are responsible for 30% (50%) of the global weathering flux, In the case of P release the contribution of hotspots to the global flux is even higher (Hartmann, personal communication). In addition, the land area of the Indonesian Archipelago, a hotspot region, is underestimated in the model due to the rather low resolution.

The uncertainty due to the parameterization of the temperature response function is large as approximated by the simulations in which E_a was varied by 20 kJ mol^{-1} (error bars in Figure 3.1). Here, more research is needed to better constrain the temperature control on weathering.

The spatial pattern of P release differs to some extent among the different climate simulations (Figure 3.2). A consistent feature is the high release rates at low latitudes and high altitudes, like Andes, Central America, Rocky Mountains, Eastern North America, Himalaya, South-East Asia, Western Central Africa and Western Europe. These are regions with a relatively high α , when averaged over regions Central America and Western Europe have the largest values for α , and/or

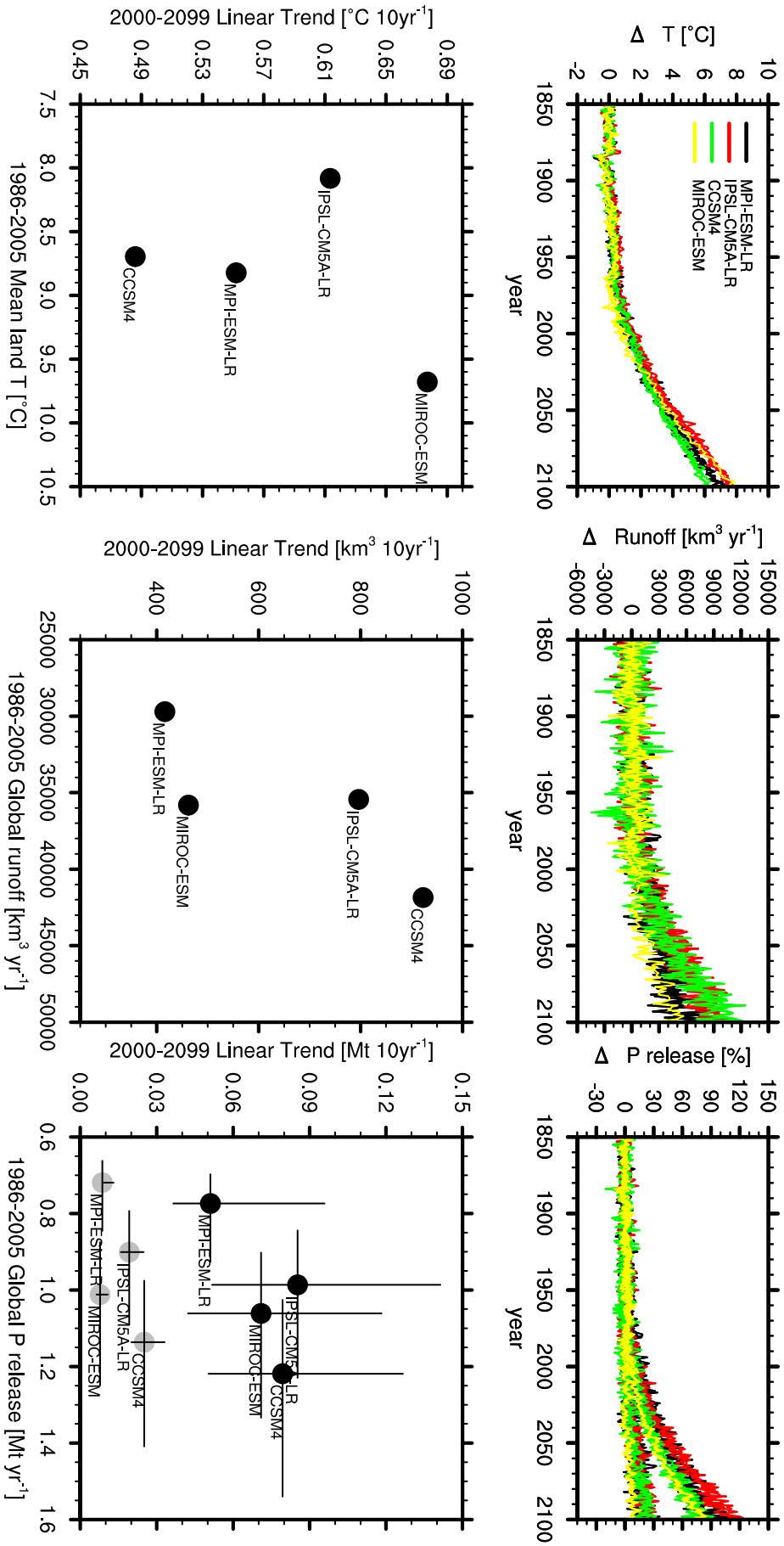


Figure 3.1: The anomalies in MAT over land (left), global SAR (center), and in P release (right) using 4 different climate forcings (1850–2100). The top panel show the temporal evolutions and lower panels the present day state and the linear trend during the projection period. In the case of P release, the results from simulation 1 with (black) and simulation 2 without warming (grey) are shown. The uncertainty bars are constrained by the simulations 3 and 4 with perturbed parameterization of the activation energy.

intense runoff.

3.3.2 Future

During the 21st century, MAT drastically increases in all forcing simulations (Figure 3.1). Depending on the ESM global MAT increases between 6 and 8 °C. Also runoff rates increase. As a result, the P release increases whereby warming has a more profound effect on release rates than changes in runoff (Figure 3.1). Changes in runoff enhances release rates by less than 25%, whereas the P release increases more than 80% when the effect of temperature on weathering is additionally accounted for. The importance of temperature is highlighted by the finding that even for the lowest temperature sensitivity the changes in P release rates are dominated by temperature. As a result, the large uncertainties in the global release rates are caused by the uncertainties in the quantification of the activation energy (Eq.(3.2)). Differences in the projected climate among the 4 ESMs contribute to a lesser extent to the uncertainty in the projected global P release.

The spatial changes in P release during the 21st century vary strongly among the models (Figure 3.3). This can be attributed to differences in the projected runoff among models, as the temperature effects are only positive and the pattern is consistent among the models (not shown). A consistent pattern is the increase in P release at high latitudes (>45°N), Central Africa, SE-Asia and the Amazon basin. The extent of the increase is strongly model dependent, for example, at the Amazon basin the P release increases between 30–80% (CCSM4 and IPSL-ESM-LR).

3.3.3 Implications of the strong increase in P weathering

The fate of additional P due to enhanced weathering is elusive. On a time scale of years to centuries, it could be incorporated into biomass, adsorbed onto soil particles or enter riverine systems. Finally, on a centennial to millennial time scale, it will end up in the ocean. Ecosystems react sensitive to P addition, irrespectively if the systems are terrestrial, aquatic or marine ones (Elser et al., 2007). As discussed in the previous chapter, land C uptake during the 21st century could be enhanced by increasing P availability. In the simulation analysed in chapter 2, natural loss rates to riverine systems decrease drastically during the 21st century. The reduction in loss rates is caused by lowered levels of inorganic P due to increased rates of immobilization and plant uptake (Chapter 2). It is therefore likely that the major part of the additionally released P will be incorporated into terrestrial biomass before it enters aquatic and marine systems.

As a first approximation to constrain the potential to store additional biomass, one can use the C:P ratio of the most P-extensive (high C:P ratio) storage tissue (wood, C:P = 1500) and the most P-intensive (low C:P ratio) one (soil organic matter, C:P = 50) (see Table A.1). When all of the P which is projected to become available due to climate change is used for the built-up of wood, land C uptake could be increased by 75 Gt from 1860 to 2100 (RCP8.5 scenario). In the case of storage in soil organic matter, the additional C uptake is with 2 Gt negligible. To refine the estimate one can use the ratio between vegetation P uptake and soil P immobilization from the results of chapter 2,

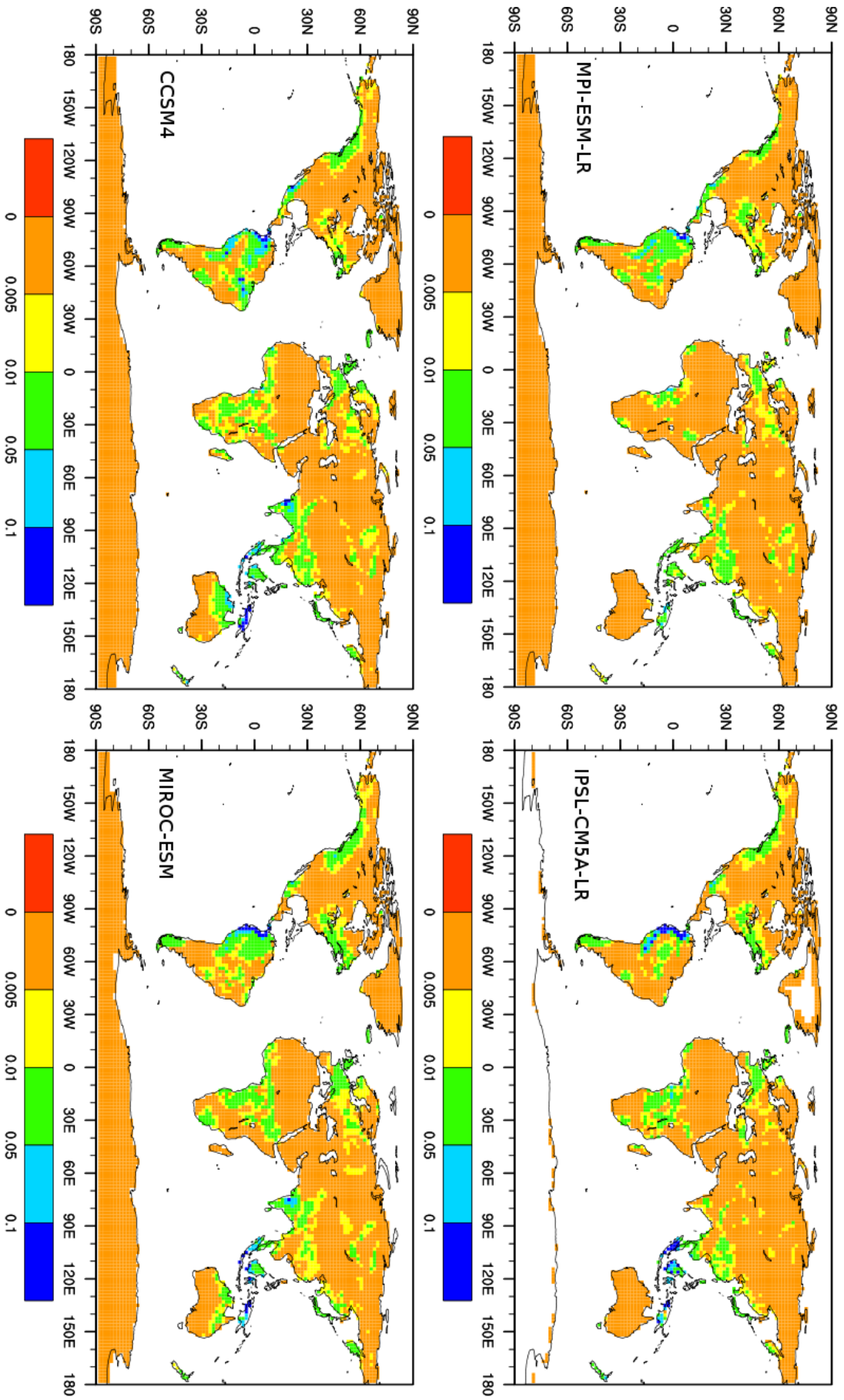


Figure 3.2: Present day P release for four different ESM models. Shown are the mean rates (1980–2009) over the whole ensemble (3).

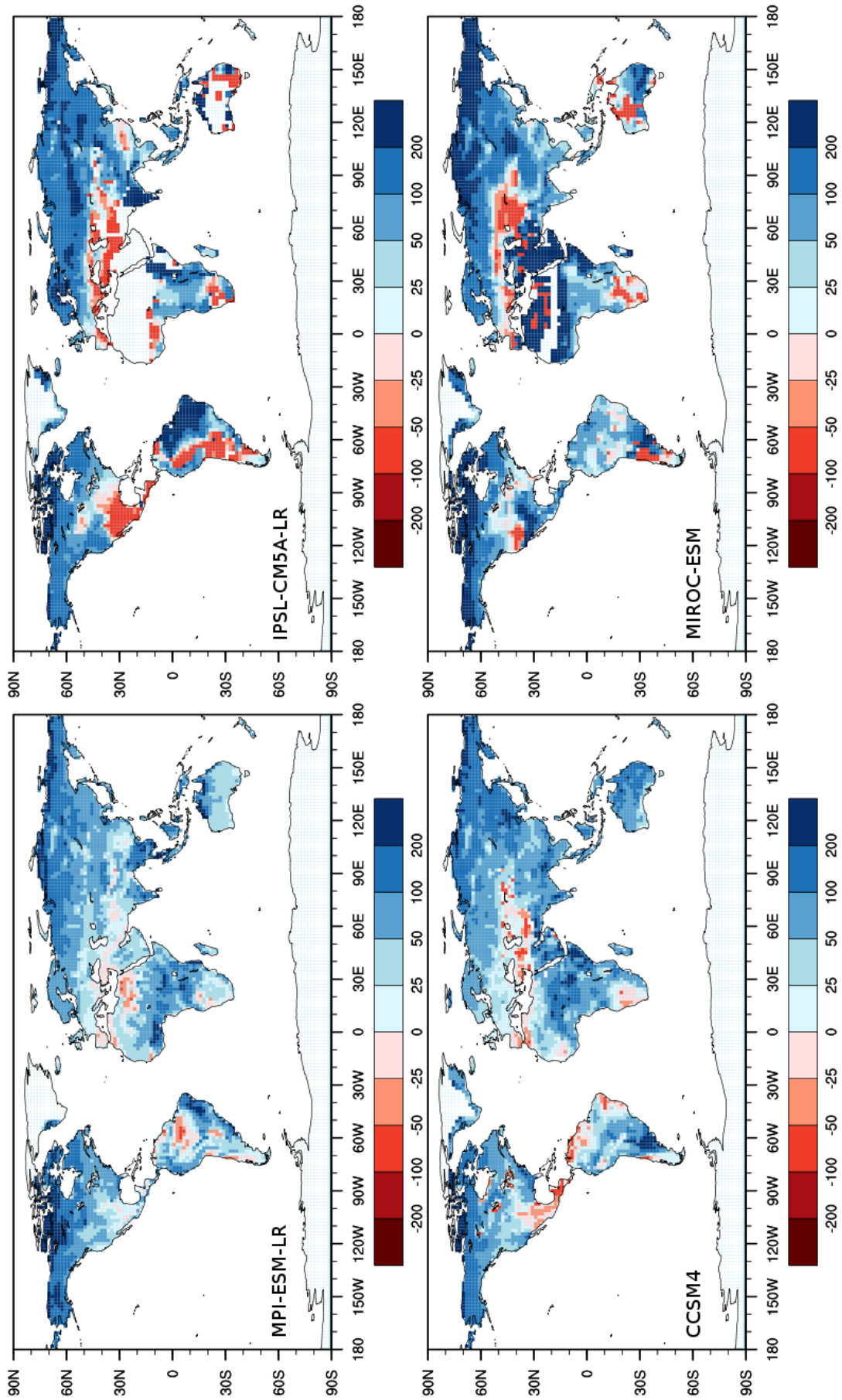


Figure 3.3: The change of P release at the end of the 21st century relative to present day. Shown are the relative differences between the mean rates for 2090–2099 and 1990–1999 averaged over the ensemble.

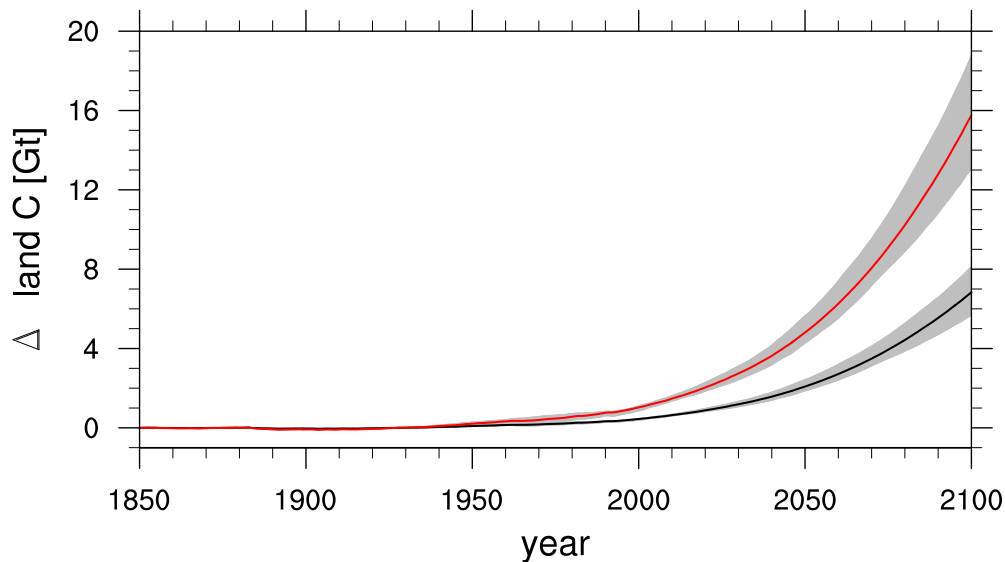


Figure 3.4: The theoretical range of possible C uptake due to the increasing P release rates. Shown is the mean over all simulations (solid line) as well as the range between maxima and minima. The upper curve (red) is based on the assumption that all P taken up by vegetation is used for woody tissue and the lower (black) curve on the assumption all P taken up is used for physiological active tissue.

which is 0.25. Using this ratio, the additional C sequestration is between 13 and 19 Gt depending on the climatic forcing (Figure 3.4, red line). Assuming all P taken up by vegetation is used for the built-up of physiological active tissue (C:P = 500) the C storage potential is reduced to 5.5–8 Gt (Figure 3.4, black line). Global model not accounting for changes in P availability project a terrestrial C uptake during the 21st of more than 300 Gt (Denman et al., 2007). Despite the large uncertainties, this simple calculation shows that changes in P release may have significant, yet likely moderate, effects on the C balance of terrestrial systems on a decadal time scale.

3.3.4 Limitations of the modelling approach

The weathering model does not account explicitly for any biological control of weathering and for a possible inhibition of P release by a saturation of soil water in respect to dissolved P. The influence of biota is implicitly accounted for, as productivity correlates with the climatic variables, runoff and temperature (Hartmann and Moosdorf, 2011). As long as the correlation between productivity and the physical environment does not change, the implicit representation of biota is sufficient. But we cannot rule out that such empirical correlations change, as the CO₂ concentration is projected to rise with a rate unseen in the geological past. Even under present conditions, the CO₂ concentration affects runoff rates due to a reduced transpiration of vegetation (Gedney et al., 2006). In general, the application of empirical models under conditions of strong changes are problematic, but the use of such models is unavoidable when alternatives are missing.

The likelihood of a saturation of soil water in respect to P due to a intensified P release is hard to judge. The concentration of P in soil water not only depends on the source strength but also on the strength of sinks, namely adsorption and immobilization by biota. While the first can be estimated

using models of adsorption, like the one used in chapter 2, the latter is hard to constrain. Root uptake and microbial activity is highly variable on a daily, annual or interannual basis. How root uptake is controlled and may change in future is also poorly understood. There remains a need to develop mechanistic models of P release, considering biological processes, like root uptake and organic P mineralization, and soil processes, like sorption, to assess changes in the availability P for biota in a more reliable manner. Such kind of models have been developed for chemical weathering in general on local and regional scale (Godderis et al., 2009), but these models lack a representation for the P release.

3.4 Conclusions

The P release by chemical weathering is expected to increase under warmer climatic conditions and may increase P availability in ecosystems. To quantify the changes in P release in a changing climate, we applied an empirical model of P weathering using CMIP5 projections of climate change for the 21st century under the RCP8.5 scenario. The empirical model accounts for spatial differences in lithological P concentrations, shielding effects, and changes in temperature and runoff as main factors controlling P release.

The simulations show that global P release could double by 2100; in absolute terms an increase in P release by 0.5 to 0.9 Mt yr⁻¹. Increasing temperatures are mainly responsible for the increase in P release, while changes in runoff are of secondary importance, contributing between 20–30% to the overall increase. This finding is contrary to the common assumption that chemical weathering is dominantly controlled by runoff and lithology (Gaillardet et al., 1999).

The increase in P availability due to enhanced weathering could partly offset the P limitation of terrestrial productivity explored in chapter 2. The best guess estimate lies between 5.5 and 19 Gt, which would reduce the reduction of land C uptake during the 21st century by P limitation as estimated in chapter 2 by 6 to 22%. In all these calculation it is assumed that P losses do not change and that all additional P is used for the built up of organic matter. Therefore the effect on C uptake is maximized.

Our results are the first quantitative estimate of changes in P availability due to climate change induced changes in chemical weathering. As the weathering model is rather simple and climate models vary substantial in the projected climate, these results must be considered as highly uncertain. This study illustrates that the temperature dependence of weathering can have profound effects on the dynamics of weathering. More research in the quantification of the weathering response to temperature changes under different environmental conditions is needed to confirm our results. We also did not account for biological enhancement of weathering due to increasing biological productivity. Secondly, the fate of the additional P—whether it will be used by ecosystems, and in which form—is elusive thus its effect on the C cycle is hard to constrain. Here we explored only a maximum/minimum range of possible C sequestration.

In summary, we have showed that climate change, in particular warming, may have profound

effects on P weathering, but further research on the processes controlling P release is needed to constrain the changes in C and P cycling.

3.5 Acknowledgements

We acknowledge the World Climate Research Programme's Working Group on Coupled Modelling, which is responsible for CMIP, and we thank the climate modeling groups (listed in Table 3.2) for producing and making available their model output. For CMIP the U.S. Department of Energy's Program for Climate Model Diagnosis and Intercomparison provides coordinating support and led development of software infrastructure in partnership with the Global Organization for Earth System Science Portals.

Chapter 4

Temperature acclimation of photosynthesis has a minor impact on present and future productivity.

4.1 Introduction

The productivity of terrestrial plants controls food supply and influences the dynamics of atmospheric CO₂. It is therefore crucial to understand and quantify productivity and to project its future response to climate change and increasing atmospheric CO₂ concentrations. For such a task, comprehensive Earth System Models (ESM) are suitable tools as they aim to account for all of the relevant processes in the earth system. As these models get increasingly more complex it is important to steadily evaluate subprocesses regarding current advances in process understanding. Recently, using an ESM, Booth et al. (2012) pointed to the temperature dependence of photosynthesis as the most important uncertainty of the climate-carbon cycle feedback.

Photosynthesis in ESMs is typically based on the Farquhar model (Farquhar et al., 1980). In this model, leaf level photosynthesis is assumed to be limited either by the maximum Rubisco carboxylation rate (V_{max}) or the maximum RubiscoBiPhosphate (RuBP) regeneration rate (J_{max}). Both biochemical processes are temperature dependent. Gross photosynthesis is small at low temperatures, rises to a maximum rate at optimal temperature and then decreases at very high temperatures. The decline at high temperatures may be related to reduced enzyme activity, in particular of Rubisco (Crafts-Brandner and Salvucci, 2000), or to temperature induced changes in the permeability of cell membranes. The common approach to describe the dependence of J_{max} and V_{max} on temperature use Arrhenius or Q_{10} equations for enzyme kinetics (Harley et al., 1992; Medlyn et al., 2002; Knorr, 2000). The parameterization of such an instantaneous temperature dependence result in quite different light-saturated photosynthesis rates at temperatures above 40 °C (compare solid lines in Fig. 4.1), which may have profound effects when models are used in scenarios of global warming.

Recent warming experiments illustrate a high variability in the photosynthetic response to elevated temperatures (see references in (Lin et al., 2012)). Part of this variability in the temperature

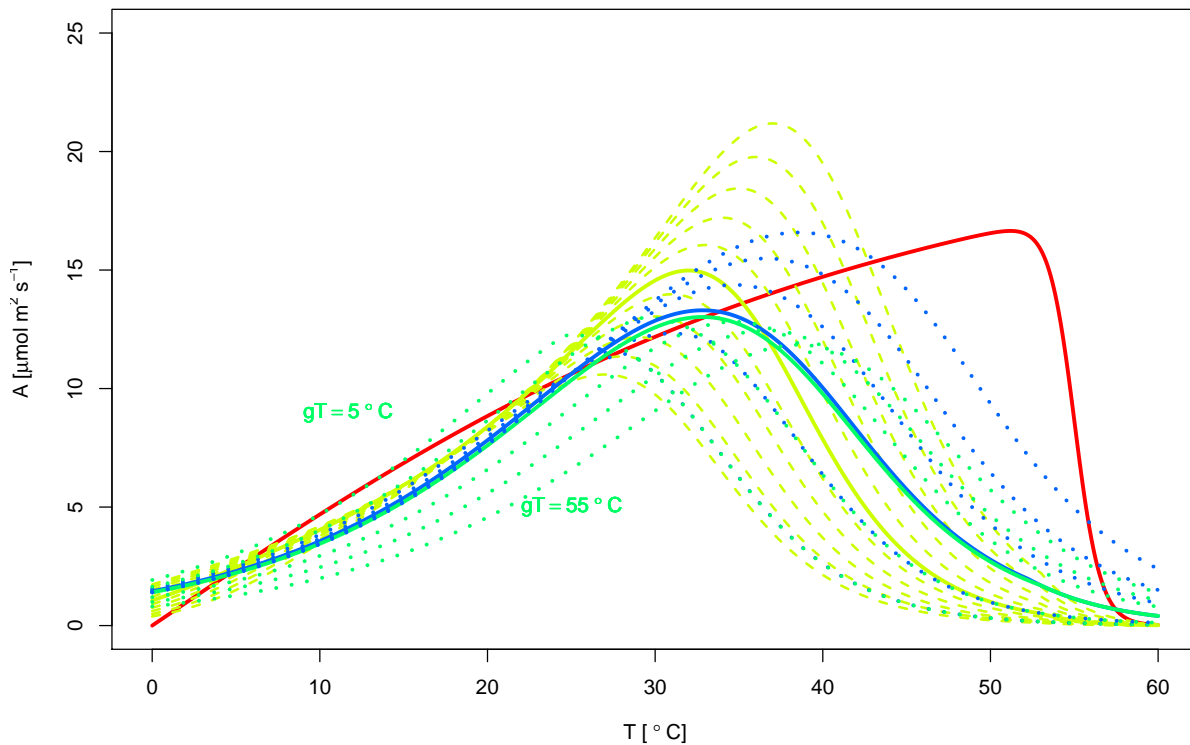


Figure 4.1: Gross CO₂ uptake per leaf area (A) at high irradiance (1500 mol(photons), 360 $\mu\text{mol}(\text{CO}_2) \text{mol}^{-1}(\text{air})$ and 0.21 $\text{mol}(\text{O}_2) \text{mol}^{-1}(\text{air})$). Shown are calculations with the Farquhar model using different temperature dependences of J_{max} and V_{max} . Knorr (2000) (red), Booth et al. (2012) (yellow) and Kattge and Knorr (2007) with rigid and flexible $r_{V,J}$ (blue and green). In the case of Kattge and Knorr (2007), the bold lines shows A at a growth temperature (gT) of 25 °C, while the dotted lines show A for gT between 5 and 55 °C. In the case of Booth et al. (2012) the bold lines show A at standard optimum temperature for broadleaf trees of 32 °C, while the broken lines show A for optimum temperature between 27 to 37 °C. Note that in the study by Booth et al. (2012) the optimum temperature was not treated dynamically (did not depend on prevailing temperatures), but was varied among a set of simulations.

response can be attributed to short to mid-term changes at the organismal level (acclimation). The acclimation of photosynthesis may result from adjustments of stomatal or respiratory processes (Lin et al., 2012), but it is most likely caused by changes in biochemical processes (Medlyn et al., 2002): changes in the heat tolerance of enzymes (Berry and Bjorkman, 1980; Hikosaka et al., 2006) or changes in the expression or activity of Calvin cycle enzymes (Stitt and Hurry, 2002). Such biochemical adjustments alter the temperature response of V_{max} and J_{max} (June et al., 2004; Onoda et al., 2005; Hikosaka et al., 2006; Kattge and Knorr, 2007). Kattge and Knorr (2007) developed a general formulation of the temperature dependence and acclimation of V_{max} and J_{max} on data for 36 plant species, spanning a wide range of plant functional types, including deciduous trees, coniferous trees, shrubs, and herbaceous species. In this formulation, the optimum temperature of V_{max} and J_{max} increases by 0.44 °C and 0.33 °C, respectively, per 1 °C increase of growth temperature (Kattge and Knorr, 2007). Although being moderate the temperature acclimation is

sufficient to double modeled photosynthesis at 40 °C, if plants are grown at 25 °C instead of 17 °C.

How global productivity is affected by temperature acclimation is unclear. From varying optimum temperature of photosynthesis, Booth et al. (2012) concluded that acclimation can have profound effects on the C balance of terrestrial ecosystems. However, the approach which had been taken by Booth et al. (2012) is problematic. Acclimation (dynamical changes in the optimum temperature to prevailing temperatures) was not taken into account explicitly. In their study the temperature dependence was treated rigidly in the model and the optimum temperature was varied among a set of simulations. In addition, in their photosynthesis formulation the maximal photosynthesis rate increases more strongly with increasing optimum temperature (yellow line in Figure 4.1), than in the temperature photosynthesis formulation derived from data (Kattge and Knorr, 2007) (blue and green lines in Figure 4.1). Therefore the approach taken by Booth et al. (2012) most likely overestimates the influence of acclimative changes in the optimum temperature on photosynthesis. Bearing in mind, that under natural conditions irradiance is suboptimal and other factors than temperature constrain photosynthesis, for example water availability, the effect of temperature acclimation as suggested by figure 4.1 may actually be less pronounced. The only study, known to the authors, which accounts explicitly for acclimation in a global model is by Friend (2010) and only a minor effect of acclimation on global fluxes was reported. In his study the formulation for the acclimation of the electron transport by June et al. (2004) was used, which was derived from measurements on a single plant species. The global applicability of the formulation by June et al. (2004) is questionable as the acclimative strength differs strongly among species (Berry and Bjorkman, 1980).

To quantify the effect of temperature acclimation of photosynthesis on global productivity, we implemented the formulations for temperature acclimation of V_{max} and J_{max} by Kattge and Knorr (2007) into the Max Planck Institute Earth System Model (MPI-ESM) and applied the model under present climatic conditions and under conditions of strong warming. In addition, we assessed how the effect of temperature acclimation on productivity is related to changes in productivity caused by the choice of the instantaneous temperature dependence, by performing simulations with two different kind of instantaneous temperature dependences (Knorr, 2000; Kattge and Knorr, 2007).

4.2 Model & experiments

We modified the land surface scheme of the MPI-ESM, JSBACH. The representation of photosynthesis in JSBACH (Knorr, 2000) is based on the Farquhar model (Farquhar et al., 1980). The temperature dependences of V_{max} and J_{max} have a sharp linear cut off at high temperatures (red curve Figure 4.1) and was originally developed and parameterized for C₄ plants (Collatz et al., 1992). We implemented a second formulation by Kattge and Knorr (2007) for these temperature dependences. This new formulation has a more gradual decline of photosynthesis at high temperatures (green/blue curves Figure 4.1). In addition, temperature acclimation is accounted for. The modified model can be used with either of the two formulations. Furthermore, the growth

temperature in the new formulation can be artificially fixed to 25 °C to disable temperature acclimation. This allows to quantify separately (i) the effect of acclimation and (ii) the effect of the two different temperature dependences of V_{max} and J_{max} independent of acclimation.

4.2.1 Model description

4.2.1.1 General photosynthesis

The implementation of photosynthesis in JSBACH originates from the BETHY model (Knorr, 2000). Gross leaf CO₂ uptake on leaf area basis, A , is calculated according to Farquhar et al. (1980) as

$$A = \min(J_C, J_E), \quad (4.1)$$

where J_C is the rate of photosynthesis when Rubisco activity is limiting photosynthesis and J_E the rate when electron transport is limiting. By subtracting the so called *dark respiration* (R_d), the non photorespiratory respiration in daylight, net CO₂ uptake is derived. Photosynthesis limited by Rubisco activity is calculated as

$$J_C = V_{max} \frac{c_i - \Gamma_*}{c_i + K_C(1 + O_i/K_O)}. \quad (4.2)$$

where V_{max} is the maximum carboxylation rate, c_i and O_i are the leaf internal CO₂ and O₂ concentrations, Γ_* is the so called CO₂ compensation point in the absence of mitochondrial respiration, and K_C and K_O are Michaelis-Menten constants parameterizing the dependence on CO₂ and O₂ concentrations. Photosynthesis limited by electron transport is calculated as

$$J_E = J(I) \frac{c_i - \Gamma_*}{4(c_i + 2\Gamma_*)} \quad (4.3)$$

with

$$J(I) = J_{max} \frac{\alpha I}{\sqrt{J_{max}^2 + \alpha^2 I^2}}. \quad (4.4)$$

where I is the photosynthetic active radiation, J_{max} the maximum electron transport rate, and α the quantum efficiency for photon capture.

In the Farquhar model, the Michaelis-Menten constants for the enzyme kinetics of Rubisco have an Arrhenius type temperature dependence (Farquhar et al., 1980)

$$K_C = K_C^{25} \exp\left(\left(\frac{T}{T_{ref,K}} - 1\right) \frac{E_C}{RT}\right) \quad (4.5)$$

$$K_O = K_O^{25} \exp\left(\left(\frac{T}{T_{ref,K}} - 1\right) \frac{E_O}{RT}\right), \quad (4.6)$$

where $K_{C,0}^{25}$ and $K_{O,0}^{25}$ are the respective Michaelis-Menten constants at 25 °C, E_C and E_O are the associated activation energies, R is the gas constant, T the temperature in K, and $T_{ref,K}$ the

reference temperature in K.

4.2.1.2 Standard temperature dependence of V_{max} and J_{max} (Knorr, 2000)

In the standard JSBACH, the temperature dependence of the maximum carboxylation rate is of Arrhenius type (Farquhar et al., 1980):

$$V_{max} = V_{max}^{25} f(T) \exp\left(\left(\frac{T}{T_{ref,K}} - 1\right) \frac{E_V}{RT}\right), \quad (4.7)$$

with V_{max}^{25} as the reference value at 25 °C and E_V as the associated activation energy. Following Collatz et al. (1992) the additional function

$$f(T) = 1/(1 + e^{1.3(T-328K)}) \quad (4.8)$$

accounts for inhibition of the biochemical processes at high temperatures outside the validity range of the Farquhar model: $f(T)$ assumes values between 0 and 1 with a sharp decrease from 1 to 0 around 55 °C.

Following once more Farquhar et al. (1980), the temperature dependence of maximum electron transport rate is

$$J_{max} = J_{max}^{25} f(T) \frac{T_C}{T_{ref,C}} \quad (T_C \text{ is } T \text{ in } ^\circ\text{C} \text{ instead of K}), \quad (4.9)$$

where J_{max}^{25} is the reference value at 25 °C, $T_{ref,C}$ is the reference temperature in °C, and the function $f(T)$ is the high temperature inhibition function (Equation 4.8).

4.2.1.3 New formulation (Kattge and Knorr, 2007)

In Kattge and Knorr (2007), the linear temperature dependence of J_{max} is changed to an Arrhenius type behavior:

$$J_{max} = J_{max}^{25} g(T, T_G) \exp\left(\left(\frac{T}{T_{ref,K}} - 1\right) \frac{E_V}{RT}\right), \quad (4.10)$$

Here, the function $g(T, T_G)$ is introduced to account for dependence of J_{max}^{25} on instantaneous leaf temperature (T) and growth temperature (T_G). We use a 30 day or 7 day running mean of surface air temperature as growth temperature. The introduction of the temperature dependence function $h(T, T_G)$ makes the heat inhibition function $f(T)$ redundant.

$$V_{max} = V_{max}^{25} h(T, T_G) \exp\left(\left(\frac{T}{T_{ref,K}} - 1\right) \frac{E_V}{RT}\right). \quad (4.11)$$

The temperature dependent functions $g(T, T_G)$ and $h(T, T_G)$ are given as

$$g(T, T_G) = \frac{1 + \exp\left(\frac{T_{ref,K}(a_{\Delta S,J} + b_{\Delta S,J}T_G - E_d)}{T_{ref,K}R}\right)}{1 + \exp\left(\frac{T(a_{\Delta S,J} + b_{\Delta S,J}T_G - E_d)}{TR}\right)}, \quad (4.12)$$

$$h(T, T_G) = \frac{1 + \exp\left(\frac{T_{ref,K}(a_{\Delta S,V} + b_{\Delta S,V}T_G - E_d)}{T_{ref,K}R}\right)}{1 + \exp\left(\frac{T(a_{\Delta S,V} + b_{\Delta S,V}T_G - E_d)}{TR}\right)}, \quad (4.13)$$

where $a_{\Delta S,V}$ and $b_{\Delta S,V}$ are the intercept and slope of the linear dependence of V_{max}^{25} on T_G (Kattge and Knorr, 2007). Accordingly, $a_{\Delta S,J}$ and $b_{\Delta S,J}$ are the parameters for the dependence of J_{max}^{25} on T_G . E_d is the deactivation energy and is set to 200 kJ mol^{-1} . To prevent acclimation of photosynthesis to temperature below 5°C the minimum value of T_G is set to 5°C .

Kattge and Knorr (2007) also found that the ratio $r_{V,J} = \frac{V_{max}^{25}}{J_{max}^{25}}$ varies with T_G . To account for this J_{max}^{25} in eq. (4.10) is replaced by

$$J_{max}^{25}(T_G) = (a_{rJ,V} + b_{rJ,V}T_G)V_{max}^{25} \quad (4.14)$$

4.2.1.4 Parameterization of frost inhibition

The temperature dependence of Kattge and Knorr (2007) predicts photosynthesis rates below 0°C (Figure 4.1), even when acclimation is restricted to temperature above 5°C . To account for frost inhibition we linearly scale V_{max} and J_{max} by introducing an additional factor F_{fr} in the equations (4.10) and (4.11). The factor F_{fr} is chosen to develop with time according to

$$F_{fr}^{t+1} = \begin{cases} \max(0, F_{fr}^t - \frac{\Delta t}{T_{ref}}) & \text{if } T_d \leq 0.0^\circ\text{C} \\ \min(1, F_{fr}^t + \frac{\Delta t}{T_{ref}}) & \text{if } T_d > 0.0^\circ\text{C} \end{cases} \quad (4.15)$$

where Δt is the time step of the model and T_d the mean surface air temperature in $^\circ\text{C}$ over the last 24h. We set the reference time T_{ref} to 5 days, as Leinonen (1996) found that photosynthesis needs 5 days to recover after a frost event.

4.2.2 Simulation setup

We performed (1) simulations on site scale with the land surface model JSBACH driven by meteorological observations (FLUXNET), (2) simulations with the MPI-ESM prescribing observed sea surface temperatures (AMIP), and (3) full coupled simulation with the MPI-ESM under conditions of strong warming. Thereby we are able to evaluate the temperature dependences by comparison of model results to observations on site scale and globally, as well as to estimate possible changes in productivity due to global warming.

We performed simulations with and without acclimation using either of the instantaneous temperature dependences described in section 4.2.1.2 and 4.2.1.3. In addition, several sensitivity simulations were performed to analyse uncertainties in the temperature acclimation formulation, namely the effects of (1) the memory time of growth temperature, (2) slope of the temperature dependence of V_{max} and J_{max} , (3) the temperature response of the ratio between V_{max} and J_{max} at 25 °C. The different model versions and in which simulations they are applied are summarized in Table 4.1.

Table 4.1: The different model versions and the simulations performed. The model versions differ in the instantaneous temperature dependence of J_{max} and V_{max} (Optimum: section 4.2.1.3, Arrhenius: section 4.2.1.2) and if and how acclimation is accounted for. The versions with acclimation differ in the memory time growth temperature, in the slopes of acclimation ($b_{\Delta S,V}$ and $b_{\Delta S,J}$) and in the temperature dependence of $r_{J,V}$.

Acronym	instantaneous	acclimation				simulations		
		memory time	slope	$r_{J,V}$	Site-Scale	AMIP	4× CO ₂	
Tacc_off	Arrhenius	n/a	n/a	n/a	n/a	x	x	x
Tacc_on	Optimum	on	30 days	std	flexible	x	x	x
Tacc_on_fT	Optimum	off	n/a	n/a	n/a	x	x	x
Tacc_on_VJ	Optimum	on	30 days	std	rigid			x
Tacc_on_gT	Optimum	on	7 days	std	flexible		x	
Tacc_on+SE	Optimum	on	30 days	+1SE	flexible		x	
Tacc_on-SE	Optimum	on	30 days	-1SE	flexible		x	

4.2.2.1 Site scale simulations using FLUXNET data

The aim of the site scale simulations is to test how the different temperature formulations perform with respect to observed fluxes. JSBACH was driven by observed meteorological data of 5 sites, which span a broad range of climates (Table 4.2). For the evaluation of simulated gross primary productivity (GPP) and heat fluxes we used eddy covariance based estimates. We use two different GPP estimates which differ mainly in respect to whether or not nighttime data was used to derive respiratory rates (Lasslop et al., 2010; Reichstein et al., 2005). For statistical analysis we calculated the Pearson correlation coefficient using model and observational data (excluding gap filled data points). In addition, percent bias (PBIAS) was calculated which measures the average tendency of the simulated values to be larger or smaller than their observed ones.

Interannual variations in GPP are driven by APAR and water availability (Archibald et al., 2009).

4.2.2.2 Simulations with prescribed SSTs

To quantify how the choice of instantaneous temperature dependence as well as temperature acclimation affects global fluxes, we performed simulation with the MPI-ESM and prescribed sea surface temperatures (Table 4.1). SSTs were prescribed to ensure comparable and as realistic as

Table 4.2: Description of FLUXNET sites used. KG-Climate are the climates after Koeppen and Geiger.

Sitename	PFT	KG-Climate	Years
CA-Qcu	Evergreen needleleaf trees	subarctic (Dfc)	2001–2006
DE-Hai	Deciduous Broadleaf Trees	maritime (Cfb)	2000–2006
FR-Hes	Deciduous Broadleaf Trees	maritime (Cfb)	1997–2006
BW-Ma1	Grass	semi-arid (Bsh)	1999–2001
ZA-Kru	Grass	semi-arid (Bsh)	2001–2003

possible boundary conditions. Thereby the model performance on seasonal and interannual time scales can be improved. Several sensitivity simulations were performed to assess the uncertainties in the parameterization of acclimation. First, we varied the memory time of acclimation as it is unclear on which time scales the temperature acclimation of V_{max} and J_{max} takes place: Gunderson et al. (2010) reported a rather short tracking of optimal temperature to daytime temperatures of the last 1–5 days for temperate deciduous trees. In the experiments from which the data used by Kattge and Knorr (2007) originate, growth temperature is considered the mean temperature of the last 30 days at least. Therefore, we performed simulations with acclimation tracking the mean temperature of the last 7 or 30 days. Second, the slope of the temperature dependence of V_{max}^{25} and J_{max}^{25} ($b_{\Delta S,V}$ and $b_{\Delta S,J}$) was varied by one standard error. When increasing or decreasing the slopes, we also changed the intercepts with the y axis, $a_{\Delta S,V}$ and $a_{\Delta S,J}$, so that the angle point (the point where the curves with the different slopes intercept each other) of the temperature dependence function is at 25 °C. In the case of the simulation with the Arrhenius type instantaneous temperature dependence (Tacc_off) we use data from an ensemble of three model simulations which has been performed under the framework of the CMIP5 project (Hurrell and Visbeck, 2011). All other experiments consist of a single simulation.

For analysis we excluded the first 5 years of the simulations as the water cycle turned out to be not in balance during the first 3 years of a simulation. We accounted for the trend in the CO₂ forcing in our statistical analysis, by testing whether the difference between the annual means of the experiments is different from zero. The averages of the annual rates as well as the standard deviations were calculated for each simulation.

4.2.2.3 4×CO₂ simulations

The discrepancy in the simulated photosynthesis rates between the different temperature dependences of V_{max} and J_{max} is largest at temperatures > 35 °C (Figure 4.1). Therefore, we performed simulation with strong global warming caused by an abrupt quadrupling of atmospheric CO₂ (4 × 280 ppm). We did not account for the direct physiological effect of increasing CO₂ concentrations on photosynthesis (Equation 4.2) by keeping c_i fixed to 280 ppm. This was done to avoid a decline in the ratio between J_E and J_C limited photosynthesis with increasing atmospheric CO₂. Under present CO₂ level, photosynthesis is not saturated in respect to CO₂, thus, under higher CO₂ lev-

els, photosynthesis will less likely be limited by the carboxylation rate (J_C), causing a decline in the ratio between J_E and J_C . The temperature effect on $r_{V,J}$ is still debated (Kattge and Knorr, 2007; Onoda et al., 2005), but can have a profound influence on photosynthesis at high temperatures (Figure 4.1). Therefore, we did a sensitivity simulation in which $r_{V,J}$ was kept constant by not accounting for eq. (4.14).

The simulations were performed with interactive ocean and dynamical vegetation (Brovkin et al., 2009) spanning 50 years each. The duration of the simulation is too short for climate and vegetation dynamics to get into an equilibrium. Therefore we used the last 30 years of the simulation and linearly detrended the time series to test if simulated GPP differs between the model versions. The averages of the annual rates as well as the standard deviations were calculated for each simulation.

4.3 Results & Discussion

4.3.1 Site scale simulations

The model has some problems in simulating GPP rates at site level, except for the temperate forest sites. At the two temperate sites (DE-Hai and FR-HES) simulated GPP and the fluxes derived from flux measurements compare reasonably well (Fig. 4.2 and 4.3). At the water-limited sites (Veenendaal et al., 2008; Archibald et al., 2009), BW-Ma1 and ZA-Kru, the model data fit is significantly worse: there the model is not able to reproduce the phase and amplitude of the annual cycle. For both sites it is reported that the observed seasonal variations of GPP are dominated by the seasonal cycle of precipitation (Veenendaal et al., 2008; Archibald et al., 2009). At the more wet site, the observed decline in GPP of the FR-Hes site during the drought 2004 is absent in the model (Fig. 4.3). In addition to the water problem, the dynamically simulated phenology causes deviations from the observations: At the boreal site (CA-Qcu), the model greatly overestimate productivity due to a model bias in the leaf area index dynamics.

The different formulations for the temperature dependence of photosynthesis have marginal effects on GPP. Temperature acclimation leads to marginally higher photosynthesis at low temperatures, but reduces photosynthesis at high temperatures. The memory time of growth temperature has no effect. The model data fit was statistically not affected by the different model versions. The Pearson correlation coefficients of the monthly averaged hourly GPP (Fig. 4.2) varied between the model versions by less than 0.02, if at all (not shown). The differences in PBIAS between the model version were also negligible (not shown).

In summary, the effects of the different temperature formulations of photosynthesis are marginal compared to the model data mismatch caused by model biases in phenology and water availability.

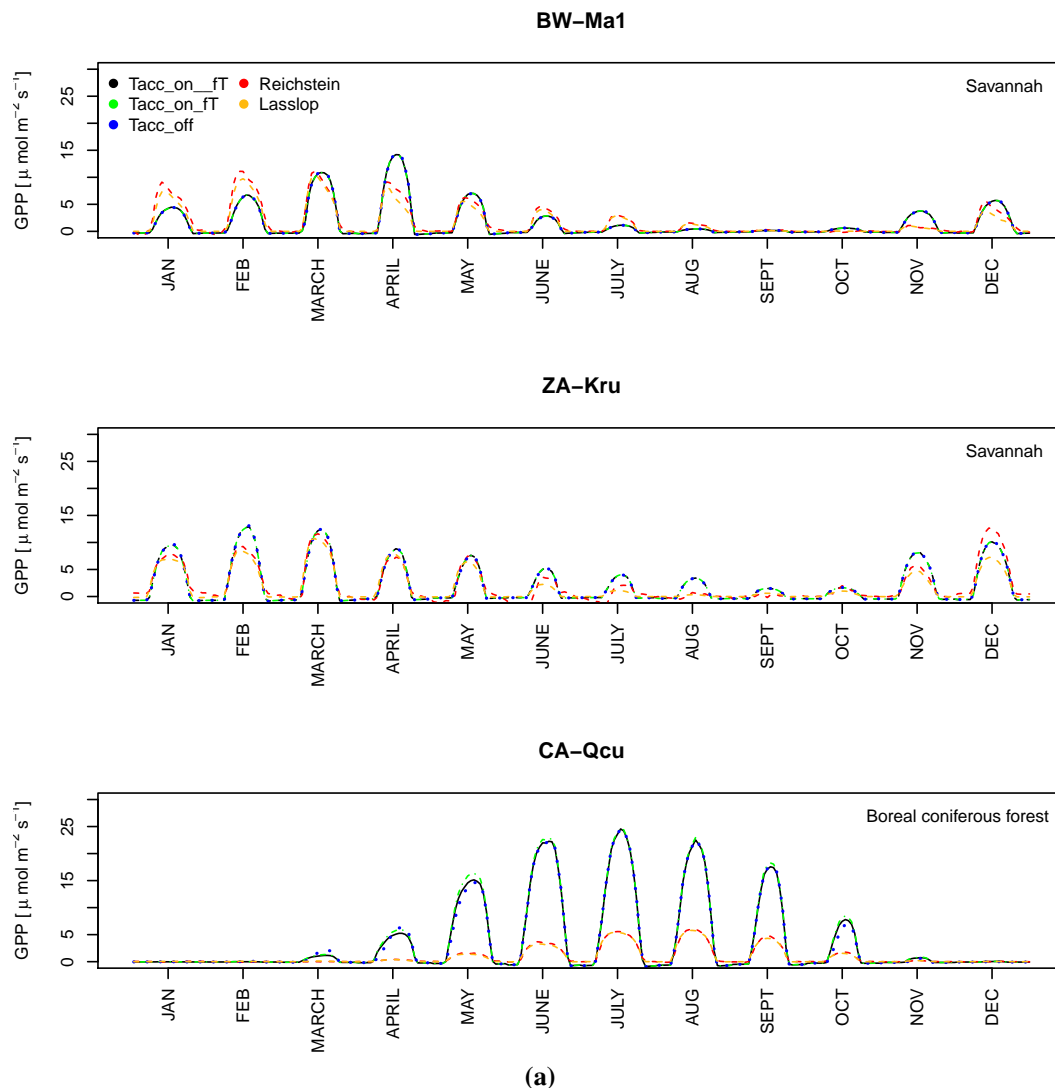


Figure 4.2: The daily cycle of GPP for every month of a year. Hourly rates are averaged over each month and the whole time series. Shown are the results from the simulations Tacc_on (green), Tacc_off (blue), Tacc_on_fT (black). Shown in addition are eddy covariance measurements based estimates after (Reichstein et al., 2005) (red) and (Lasslop et al., 2010) (yellow).

4.3.2 Simulations with prescribed SSTs

The differences in global GPP between all simulations with prescribed SSTs are small (Table 4.3). In the following, the discussed differences are statistically significant on a 0.95 significance level if not stated else (for statistical significance see Table 4.4). The exchange of the original (Arrhenius type) instantaneous temperature dependence (Tacc_off) with the new (optimum type) formulation (Tacc_on_fT) reduced global GPP and NPP by 1.2% and 1.0%, respectively. When temperature acclimation is accounted for (difference between Tacc_on_fT and Tacc_on) global GPP and NPP is increased by 1.9% and 2.3%, respectively. The increase in NPP due to acclimation is close to the findings by Friend (2010). Using a comprehensive model, Friend (2010) simulated a 2.5% increase in global NPP due to temperature acclimation of the chloroplast electron transport.

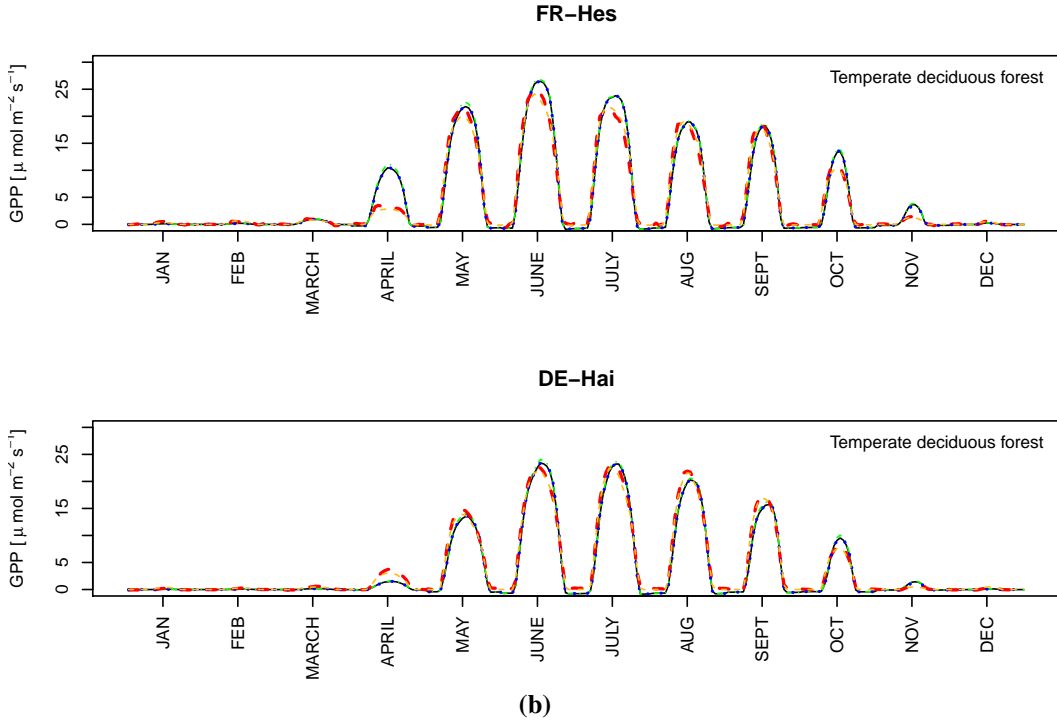


Figure 4.2: continued

The increase in global productivity due to temperature acclimation is mainly contributed by extra-tropical regions. When averaged over extra-tropical regions, GPP and NPP were respectively 5.4% and 6.1% higher in the simulation with temperature acclimation (Tacc_on) than in the simulations without (Tacc_on_fT). Regionally, change in GPP of more than $100 \text{ g m}^2 \text{ yr}$ can occur (Figure. 4.4), which are relative to annual GPP in the low single-digit range. The variance of tropical GPP is statistically significant reduced by acclimation, which is expected if plants acclimate to prevailing temperatures. The same seems to hold true for extra tropical regions but is statistically not significant.

The exchange of the original instantaneous temperature dependence (Tacc_off) with the new formulation (Tacc_on_fT) did not result in statistically significant (0.95) different rates when averaged over tropical and extra-tropical regions (Table. 4.5). But regionally differences in annual GPP occur (Figure. 4.5), which are in the same order of magnitude as the changes caused by temperature acclimation (Figure 4.4).

The sensitivity experiments show that global GPP is rather insensitive to the strength of acclimation and the choice of target temperature. The fluxes in the simulations in which we increased or decreased the slope of eq. 4.12 and 4.13 ($b_{\Delta S, V}$ and $b_{\Delta S, J}$) governing the strength of acclimation (Tacc_on+SE and Tacc_on-SE) were not significantly different (0.95) from the simulation with standard parameterization (Tacc_on). There are also no statistically significant (0.95) differences between the simulations with a differing target temperature (Tacc_on and Tacc_on_gT).

Latent heat fluxes were marginally affected and no statistically significant (0.95) effects were found (not shown).

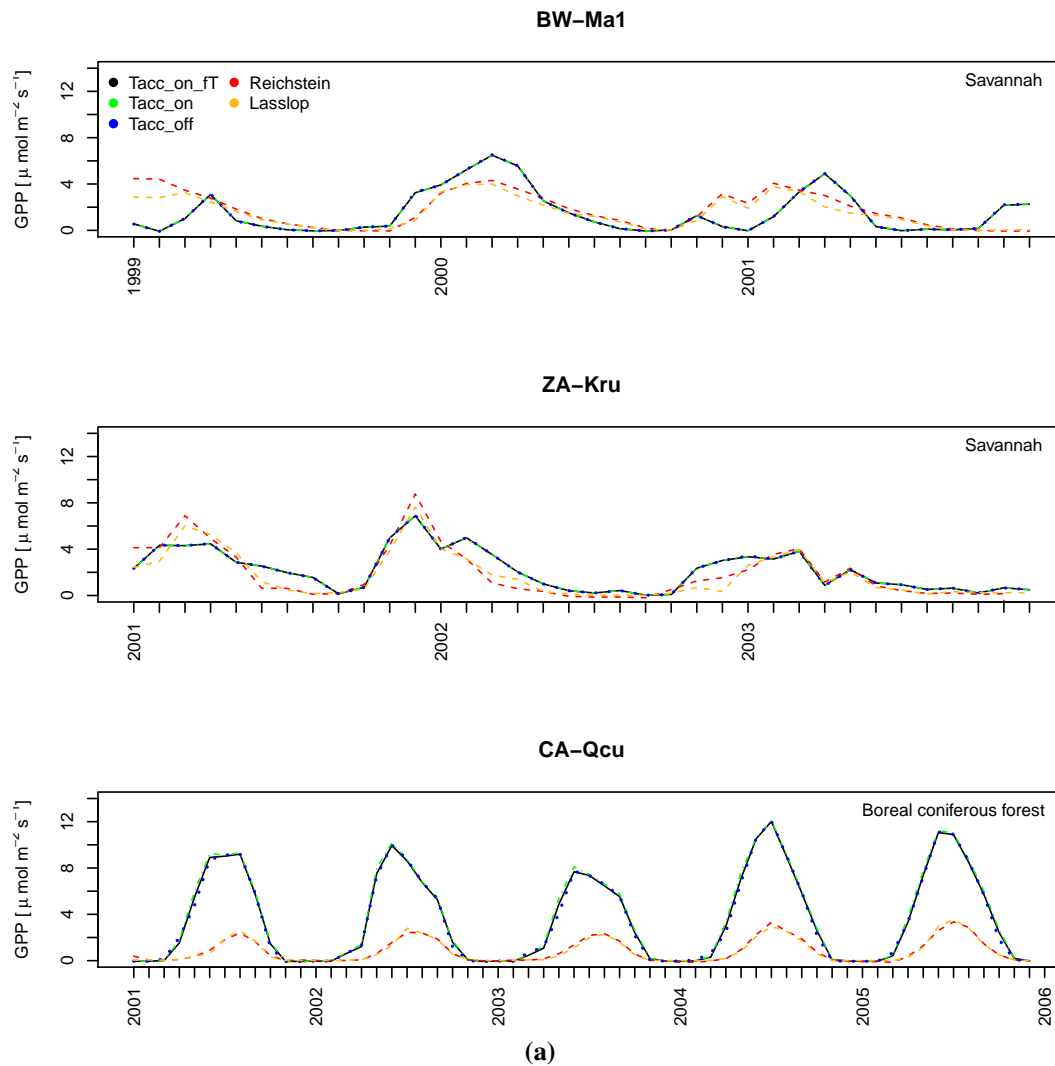


Figure 4.3: The annual cycle of GPP. The rates are monthly averages. Shown are the results from the simulations Tacc_on (green), Tacc_off (blue), Tacc_on_fT (black). Shown in addition are eddy covariance measurements based estimates after (Reichstein et al., 2005) (red) and (Lasslop et al., 2010) (yellow).

Table 4.3: Global mean fluxes of GPP, NPP, and latent heat (\pm standard deviation) in simulations with prescribed SSTs.

Acronym	GPP [Pg a^{-1}]	NPP [Pg a^{-1}]	latH [W m^{-2}]
Tacc_off	158.12 ± 3.50	76.97 ± 1.84	-39.41 ± 0.68
Tacc_on_fT	156.36 ± 4.10	76.18 ± 2.11	-39.15 ± 0.64
Tacc_on	159.29 ± 3.75	77.95 ± 1.86	-39.17 ± 0.61
Tacc_on+SE	158.81 ± 3.52	77.69 ± 1.67	-39.17 ± 0.55
Tacc_on-SE	159.07 ± 4.24	77.87 ± 2.07	-39.98 ± 0.75
Tacc_on_gT	159.10 ± 3.62	77.89 ± 1.84	-39.14 ± 0.61

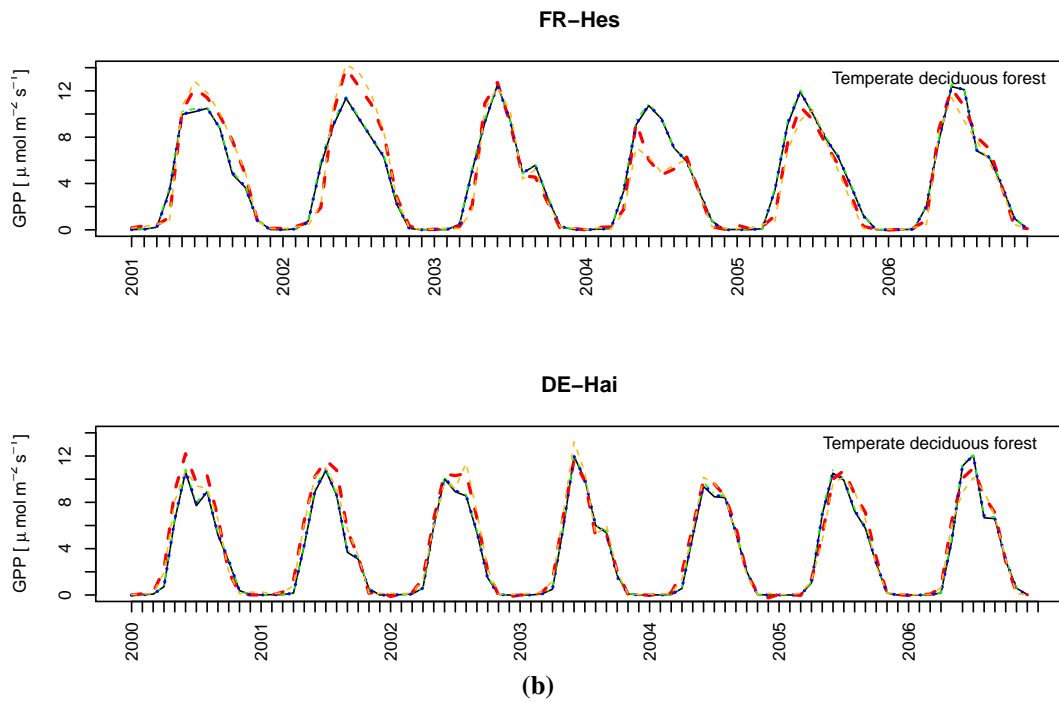


Figure 4.3: continued

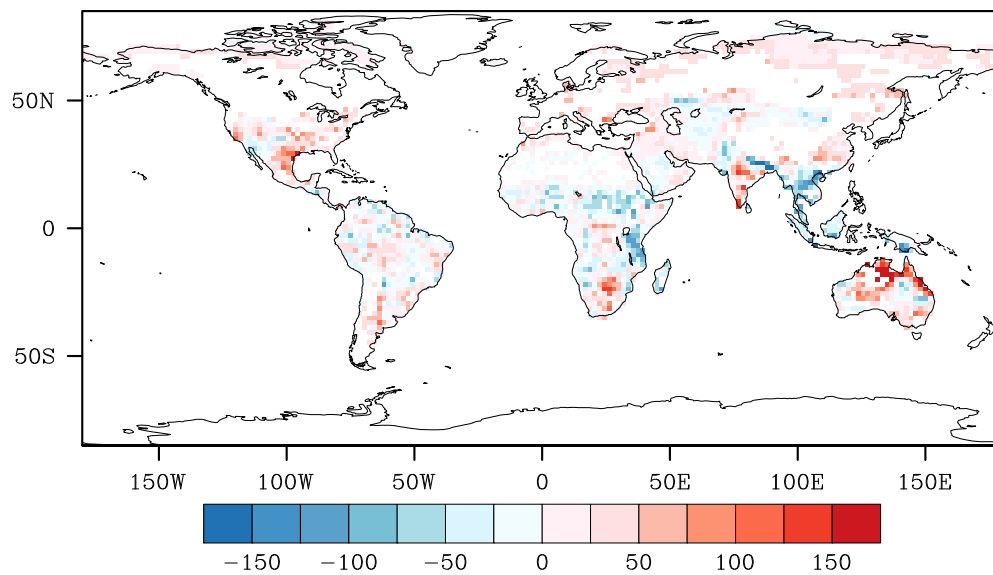


Figure 4.4: The difference in GPP between the prescribed SSTs simulation with (Tacc_on) and the simulation without acclimation (Tacc_on_fT). Only differences which are significantly different from zero on a .95 level are shown.

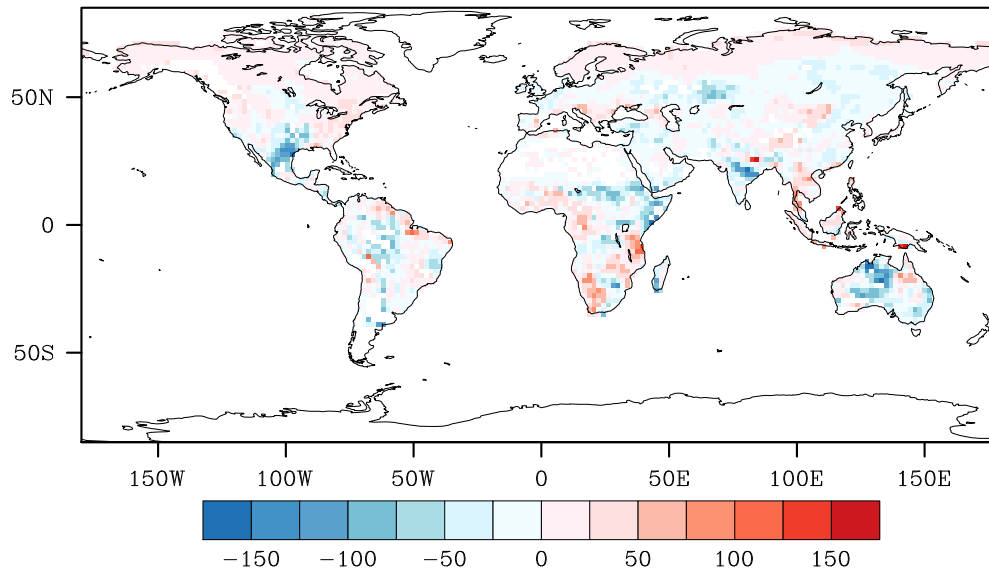


Figure 4.5: The difference in GPP between the prescribed SSTs simulation with optimum function (Tacc_on_fT) and the one with truncated Arrhenius function (Tacc_off). Only differences which are significantly different from zero on a .95 level are shown.

Table 4.4: Significance of the differences in GPP in simulations with prescribed SSTs: tabulated are the α values ($\alpha = (1 - tvalue) * 100$) of the two tailed t-test performed on the difference in global GPP between two simulation. If α is greater than 95 the two fluxes are significantly different from each other on a 0.95 significance level.

	Tacc_on	Tacc_on_fT	Tacc_off	Tacc_on+SE	Tacc_on-SE
Tacc_on_fT	100.00				
Tacc_off	96.44	99.74			
Tacc_on+SE	68.89	99.89	74.86		
Tacc_on-SE	27.08	99.99	87.56	29.06	
Tacc_on_gT	31.39	100.00	95.31	45.23	03.87

Given the large uncertainties in estimation of present day GPP (Beer et al., 2010; Welp et al., 2011), one can not judge which of the formulation is more accurate because the changes in annual rates are in the range of a few percents. In summary, for present day climate temperature acclimation cause a slight increase in extra-tropical productivity. We further showed that the uncertainty originating from the slope of the acclimation function is negligible.

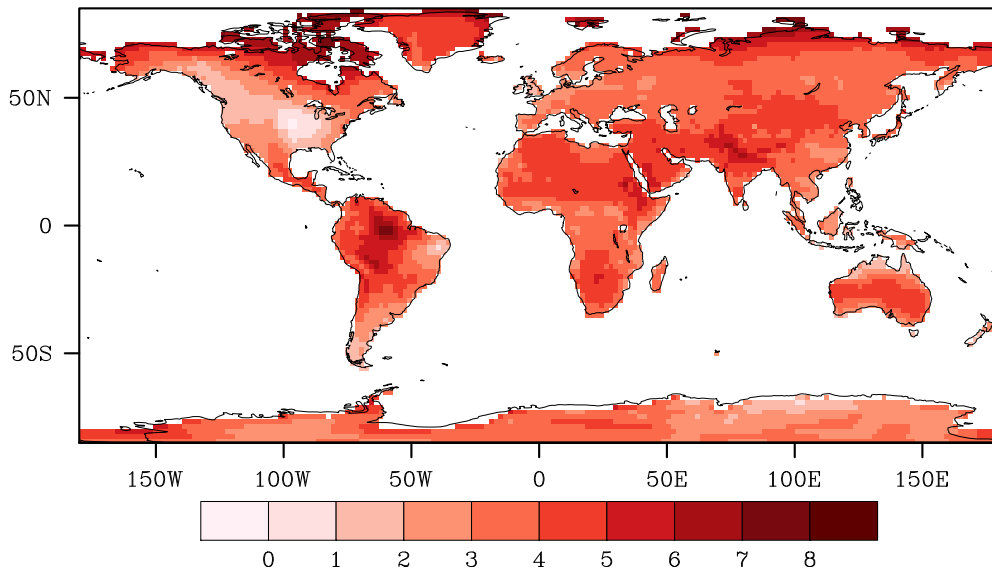
4.3.3 $4 \times \text{CO}_2$

Due to the quadrupling of atmospheric CO_2 , temperature over land is in the mean 6 K higher than in the control simulation (280ppm), with local temperatures up to >10 K higher (Figure 4.6). Such an increase in temperature causes a 1.2% drop in global GPP in the model. Regionally, the sign of the temperature effect differs. Tropical GPP decreases by 7%, while extra-tropical GPP is increased in the same order of magnitude. As warming also enhances respiration rates, global

Table 4.5: Regionally averaged fluxes of GPP, NPP, and latent heat (\pm standard deviation) in simulations with prescribed SSTs.

Acronym	GPP[g m ⁻² a ⁻¹]	NPP[g m ⁻² a ⁻¹]	latH [W m ⁻²]
tropical [30 °S - 30 °N]			
Tacc_off	1719.17 \pm 50.36	788.75 \pm 27.75	-58.50 \pm 1.39
Tacc_on_fT	1708.13 \pm 58.45	782.60 \pm 32.94	-58.27 \pm 1.50
Tacc_on	1709.36 \pm 45.40	782.91 \pm 25.75	-58.14 \pm 1.45
extra tropical [30 °N - 90 °N]			
Tacc_off	610.75 \pm 20.4	342.19 \pm 12.56	-25.40 \pm 0.56
Tacc_on_fT	612.64 \pm 18.26	345.12 \pm 10.96	-25.26 \pm 0.53
Tacc_on	645.95 \pm 20.00	366.42 \pm 12.15	-25.39 \pm 0.48

NPP decrease more strongly than GPP by -13% .

**Figure 4.6:** Temperature difference between the $4\times\text{CO}_2$ simulation Tacc_off and the control simulation (280ppm).

Global GPP differs up to 3% between the simulations with the different temperature dependences of photosynthesis. Whereby the choice of the instantaneous temperature response function affects global GPP as strong as whether or not temperature acclimation is accounted for (Table 4.6). But the effect of acclimation strongly depends on how $r_{V,J}$ is handled in the model. When $r_{V,J}$ is T independent simulated GPP is slightly higher than in the simulation with the original formulation for the instantaneous temperature dependence, while with flexible $r_{V,J}$ the effect of acclimation is negligible.

As these simulation were performed with dynamical vegetation (climatic and productivity related changes in the distribution of vegetation), we further analysed the mean GPP per PFT to separate the effects of temperature on photosynthesis from the ones on vegetation distribution. We found that the effects of vegetation dynamics in tropical regions are significantly contributing

Table 4.6: The global fluxes of GPP, NPP, and latent Heat (mean \pm standard deviation) in the $4\times\text{CO}_2$ simulations.

Acronym	GPP[Pg a ⁻¹]	NPP[Pg a ⁻¹]	latH [W m ⁻²]
Tacc_off	143.12 \pm 3.4	64.48 \pm 2.14	-42.49 \pm 0.98
Tacc_on_fT	141.64 \pm 3.14	63.42 \pm 1.93	-42.33 \pm 0.85
Tacc_on	143.80 \pm 3.28	64.91 \pm 2.02	-42.34 \pm 0.93
Tacc_on_VJ	144.40 \pm 3.71	65.40 \pm 2.14	-42.53 \pm 1.03

Table 4.7: Significance of the differences in GPP in simulations with $4\times\text{CO}_2$: tabulated are the α values ($\alpha = (1 - tvalue) * 100$) of the two tailed t-test performed on the difference in global GPP between two simulation. If α is greater than 95 the two fluxes are significantly different from each other on a 0.95 significance level.

	Tacc_on	Tacc_on_fT	Tacc_off
Tacc_on_fT	97.78		
Tacc_off	45.64	99.72	
Tacc_on_VJ	55.06	91.16	77.55

to the reduction in GPP. The overall tropical GPP decreases due to increasing temperatures by 7% while the dominating PFTs (tropical forest and C4 grasslands) decrease by 4.5% and 2.5%, respectively. In the extra-tropics vegetation dynamics contribute to the increase in GPP: the overall increase of 20% is larger than the increases in GPP of the dominant PFTs lying in the range of 11-16%. This shows that the effects of vegetation dynamics and of temperature acclimation are pointing into the same direction.

Overall, the effects of the different temperature dependences on regional level (including the effects vegetation dynamics) (Table 4.8) and on PFT-level (excluding the effects of vegetation dynamics) (not shown) are small and qualitatively similar to the simulations with prescribed SSTs.

Table 4.8: Regional fluxes of GPP, NPP, and latent heat (mean \pm standard deviation) in the $4\times\text{CO}_2$ simulations.

Acronym	GPP[g m ⁻² a ⁻¹]	NPP[g m ⁻² a ⁻¹]	latH [W m ⁻²]
tropical [30 °S - 30 °N]			
Tacc_off	1428.76 \pm 63.00	610.02 \pm 40.19	-62.71 \pm 2.65
Tacc_on_fT	1400.37 \pm 56.44	686.98 \pm 34.91	-62.35 \pm 2.34
Tacc_on	1393.07 \pm 59.45	584.29 \pm 37.42	-61.84 \pm 2.47
Tacc_on_VJ	1421.49 \pm 70.83	602.58 \pm 44.10	-62.81 \pm 3.01
extra tropical [30 °N - 90 °N]			
Tacc_off	622.57 \pm 18.40	312.96 \pm 10.74	-28.09 \pm 0.84
Tacc_on_fT	630.35 \pm 16.15	319.03 \pm 9.19	-28.14 \pm 0.69
Tacc_on	659.40 \pm 16.63	337.96 \pm 9.03	-28.44 \pm 0.66
Tacc_on_VJ	647.68 \pm 18.40	331.53 \pm 10.74	-28.13 \pm 0.84

In summary, temperature acclimation effects on global GPP are of the same order of magnitude as the effect of the instantaneous temperature dependence formulation. Changes in the temperature dependence of autotrophic respiration (Atkin et al., 2008), leaf phenology (Wolkovich et al., 2012), and vegetation dynamics may be more important for the response of ecosystem productivity to warming, but are even less understood than the temperature dependence of photosynthesis.

4.4 Conclusions

We found that acclimation of photosynthesis to growth temperatures has only a minor effect on global productivity. The effect is of similar strength to the modelling results by Friend (2010). The minor effect of acclimation on global GPP stands in contrast to the conclusions drawn by Booth et al. (2012). As Booth et al. (2012) did not account for acclimation but varied the short-term optimum temperature of photosynthesis they might have overestimated the importance of the optimum temperature.

The evaluation of the different temperature dependences using observational data is hampered by model biases in phenology and water availability in combination with the low accuracy of observation based estimates. There are two major uncertainties regarding temperature acclimation. First, the temperature dependence of $r_{V,J}$ affects photosynthesis rates at high temperature substantially, but experimental data is insufficient to constrain the behavior of $r_{V,J}$. Second, there may be differences in the acclimation strength between different vegetation types which are not accounted for in our study. The acclimation response of tropical trees may be less than of temperate ones (Berry and Bjorkman, 1980; Read and Busby, 1990; S. and J., 2002; Cunningham and Read, 2003). If tropical trees indeed acclimate less or not the positive effect of acclimation on global GPP could be slightly larger than our simulations suggest, as acclimation tends to reduce tropical productivity in our simulations.

An underestimation of the effect of acclimation may also result from missing interactions between the LAI and the C cycle in the model. The LAI is computed independently of the actual leaf C. Therefore the LAI, by which leaf level photosynthesis is scaled up to GPP, is in all simulation similar. A possible positive feedback which would enhance the acclimation effects, is therefore not accounted for in JSBACH.

We conclude that long-term projections done with the MPI-ESM, as for example for the CMIP5 project, would not be strongly affected by the omission of acclimation, unlike suggested by Booth. We even suggest to wait with the implementation of acclimation into ESMs until a better understanding of $r_{V,J}$ and the acclimative strength of tropical trees has been achieved.

4.5 Acknowledgements

We thank Gitta Lasslop for the provision of her FLUXNET GPP products.

Chapter 5

Summary & Conclusions

5.1 Summary of findings

5.1.1 Nutrient limitation

5.1.1.1 How much and where is N and P availability limiting land C uptake in this century?

In direct comparison with simulations which do not consider nutrient cycles, the accumulated land C uptake between 1860 and 2100 (SRES A1B scenario) is 13 % and 16 % lower in simulations with N and P cycling, respectively. The combined effect of both nutrients reduces land C uptake by 25 % (-138 Gt) compared to simulations without N or P cycling. The model reveals a distinct geographic pattern of P and N limitation, where P limitation dominates low-latitude systems and N limitation is more restricted to higher latitudes.

5.1.1.2 What is the long-term (multi-centennial) evolution of N and P limitation?

After 2100, increased temperatures and high CO₂ concentrations cause a shift from N to P limitation at high latitudes, while nutrient limitation in the tropics declines. The increase in P limitation at high-latitudes is induced by a strong increase in NPP and the low P sorption capacity of soils, while a decline in tropical NPP due to high autotrophic respiration rates alleviates N and P limitations.

5.1.1.3 What are the main uncertainties in projecting terrestrial P availability?

The poorly constrained processes of soil P sorption and biochemical mineralization are identified as the main uncertainties in the strength of P limitation. Changes in stoichiometry (flexibility), although commonly discussed as a possible mechanisms to improve nutrient use and therefore counteract nutrient limitation, have a very minor effect on the evolution and strength of N and P limitation.

5.1.1.4 How much and where is the P release by chemical weathering altered due to climate change?

Under the RCP8.5 scenario, global P release by chemical weathering doubles (80%–110%) by 2100. However, the uncertainties are large, mainly due to the parameterization of the temperature response of P release. A robust outcome is an increase in P release at high latitudes (>45°N), Central Africa, SE-Asia and the Amazon basin. To what extent release rates increase strongly depends on the climatic forcing, for example, at the Amazon basin the increase in P release varies between 30–80%.

5.1.1.5 To what extent do changes in temperature and runoff contribute to the overall change in P release?

Changes in runoff enhances P release rates by less than 25%, whereas the P release increases more than 80% when the effect of temperature on weathering is additionally accounted for. This finding is contrary to the common assumption that chemical weathering is dominantly controlled by runoff and lithology. The uncertainties in the global release rates are large due to the high sensitivity to the parameterization of the temperature response formulation. The runoff projections on regional scale differ strongly among the different climatic forcings. Therefore runoff is mainly responsible for the uncertainty in the release rates on regional scale.

5.1.1.6 To what extent could land C uptake be affected by the expected changes in P release?

Back-on-the-envelope calculations show that the enhanced P release most likely result in the sequestration of 5.5–22 Gt of C between 1860 and 2100. This is a minor sequestration given that current annual land C uptake is about 2.6 Gt yr⁻¹ (Friedlingstein et al., 2010) and most models predict a cumulative uptake of more than 300 Gt during the 21st century (Hungate et al., 2003; Friedlingstein et al., 2006).

5.1.2 Temperature acclimation of photosynthesis

5.1.2.1 How much and where is present productivity and productivity in a warmer climate affected by temperature acclimation?

Acclimation of photosynthesis to prevailing temperatures has only a minor effect on global productivity. Temperature acclimation slightly increases extra-tropical productivity under present climatic conditions by 5% and under future climatic conditions by 7%. Present day productivity of tropical ecosystems is not affected by acclimation. In future, tropical productivity may increase or decrease due to acclimation depending on the parameterization of the temperature acclimation formulation.

5.1.2.2 How does this effect relate to changes in productivity due to other factors constraining the temperature response of photosynthesis?

The effect of temperature acclimation is of the same magnitude as the effect of the parameterization of the instantaneous heat inhibition of photosynthesis at high temperatures.

5.1.2.3 What are the main uncertainties in the quantification of the effect of temperature acclimation on productivity?

The effect of temperature acclimation on tropical ecosystems is elusive. On the one hand, it is under debate if tropical trees do acclimate to temperature at all, as temperatures at low latitudes do not vary much during the year. On the other hand, if they acclimate, the sign of their response to warming depends on the temperature response of the ratio between carboxylation limited and electron-transport limited photosynthesis ($r_{V,J}$), which can not be constrained from the limited availability of data. In particular, photosynthesis measurements from tropical and subtropical vegetation are needed.

5.2 Conclusions

The findings indicate that terrestrial sink during the 21st century is likely overestimated in models that neglect P and N limitations, like the models used in the CMIP5 project. To my knowledge, this study is the first one which shows that high latitude ecosystem can become P limited. This has profound implications for C cycle projections, as P availability is commonly not considered as an uncertainty in projections of the C balance of mid to high latitudes. I identified P soil sorption and biochemical mineralization as the main processes that control terrestrial P availability. Both processes are poorly understood or even not yet quantified with empirical data. Changes in P release by chemical weathering may be of minor importance for the C balance during the 21st century, but can have significant effects on the C balance on longer time scales. Based on these findings, I argue that P limitation is of global significance and that the P cycle must be included in global models used for C cycle projections.

Regarding temperature acclimation of photosynthesis, I conclude that the omission of acclimation in models does not significantly affect the projected terrestrial sink, unlike previously suggested (Booth et al., 2012). My studies is an example that the analysis of the photosynthetic response to a single factor, here temperature, is a rather poor predictor for the actual response of productivity on the level of an ecosystem, because other factors may constrain productivity under natural conditions. Due to small but highly uncertain changes in productivity caused by acclimation, I rather recommend to wait with the implementation of acclimation into ESMs until a better understanding of the biochemical processes and the acclimative strength of tropical trees has been achieved.

5.3 Implications for further model developments

In this study the influence of nutrient limitation and temperature acclimation on the productivity of terrestrial ecosystems is investigated without taking into account (1) processes driven by land use change and management and (2) feedbacks between climate and vegetation. These aspects are omitted to provide a idealized test case which facilitates the analysis of the processes under investigation. Changes in land use are of major importance for the terrestrial C balance (Denman et al., 2007). The strength of nutrient limitation, as found in my study, may be dampened or amplified by climate-vegetation feedbacks (Denman et al., 2007). Therefore, it must be the overall goal to investigate nutrient limitation and temperature acclimation in a more inclusive framework.

Before such studies can be conducted, several aspects in the representation of the C cycle in the MPI-ESM must be improved. There are two reason to focus on the C cycle first, before a more comprehensive representation of nutrient cycling and its interactions with the C or water cycle can be implemented. Firstly, the strength of nutrient limitation is inherit to the C cycle, as nutrient limitation depends on the accuracy of the C cycle model itself in simulating actual C cycling. Secondly, the representation of the C cycle in an ESM is a strong simplification of what is actually known from theory (Canadell et al., 2007). Several aspects of the C cycle which are not accounted for in the model become relevant when the cycles of nutrients are incorporated. As the C cycle is far better understood and documented than the cycles of N or P, the merit of improving the C cycle is that uncertainties can be kept rather low.

In particular, the dynamics of soil C are implemented in the MPI-ESM in the most simplistic way, as one pool, which is problematic. Such a representation is commonly criticized (Knorr et al. (2005)) for providing an inaccurate characterization of the soil C response to climate change. The dependency of soil C to climate and how it is represented in models is a large uncertainty in the estimation of the land C uptake (Jones et al., 2005; Thum et al., 2011) and land use emissions (Reick et al., 2010). Warming experiments show that the response of soil C to warming is insufficiently represented by the commonly used Arrhenius or Q_{10} formulations (Reth et al., 2009). Yet it is unclear, if simple soil models over- (Luo et al., 2001; Knorr et al., 2005) or underestimate (Ise and Moorcroft, 2006; Reth et al., 2009) the response to warming. To improve the reliability, more mechanistic models of soil C cycling which separates soil carbon in fraction of differing accessibility for heterotrophs and account for environmental constrains, other than temperature and water availability, are needed (Giardina and Ryan, 2000; Davidson and Janssens, 2006). The decomposition of soil organic matter is closely interlinked with the mineralization of N and P (Janssens et al., 2010). Thus it may be beneficial to account for nutrient constrains already during the basic development of soil C models, rather than expand these models with nutrient cycles later.

A second problematic aspect in JSBACH is that the LAI, which is used to upscale leaf level photosynthesis rates to canopy level, is independent of the actual amount of leaf carbon in the model. An evaluation of processes which affect productivity, for example temperature acclimation, is problematic, if the positive feedback between higher photosynthesis and LAI is not captured by

the model.

For the coupling of the CNP model with an atmospheric model, the limited understanding how nutrient limitation affects autotrophic respiration is the main challenge for estimating the effect of nutrients in a coupled system (Zaehle and Dalmonech, 2011). It is unclear from experiments, if a reduction in plant productivity due to nutrient limitation must be attributed to a reduction in net photosynthesis or an increase in respiration. While a reduction in photosynthesis would affect evapotranspiration, an increase in respiration would not.

In summary, while the inter-linkage between the LAI and the C cycle can easily be incorporated in models, for the other two aspects, the soil C and the water nutrient interactions several alternative hypotheses exist and current data availability is hardly sufficient to test these. As long as the data is insufficient, it is crucial to test each of these hypothesis in a common model framework and carefully assess their relevance. Thereby models can help to guide further experimental research which is needed to permit more inclusive simulations.

5.4 Implications for studies on past climate and marine systems

The main focus of this thesis is on the terrestrial C sink during the 21st century and beyond. Nonetheless, my work is also relevant for (1) studies of the climate of the past and (2) for the coupling of land and marine systems, as the productivity of terrestrial, aquatic and marine system is assumed to be limited by P availability on a time scale of hundred thousands to millions of years. In this thesis I showed that the terrestrial P cycle is indeed relevant for the terrestrial C balance, even on shorter time scales. To study the terrestrial P cycling of the past, simple box models are currently applied, for example, to test if the terrestrial P cycle is responsible for the observed resilience of atmospheric O₂ concentrations on geological time scale (Lenton and Watson, 2011). Although not being directly applicable to paleo studies, the developed mechanistic model of combined C, N, and P cycling and the identification of the main processes controlling P availability (Chapter 2), are an important step forward regarding the role of P for the climate of the past.

The newly developed model also facilitates studies on the coupling between marine systems and terrestrial system via terrestrial nutrient export. In combination with the P release model by Hartmann and Moosdorf (2011), the developed CNP model is able to provide dynamical boundary conditions for studies on aquatic productivity. Yet, the model is not directly applicable for marine studies as soil erosion and the riverine transport of organic and inorganic matter are not represented in the MPI-ESM. Nonetheless, the incorporation of a P cycle in an ESM is an important step forward into the direction of a models which account for all processes relevant for the climate system.

Bibliography

- Aerts, R. and Chapin, F.: The mineral nutrition of wild plants revisited: A re-evaluation of processes and patterns, in: *Advances in Ecological Research*, Vol 30, vol. 30 of *Advances in Ecological Research*, pp. 1–67, Academic Press Inc, 525 B Street, Suite 1900, San Diego, CA 92101-4495 USA, 2000.
- Agren, G.: Stoichiometry and Nutrition of Plant Growth in Natural Communities, *Annu. Rev. Ecol. Evol. Syst.*, 39, 153–170, doi:10.1146/annurev.ecolsys.39.110707.173515, 2008.
- Anisimov, O., Shiklomanov, N., and Nelson, F.: Global warming and active-layer thickness: results from transient general circulation models, *Global Planet. Change*, 15, 61–77, doi: 10.1016/S0921-8181(97)00009-X, 1997.
- Aponte, C., Maranon, T., and Garcia, L.: Microbial C, N and P in soils of Mediterranean oak forests: influence of season, canopy cover and soil depth, *Biogeochemistry*, 101, 77–92, doi: 10.1007/s10533-010-9418-5, 6th International Symposium on Ecosystem Behavior, Helsinki, FINLAND, JUN 29-JUL 03, 2009, 2010.
- Archibald, S. A., Kirton, A., Merwe, M. R. V. D., Scholes, R. J., Williams, C. A., Hanan, N., Resources, N., and Africa, S.: Drivers of inter-annual variability in Net Ecosystem Exchange in a semi-arid savanna ecosystem, South Africa, pp. 251–266, 2009.
- Atkin, O. and Tjoelker, M.: Thermal acclimation and the dynamic response of plant respiration to temperature, *Trends Plant Sci.*, 8, 343–351, doi:10.1016/S1360-1385(03)00136-5, 2003.
- Atkin, O. K., Atkinson, L. J., Fisher, R. A., Campbell, C. D., Zaragoza-Castells, J., Pitchford, J. W., Woodward, F. I., and Hurry, V.: Using temperature-dependent changes in leaf scaling relationships to quantitatively account for thermal acclimation of respiration in a coupled global climate-vegetation model, *Global change biology*, 14, 2709–2726, doi:10.1111/j.1365-2486.2008.01664.x, 2008.
- Baker, T., Phillips, O., Laurance, W., Pitman, N. A., Almeida, S., Arroyo, L., DiFiore, A., Erwin, T., Higuchi, N., Killeen, T., Laurance, S., Nascimento, H., Monteagudo, A., Neill, D., Silva, J., Malhi, Y., Gonzalez, G. L., Peacock, J., Quesada, C., Lewis, S., and Lloyd, J.: Do species traits determine patterns of wood production in Amazonian forests?, *Biogeosciences*, 6, 297–307, 2009.
- Bakker, C., Rodenburg, J., and van Bodegom, P.: Effects of Ca- and Fe-rich seepage on P availability and plant performance in calcareous dune soils, *Plant Soil*, 275, 111–122, doi: 10.1007/s11104-005-0438-1, 2005.

BIBLIOGRAPHY

- Bakker, C., Van Bodegom, P., Nelissen, H., Ernst, W. H., and Aerts, R.: Plant responses to rising water tables and nutrient management in calcareous dune slacks, *Plant Ecol.*, 185, 19–28, doi: 10.1007/s11258-005-9080-5, 2006.
- Banfield, J. F., Barker, W. W., Welch, S. A., and Taunton, A.: Colloquium Paper: Biological impact on mineral dissolution: Application of the lichen model to understanding mineral weathering in the rhizosphere, *Proceedings of the National Academy of Sciences*, 96, 3404–3411, URL <http://www.pnas.org/cgi/content/abstract/96/7/3404>, 1999.
- Barron, A. R., Wurzbarger, N., Bellenger, J. P., Wright, S. J., Kraepiel, A. M. L., and Hedin, L. O.: Molybdenum limitation of asymbiotic nitrogen fixation in tropical forest soils, *Nature Geoscience*, 2, 42–45, URL <http://dx.doi.org/10.1038/ngeo366>, 2008.
- Batjes, N.: Total carbon and nitrogen in the soils of the world, *Eur. J. Soil Sci.*, 47, 151–163, 1996.
- Beer, C., Reichstein, M., Tomelleri, E., Ciais, P., Jung, M., Carvalhais, N., Roedenbeck, C., Arain, M. A., Baldocchi, D., Bonan, G. B., Bondeau, A., Cescatti, A., Lasslop, G., Lindroth, A., Lomas, M., Luyssaert, S., Margolis, H., Oleson, K. W., Roupsard, O., Veenendaal, E., Viovy, N., Williams, C., Woodward, F. I., Papale, D., and Rödenbeck, C.: Terrestrial Gross Carbon Dioxide Uptake: Global Distribution and Covariation with Climate, *Science*, 329, 834–838, doi: 10.1126/science.1184984, URL <http://www.ncbi.nlm.nih.gov/pubmed/20603496>, 2010.
- Berkeley Earth: Berkeley Earth Surface Temperature, URL <http://berkeleyearth.org>.
- Berry, J. A. and Bjorkman, O.: Photosynthetic response and adaptation to temperature in higher plants, *Annual Review of Plant Physiology and Plant Molecular Biology*, 16, 81–89, 1980.
- Booth, B. B. B., Jones, C. D., Collins, M., Totterdell, I. J., Cox, P. M., Sitch, S., Huntingford, C., Betts, R. A., Harris, G. R., and Lloyd, J.: High sensitivity of future global warming to land carbon cycle processes, *Environmental Research Letters*, 7, 024002, URL <http://stacks.iop.org/1748-9326/7/i=2/a=024002>, 2012.
- Bradford, M. E. and Peters, R. H.: The relationship between chemically analyzed phosphorus fractions and bioavailable phosphorus1 Bioavailable phosphorus, 32, 1124–1137, 1987.
- Brady, P. V. and Carroll, S. A.: LETTER Direct effects of CO₂ and temperature on silicate weathering: Possible implications for climate control, 58, 1853–1856, 1994.
- Brovkin, V., Raddatz, T., Reick, C. H., Claussen, M., and Gayler, V.: Global biogeophysical interactions between forest and climate, *Geophysical research letters*, 36, doi:10.1029/2009GL037543, 2009.
- Buendía, C., Kleidon, a., and Porporato, a.: The role of tectonic uplift, climate, and vegetation in the long-term terrestrial phosphorous cycle, *Biogeosciences*, 7, 2025–2038, doi:10.5194/bg-7-2025-2010, URL <http://www.biogeosciences.net/7/2025/2010/>, 2010.

- Canadell, J. G., Pataki, D. E., and Pitelka, L. F., eds.: *Terrestrial Ecosystems in a Changing World*, Global Change — The IGBP Series, Springer Berlin Heidelberg, Berlin, Heidelberg, URL <http://www.springerlink.com/content/r818418228837370>, 2007.
- Catling, D. C., Glein, C. R., Zahnle, K. J., and McKay, C. P.: Why O₂ is required by Complex Life on Habitable Planets and the Concept of Planetary 'Oxygenation Time', *Astrobiology*, 5, 415–438, 2005.
- Clark, D.: Sources or sinks? The responses of tropical forests to current and future climate and atmospheric composition, *Philos. T. Roy. Soc. B.*, 359, 477–491, doi:10.1098/rstb.2003.1426, Annual Meeting of the Association-for-Tropical-Biology-and -Conservation, Panama City, Panama, July, 2002, 2004.
- Claussen, M., Mysak, L., Weaver, A., Crucifix, M., Fichet, T., Loutre, M.-F., Weber, S., Alcamo, J., Alexeev, V., Berger, A., Calov, R., Ganopolski, A., Goosse, H., Lohmann, G., Lunkeit, F., Mokhov, I., Petoukhov, V., Stone, P., and Wang, Z.: Earth system models of intermediate complexity: closing the gap in the spectrum of climate system models, *Climate Dynamics*, 18, 579–586, doi:10.1007/s00382-001-0200-1, URL <http://www.springerlink.com/openurl.asp?genre=article&id=doi:10.1007/s00382-001-0200-1>, 2002.
- Cleveland, C. and Liptzin, D.: C : N : P stoichiometry in soil: is there a “Redfield ratio” for the microbial biomass?, *Biogeochemistry*, 85, 235–252, doi:10.1007/s10533-007-9132-0, 2007.
- Cleveland, C. C., Townsend, A. R., Schimel, D. S., Fisher, H., Howarth, R. W., Hedin, L. O., Perakis, S. S., Latty, E. F., Von Fischer, J. C., Elseroad, A., and Wasson, M. F.: Global patterns of terrestrial biological nitrogen (N₂) fixation in natural ecosystems, *Global Biogeochemical Cycles*, 13, 623, URL <http://www.agu.org/pubs/crossref/1999/1999GB900014.shtml>, 1999.
- Cole, C., Innis, G., and Stewart, J.: Simulation of phosphorus in semiarid grasslands, *Ecology*, 58, 1–15, doi:10.2307/1935104, 1977.
- Collatz, G., Ribas-Carbo, M., and Berry, J.: Coupled photosynthesis-stomatal conductance model for leaves of C₄ plants, *Australian journal of plant physiology*, 19, 519–538, 1992.
- Cornelissen, J.: An experimental comparison of leaf decomposition rates in a wide range of temperate plant species and types, *J. Ecol.*, 84, 573–582, doi:10.2307/2261479, 1996.
- Cornelissen, J., Diez, P., and Hunt, R.: Seedling growth, allocation and leaf attributes in a wide range of woody plant species and types, *J. Ecol.*, 84, 755–765, doi:10.2307/2261337, 1996.
- Cornelissen, J., Cerabolini, B., Castro-Diez, P., Villar-Salvador, P., Montserrat-Marti, G., Puyravaud, J., Maestro, M., Werger, M., and Aerts, R.: Functional traits of woody plants: correspondence of species rankings between field adults and laboratory-grown seedlings?, *J. Veg. Sci.*, 14, 311–322, doi:10.1658/1100-9233(2003)014, 2003.

BIBLIOGRAPHY

- Cornelissen, J., Queded, H., Gwynn-Jones, D., Van Logtestijn, R., De Beus, M., Kondratchuk, A., Callaghan, T., and Aerts, R.: Leaf digestibility and litter decomposability are related in a wide range of subarctic plant species and types, *Funct. Ecol.*, 18, 779–786, doi:10.1111/j.0269-8463.2004.00900.x, 2004.
- Coss, A. and Schlesinger, W.: A literature-review and evaluation of the hedley fractionation - applications to the biogeochemical cycle of soil-phosphorus in natural ecosystems, *Geoderma*, 64, 197–214, 1995.
- Crafts-Brandner, S. J. and Salvucci, M. E.: Rubisco activase constrains the photosynthetic potential of leaves at high temperature and CO₂, *Proceedings of the National Academy of Sciences*, 97, 13 430–13 435, 2000.
- Craine, J., Lee, W., Bond, W., Williams, R., and Johnson, L.: Environmental constraints on a global relationship among leaf and root traits of grasses, *Ecology*, 86, 12–19, doi:10.1890/04-1075, 2005.
- Craine, J., Elmore, A., Aidar, M., Bustamante, M., Dawson, T., Hobbie, E., Kahmen, A., Mack, M., McLauchlan, K., Michelsen, A., Nardoto, G., Pardo, L., Penuelas, J., Reich, P., Schuur, E., Stock, W., Templer, P., Virginia, R., Welker, J., and Wright, I. J.: Global patterns of foliar nitrogen isotopes and their relationships with climate, mycorrhizal fungi, foliar nutrient concentrations, and nitrogen availability, *New Phytol.*, 183, 980–992, doi: 10.1111/j.1469-8137.2009.02917.x, 2009.
- Cunningham, S. C. and Read, J.: Do temperate rainforest trees have a greater ability to acclimate to changing temperatures than tropical rainforest trees?, *New Phytologist*, 157, 55–64, doi:10.1046/j.1469-8137.2003.00652.x, URL <http://doi.wiley.com/10.1046/j.1469-8137.2003.00652.x>, 2003.
- Davidson, E., de Carvalho, C., Figueira, A., Ishida, F., Ometto, J., Nardoto, G., Saba, R., Hayashi, S., Leal, E., Vieira, I., and Martinelli, L.: Recuperation of nitrogen cycling in Amazonian forests following agricultural abandonment, *Nature*, 447, 995–998, doi:10.1038/nature05900, 2007.
- Davidson, E. a. and Janssens, I. a.: Temperature sensitivity of soil carbon decomposition and feedbacks to climate change., *Nature*, 440, 165–73, doi:10.1038/nature04514, URL <http://www.ncbi.nlm.nih.gov/pubmed/16525463>, 2006.
- Denman, K. L., Brasseur, G., Chidthaisong, A., Ciais, P., Cox, P. M., Dickinson, R. E., Hauglustaine, D., Heinze, C., Holland, E., Jacob, D., Lohmann, U., Ramachandran, S., da Silva Dias, P. L., Wofsy, S. C., and Zhang, X.: Couplings Between Changes in the Climate System and Biogeochemistry, in: *Climate Change 2007: The Physical Science Basis. Contribution of Working Group I to the Fourth Assessment Report of the Intergovernmental Panel on Climate Change*, edited by Solomon, S., Qin, D., Manning, M., Chen, Z., Marquis, M., Averyt, K. B., Tignor, M., and Miller, H. L., Cambridge University Press, Cambridge, United Kingdom and New York, NY, USA, 2007.

- Dentener, F., Drevet, J., Lamarque, J., Bey, I., Eickhout, B., Fiore, A., Hauglustaine, D., Horowitz, L., Krol, M., Kulshrestha, U., Lawrence, M., Galy-Lacaux, C., Rast, S., Shindell, D., Stevenson, D., Van Noije, T., Atherton, C., Bell, N., Bergman, D., Butler, T., Cofala, J., Collins, B., Doherty, R., Ellingsen, K., Galloway, J., Gauss, M., Montanaro, V., Mueller, J., Pitari, G., Rodriguez, J., Sanderson, M., Solomon, F., Strahan, S., Schultz, M., Sudo, K., Szopa, S., and Wild, O.: Nitrogen and sulfur deposition on regional and global scales: A multimodel evaluation, *Global Biogeochem. Cy.*, 20, doi:10.1029/2005GB002672, 2006.
- Diaz, S., Hodgson, J., Thompson, K., Cabido, M., Cornelissen, J., Jalili, A., Montserrat-Marti, G., Grime, J., Zarrinkamar, F., Asri, Y., Band, S., Basconcelo, S., Castro-Diez, P., Funes, G., Hamzehee, B., Khoshnevi, M., Perez-Harguindeguy, N., Perez-Rontome, M., Shirvany, F., Vendramini, F., Yazdani, S., Abbas-Azimi, R., Bogaard, A., Boustani, S., Charles, M., Dehghan, M., de Torres-Espuny, L., Falczuk, V., Guerrero-Campo, J., Hynd, A., Jones, G., Kowsary, E., Kazemi-Saeed, F., Maestro-Martinez, M., Romo-Diez, A., Shaw, S., Siavash, B., Villar-Salvador, P., and Zak, M.: The plant traits that drive ecosystems: Evidence from three continents, *J. Veg. Sci.*, 15, 295–304, doi:10.1658/1100-9233(2004)015, 2004.
- Drever, J. I.: The effect of land plants on weathering rates of silicate minerals, *Geochimica et Cosmochimica Acta*, 58, 2325–2332, URL [http://dx.doi.org/10.1016/0016-7037\(94\)90013-2](http://dx.doi.org/10.1016/0016-7037(94)90013-2), 1994.
- Elser, J. J., Bracken, M. E. S., Cleland, E. E., Gruner, D. S., Harpole, W. S., Hillebrand, H., Ngai, J. T., Seabloom, E. W., Shurin, J. B., and Smith, J. E.: Global analysis of nitrogen and phosphorus limitation of primary producers in freshwater, marine and terrestrial ecosystems, *ECOLOGY LETTERS*, 10, 1135–1142, doi:10.1111/j.1461-0248.2007.01113.x, 2007.
- Esser, G., Kattge, J., and Sakalli, A.: Feedback of carbon and nitrogen cycles enhances carbon sequestration in the terrestrial biosphere, *Global Change Biol.*, 17, 819–842, doi:10.1111/j.1365-2486.2010.02261.x, 2011.
- FAO: Current world fertilizer trend and outlook 2015, Tech. rep., Food & Agriculture Organization of the United Nations, Rome, 2012.
- Farquhar, G., Caemmerer, S., and Berry, J.: A biochemical model of photosynthetic CO₂ assimilation in leaves of C-3 species, *Planta*, 149, 78–90, 1980.
- Feeley, K. J., Joseph Wright, S., Nur Supardi, M. N., Kassim, A. R., and Davies, S. J.: Decelerating growth in tropical forest trees., *Ecology letters*, 10, 461–9, URL <http://www.ncbi.nlm.nih.gov/pubmed/17498145>, 2007.
- Fekete, B. M.: High-resolution fields of global runoff combining observed river discharge and simulated water balances, *Global Biogeochemical Cycles*, 16, 1042, URL <http://www.agu.org/pubs/crossref/2002/1999GB001254.shtml>, 2002.
- Field, C., Chapin, F., Matson, P., and Mooney, H.: Responses of terrestrial ecosystem to the changing atmosphere - a resource-based approach, *Annu. Rev. Ecol. Syst.*, 23, 201–235, 1992.

BIBLIOGRAPHY

- Field, C., Behrenfeld, M., Randerson, J., and Falkowski, P.: Primary production of the biosphere: Integrating terrestrial and oceanic components, *Science*, 281, 237–240, 1998.
- Fisher, J. B., Sitch, S., Malhi, Y., Fisher, R. a., Huntingford, C., and Tan, S.-Y.: Carbon cost of plant nitrogen acquisition: A mechanistic, globally applicable model of plant nitrogen uptake, retranslocation, and fixation, *Global Biogeochemical Cycles*, 24, 1–17, doi:10.1029/2009GB003621, URL <http://www.agu.org/pubs/crossref/2010/2009GB003621.shtml>, 2010.
- Fisher, J. B., Badgley, G., and Blyth, E.: Global nutrient limitation in terrestrial vegetation, *Global Biogeochemical Cycles*, 26, URL <http://www.agu.org/pubs/crossref/pip/2011GB004252.shtml>, 2012.
- Fortunel, C., Garnier, E., Joffre, R., Kazakou, E., Quested, H., Grigulis, K., Lavorel, S., Ansquer, P., Castro, H., Cruz, P., Dolezal, J., Eriksson, O., Freitas, H., Golodets, C., Jouany, C., Kigel, J., Kleyer, M., Lehsten, V., Leps, J., Meier, T., Pakeman, R., Papadimitriou, M., Papanastasis, V., Quetier, F., Robson, M., Sternberg, M., Theau, J.-P., Thebault, A., and Zarovali, M.: Leaf traits capture the effects of land use changes and climate on litter decomposability of grasslands across Europe, *Ecology*, 90, 598–611, doi:10.1890/08-0418.1, 2009.
- Friedlingstein, P., Cox, P., Betts, R., Bopp, L., Von Bloh, W., Brovkin, V., Cadule, P., Doney, S., Eby, M., Fung, I., Bala, G., John, J., Jones, C., Joos, F., Kato, T., Kawamiya, M., Knorr, W., Lindsay, K., Matthews, H., Raddatz, T., Rayner, P., Reick, C., Roeckner, E., Schnitzler, K.-G., Schnur, R., Strassmann, K., Weaver, A., Yoshikawa, C., and Zeng, N.: Climate-carbon cycle feedback analysis: Results from the (CMIP)-M-4 model intercomparison, *J. Climate*, 19, 3337–3353, 2006.
- Friedlingstein, P., Houghton, R., Marland, G., Hackler, J., Boden, T., Conway, T., Canadell, J., Raupach, M., Ciais, P., and Le Quere, C.: Update on CO₂ emissions, *Nature Geosci.*, 3, 811–812, doi:10.1038/ngeo1022, 2010.
- Friend, A. D.: Terrestrial plant production and climate change, *Journal of experimental botany*, 61, 1293–1309, doi:10.1093/jxb, 2010.
- Fyllas, N., Patino, S., Baker, T., Nardoto, G., Martinelli, L., Quesada, C., Paiva, R., Schwarz, M., Horna, V., Mercado, L., Santos, A., Arroyo, L., Jimenez, E., Luizao, F., Neill, D., Silva, N., Prieto, A., Rudas, A., Silviera, M., Vieira, I., Lopez-Gonzalez, G., Malhi, Y., Phillips, O., and Lloyd, J.: Basin-wide variations in foliar properties of Amazonian forest: phylogeny, soils and climate, *Biogeosciences*, 6, 2677–2708, 2009.
- Gaillardet, J., Dupre, B., Louvat, P., and Allegre, C. J.: Global silicate weathering and CO₂ consumption rates deduced from the chemistry of large rivers, *Chemical Geology*, 159, 3–30, 1999.
- Galloway, J., Dentener, F., Capone, D., Boyer, E., Howarth, R., Seitzinger, S., Asner, G., Cleveland, C., Green, P., Holland, E., Karl, D., Michaels, A., Porter, J., and Townsend, A. a. V. C.: Nitrogen cycles: past, present, and future, *Biogeochemistry*, 70, 153–226, 2004.

- Garnier, E., Lavorel, S., Ansquer, P., Castro, H., Cruz, P., Dolezal, J., Eriksson, O., Fortunel, C., Freitas, H., Golodets, C., Grigulis, K., Jouany, C., Kazakou, E., Kigel, J., Kleyer, M., Lehsten, V., Leps, J., Meier, T., Pakeman, R., Papadimitriou, M., Papanastasis, V., Queded, H., Quetier, F., Robson, M., Roumet, C., Rusch, G., Skarpe, C., Sternberg, M., Theau, J.-P., Thebault, A., Vile, D., and Zarovali, M.: Assessing the effects of land-use change on plant traits, communities and ecosystem functioning in grasslands: A standardized methodology and lessons from an application to 11 European sites, *Ann. Bot.*, 99, 967–985, doi:10.1093/aob, 90th Annual Meeting of the Ecological-Society-of-America/9th International Congress of Ecology, Montreal, CANADA, AUG, 2005, 2007.
- Gedney, N., Cox, P. M., Betts, R. A., Boucher, O., Huntingford, C., and Stott, P. A.: Detection of a direct carbon dioxide effect in continental river runoff records., *Nature*, 439, 835–8, URL <http://dx.doi.org/10.1038/nature04504>, 2006.
- Gerber, S., Hedin, L., Oppenheimer, M., Pacala, S., and Shevliakova, E.: Nitrogen cycling and feedbacks in a global dynamic land model, *Global Biogeochem. Cy.*, 24, doi:10.1029/2008GB003336, 2010.
- Giardina, C. and Ryan, M.: Evidence that decomposition rates of organic carbon in mineral soil do not vary with temperature, *Nature*, 404, 858–861, 2000.
- Gilbert, N.: Environment: The disappearing nutrient., *Nature*, 461, 716–8, URL <http://www.nature.com/news/2009/091007/full/461716a.html>, 2009.
- Godderis, Y., Roelandt, C., Schott, J., Pierret, M.-C., and Francois, L. M.: Towards an Integrated Model of Weathering, Climate, and Biospheric Processes, *Reviews in Mineralogy and Geochemistry*, 70, 411–434, doi:10.2138/rmg.2009.70.9, URL <http://ring.geoscienceworld.org/cgi/doi/10.2138/rmg.2009.70.9>, 2009.
- Goll, D. S., Brovkin, V., Parida, B. R., Reick, C. H., Kattge, J., Reich, P. B., van Bodegom, P. M., and Niinemets, U.: Nutrient limitation reduces land carbon uptake in simulations with a model of combined carbon, nitrogen and phosphorus cycling, *Biogeosciences*, 9, 3547–3569, doi: 10.5194/bg-9-3547-2012, URL <http://www.biogeosciences.net/9/3547/2012/>, 2012.
- Gruber, N. and Galloway, J.: An earth-system perspective of the global nitrogen cycle, *Nature*, 451, 293–296, doi:10.1038/nature06592, 2008.
- Gunderson, C. A., O'Hara, K. H., Campion, C. M., Walker, A. V., and Edwards, N. T.: Thermal plasticity of photosynthesis: the role of acclimation in forest responses to a warming climate, *Global change biology*, 16, 2272–2286, doi:10.1111/j.1365-2486.2009.02090.x, 2010.
- Han, W., Fang, J., Guo, D., and Zhang, Y.: Leaf nitrogen and phosphorus stoichiometry across 753 terrestrial plant species in China, *New Phytol.*, 168, 377–385, doi:10.1111/j.1469-8137.2005.01530.x, 2005.

BIBLIOGRAPHY

- Harley, P., Thomas, R., Reynolds, J., and Strain, B.: Modeling photosynthesis of cotton grown in elevated CO₂, *Plant cell and environment*, 15, 271–282, doi:10.1111/j.1365-3040.1992.tb00974.x, 1992.
- Harrison, J. a.: Dissolved inorganic phosphorus export to the coastal zone: Results from a spatially explicit, global model, *Global Biogeochemical Cycles*, 19, doi:10.1029/2004GB002357, URL <http://www.agu.org/pubs/crossref/2005/2004GB002357.shtml>, 2005.
- Hartmann, J. and Moosdorf, N.: Chemical weathering rates of silicate-dominated lithological classes and associated liberation rates of phosphorus on the Japanese Archipelago—Implications for global scale analysis, *Chemical Geology*, 287, 125–157, doi:10.1016/j.chemgeo.2010.12.004, URL <http://linkinghub.elsevier.com/retrieve/pii/S0009254110004389>, 2011.
- Hartmann, J., Jansen, N., Dürr, H. H., Kempe, S., and Köhler, P.: Global CO₂-consumption by chemical weathering: What is the contribution of highly active weathering regions?, *Global and Planetary Change*, 69, 185–194, URL <http://dx.doi.org/10.1016/j.gloplacha.2009.07.007>, 2009.
- Hartmann, J., Dürr, H. H., Moosdorf, N., Meybeck, M., and Kempe, S.: The geochemical composition of the terrestrial surface (without soils) and comparison with the upper continental crust, *International Journal of Earth Sciences*, 101, 365–376, doi:10.1007/s00531-010-0635-x, URL <http://www.springerlink.com/index/10.1007/s00531-010-0635-x>, 2012.
- He, J., Wang, Z., Wang, X., Schmid, B., Zuo, W., Zhou, M., Zheng, C., Wang, M., and Fang, J.: A test of the generality of leaf trait relationships on the Tibetan Plateau, *New Phytol.*, 170, 835–848, doi:10.1111/j.1469-8137.2006.01704.x, 2006.
- He, J.-S., Wang, L., Flynn, D., Wang, X., Ma, W., and Fang, J.: Leaf nitrogen : phosphorus stoichiometry across Chinese grassland biomes, *Oecologia*, 155, 301–310, doi:10.1007/s00442-007-0912-y, 2008.
- Hickler, T., Smith, B., Prentice, I., Mjofors, K., Miller, P., Arneth, A., and Sykes, M.: CO₂ fertilization in temperate FACE experiments not representative of boreal and tropical forests, *Global Change Biol.*, 14, 1531–1542, doi:10.1111/j.1365-2486.2008.01598.x, 2008.
- Hikosaka, K., Ishikawa, K., Borjigidai, A., Muller, O., and Onoda, Y.: Temperature acclimation of photosynthesis: mechanisms involved in the changes in temperature dependence of photosynthetic rate, *Journal of experimental botany*, 57, 291–302, doi:10.1093/jxb, 2006.
- Hoenisch, B., Hemming, N., Archer, D., Siddall, M., and McManus, J.: Atmospheric carbon dioxide concentration across the mid-pleistocene transition, *Science*, 324, 1551–1554, doi:10.1126/science.1171477, 2009.
- Hogberg, M., Baath, E., Nordgren, A., Arnebrant, K., and Hogberg, P.: Contrasting effects of nitrogen availability on plant carbon supply to mycorrhizal fungi and saprotrophs - a

- hypothesis based on field observations in boreal forest, *New Phytol.*, 160, 225–238, doi:10.1046/j.1469-8137.2003.00867.x, 2003.
- Houlton, B., Wang, Y.-P., Vitousek, P., and Field, C.: A unifying framework for dinitrogen fixation in the terrestrial biosphere, *Nature*, 454, 327–U34, doi:10.1038/nature07028, 2008.
- Hungate, B., Dukes, J., Shaw, M., Luo, Y., and Field, C.: Nitrogen and climate change, *Science*, 302, 1512–1513, doi:10.1126/science.1091390, URL <http://www.sciencemag.org/content/302/5650/1512.short>, 2003.
- Hurrell, J. and Visbeck, M.: WCRP Coupled Model Intercomparison Project - Phase 5 Editorial WCRP Modelling Strategy Developments, 16, 2011.
- Ise, T. and Moorcroft, P. R.: The global-scale temperature and moisture dependencies of soil organic carbon decomposition: an analysis using a mechanistic decomposition model, *Biogeochemistry*, 80, 217–231, doi:10.1007/s10533-006-9019-5, URL <http://www.springerlink.com/index/10.1007/s10533-006-9019-5>, 2006.
- Jahnke, R.: The phosphorus cycle, pp. 301–315, *Global Biogeochem. Cy.*, Academic Press, London, 1992.
- Jain, A., Yang, X., Kheshgi, H., McGuire, a. D., Post, W., and Kicklighter, D.: Nitrogen attenuation of terrestrial carbon cycle response to global environmental factors, *Global Biogeochemical Cycles*, 23, 1–13, doi:10.1029/2009GB003519, URL <http://www.agu.org/pubs/crossref/2009/2009GB003519.shtml>, 2009.
- Janssens, I. a., Dieleman, W., Luysaert, S., Subke, J.-a., Reichstein, M., Ceulemans, R., Ciais, P., Dolman, a. J., Grace, J., Matteucci, G., Papale, D., Piao, S. L., Schulze, E.-D., Tang, J., and Law, B.: Reduction of forest soil respiration in response to nitrogen deposition, *Nature Geoscience*, 3, 315–322, doi:10.1038/ngeo844, URL <http://www.nature.com/doifinder/10.1038/ngeo844>, 2010.
- Johnson, A., Frizano, J., and Vann, D.: Biogeochemical implications of labile phosphorus in forest soils determined by the Hedley fractionation procedure, *Oecologia*, 135, 487–499, doi:10.1007/s00442-002-1164-5, 2003.
- Johnson, D., Cheng, W., Joslin, J., Norby, R., Edwards, N., and Todd, D.: Effects of elevated CO₂ on nutrient cycling in a sweetgum plantation, *Biogeochemistry*, 69, 379–403, doi:10.1023/B: BIOG.0000031054.19158.7c, 2004.
- Jones, C., McConnell, C., Coleman, K., Cox, P., Falloon, P., Jenkinson, D., and Powlson, D.: Global climate change and soil carbon stocks; predictions from two contrasting models for the turnover of organic carbon in soil, *Global Change Biology*, 11, 154–166, doi:10.1111/j.1365-2486.2004.00885.x, URL <http://doi.wiley.com/10.1111/j.1365-2486.2004.00885.x>, 2005.

BIBLIOGRAPHY

- June, T., Evans, J., and Farquhar, G.: A simple new equation for the reversible temperature dependence of photosynthetic electron transport: a study on soybean leaf, *Functional plant biology*, 31, 275–283, doi:10.1071/FP03250, 2004.
- Kattge, J. and Knorr, W.: Temperature acclimation in a biochemical model of photosynthesis: a reanalysis of data from 36 species, *Plant cell and environment*, 30, 1176–1190, doi:10.1111/j.1365-3040.2007.01690.x, 2007.
- Kattge, J., Diaz, S., Lavorel, S., Prentice, I., Leadley, P., Bonisch, G., Garnier, E., Westoby, M., Reich, P., Wright, I., Cornelissen, J., Violle, C., Harrison, S., van Bodegom, P., Reichstein, M., Enquist, B., Soudzilovskaia, N., Ackerly, D., Ananad, M., Atkin, O., Bahn, M., Baker, T., Baldocchi, D., Bekker, R., Blanco, C., Blonder, B., Bond, W., Bradstock, R., Bunker, D., Casanoves, F., Cavender-Bares, J., Chambers, J., Chapin, F., Chave, J., Coomes, D., Cornwell, W., Craine, J., Dobrin, B., Duarte, L., Durka, W., Elser, J., Esser, G., Estiarte, M., Fagan, W., Fang, J., Fernandez-Mendez, F., Fidelis, A., Finegan, B., Flores, O., Ford, H., Frank, D., Freschet, G., Fyllas, N., Gallagher, R., Green, W., Guitierrez, A., Hickler, T., Higgins, S., Hodgson, J., Jalili, A., Jansen, S., Joly, C., Kerkhoff, A., Kirkup, D., Kitajima, K., Kleyer, M., Klotz, S., Knops, J., Kramer, K., Kuhn, I., Kurokawa, H., Laughlin, D., Lee, T., Leishman, M., Lens, F., Lenz, T., Lewis, S., Lloyd, J., Llusia, J., Louault, F., Ma, S., Mahecha, M., Manning, P., Massad, T., Medlyn, B., Messier, J., Moles, A., Muller, S., Nadrowski, K., Naeem, S., Niinemets, U., Nollert, S., Nuske, A., Ogaya, R., Oleksyn, J., Onipchenko, V., Onoda, Y., Ordonez, J., Overbeck, G., Ozinga, W., Patino, S., Paula, S., Pausas, J., Penuelas, J., Phillips, O., Pillar, V., Poorter, H., Poorter, L., Poschlod, P., Prinzing, A., Proulx, R., Rammig, A., Reinsch, S., Reu, B., Sack, L., Salgado-Negret, B., Sardans, J., Shiodera, S., Shipley, B., Sieffert, A., Sosinski, E., Soussana, J.-F., Swaine, E., Swenson, N., Thompson, K., Thornton, P., Waldram, M., Weiher, E., White, M., White, S., Wright, S., Yguel, B., Zaehle, S., Zanne, A., and Wirth, C.: TRY – a global database of plant traits, *Global Change Biol.*, pp. no–no, doi:10.1111/j.1365-2486.2011.02451.x, URL <http://dx.doi.org/10.1111/j.1365-2486.2011.02451.x>, 2011.
- Kattge, J., Knorr, W., Raddatz, T., and Wirth, C.: Quantifying photosynthetic capacity and its relationship to leaf nitrogen content for global-scale terrestrial biosphere models, *Glob. Change Biol.*, 15, 976–991, doi:10.1111/j.1365-2486.2008.01744.x, 2009.
- Kazakou, E., Vile, D., Shipley, B., Gallet, C., and Garnier, E.: Co-variations in litter decomposition, leaf traits and plant growth in species from a Mediterranean old-field succession, *Funct. Ecol.*, 20, 21–30, doi:10.1111/j.1365-2435.2006.01080.x, 2006.
- Khan, F., Lukac, M., Turner, G., and Godbold, D.: Elevated atmospheric CO₂ changes phosphorus fractions in soils under a short rotation poplar plantation (EuroFACE), *Soil Biol. Biochem.*, 40, 1716–1723, doi:10.1016/j.soilbio.2008.02.008, 2008.
- Knorr, W.: Annual and interannual CO₂ exchanges of the terrestrial biosphere: process-based simulations and uncertainties, *Global ecology and biogeography*, 9, 225–252, 2000.

- Knorr, W., Prentice, I. C., House, J. I., and Holland, E. A.: Long-term sensitivity of soil carbon turnover to warming, *Nature*, 433, 298–301, doi:doi:10.1038/nature03226, 2005.
- Körner, C.: Biosphere responses to CO₂ enrichment, *Ecological Applications*, 10, 1590–1619, 2000.
- Lasslop, G., Reichstein, M., Papale, D., Richardson, A. D., Arneth, A., Barr, A., Stoy, P., and Wohlfahrt, G.: Separation of net ecosystem exchange into assimilation and respiration using a light response curve approach: critical issues and global evaluation, *Global Change Biology*, 16, 187–208, doi:10.1111/j.1365-2486.2009.02041.x, URL <http://doi.wiley.com/10.1111/j.1365-2486.2009.02041.x>, 2010.
- Laughlin, D., Leppert, J., Moore, M., and Sieg, C.: A multi-trait test of the leaf-height-seed plant strategy scheme with 133 species from a pine forest flora, *Funct. Ecol.*, 24, 493–501, doi:10.1111/j.1365-2435.2009.01672.x, 2010.
- Leinonen, I.: A Simulation Model for the Annual Frost Hardiness and Freeze Damage of Scots Pine, *Annals of Botany*, 78, 687–693, doi:10.1006/anbo.1996.0178, URL <http://aob.oxfordjournals.org/content/78/6/687.abstract>, 1996.
- Lenton, T. and Watson, A.: *Revolutions that Made the Earth*, Oxford University Press, USA, 2011.
- Lenton, T. M.: The role of land plants, phosphorus weathering and fire in the rise and regulation of atmospheric oxygen, *Global Change Biology*, 7, 613–629, URL <http://doi.wiley.com/10.1046/j.1354-1013.2001.00429.x>, 2001.
- Lieth, H.: Modeling the primary productivity of the world, *Archivio Botanico e Biogeografico Italiano*, 48, 11–16, 1972.
- Lin, Y.-S., Medlyn, B. E., and Ellsworth, D. S.: Temperature responses of leaf net photosynthesis: the role of component processes, *Tree physiology*, 32, 219–231, doi:10.1093/treephys, 2012.
- Lloyd, J. and Farquhar, G. D.: Effects of rising temperatures and [CO₂] on the physiology of tropical forest trees., *Philosophical transactions of the Royal Society of London. Series B, Biological sciences*, 363, 1811–7, URL <http://rstb.royalsocietypublishing.org/cgi/content/abstract/363/1498/1811>, 2008.
- Luethi, D., Le Floch, M., Bereiter, B., Blunier, T., Barnola, J.-M., Siegenthaler, U., Raynaud, D., Jouzel, J., Fischer, H., Kawamura, K., and Stocker, T.: High-resolution carbon dioxide concentration record 650,000–800,000 years before present, *Nature*, 453, 379–382, doi:10.1038/nature06949, 2008.
- Luo, Y., Wan, S., Hui, D., and Wallace, L. L.: Acclimatization of soil respiration to warming in a tall grass prairie., *Nature*, 413, 622–5, doi:10.1038/35098065, URL <http://www.ncbi.nlm.nih.gov/pubmed/11675783>, 2001.

BIBLIOGRAPHY

- Luo, Y., Su, B., Currie, W., Dukes, J., Finzi, A., Hartwig, U., Hungate, B., McMurtrie, R., Oren, R., Parton, W., Pataki, D., Shaw, M., Zak, D., and Field, C.: Progressive nitrogen limitation of ecosystem responses to rising atmospheric carbon dioxide, *Bioscience*, 54, 731–739, 2004.
- Mahowald, N., Jickells, T., Baker, A., Artaxo, P., Benitez-Nelson, C., Bergametti, G., Bond, T., Chen, Y., Cohen, D., Herut, B., Kubilay, N., Losno, R., Luo, C., Maenhaut, W., McGee, K., Okin, G., Siefert, R., and Tsukuda, S.: Global distribution of atmospheric phosphorus sources, concentrations and deposition rates, and anthropogenic impacts, *Global Biogeochem. Cy.*, 22, doi:10.1029/2008GB003240, 2008.
- Marklein, A. R. and Houlton, B. Z.: Nitrogen inputs accelerate phosphorus cycling rates across a wide variety of terrestrial ecosystems., *The New phytologist*, 193, 696–704, URL <http://www.ncbi.nlm.nih.gov/pubmed/22122515>, 2012.
- Marsland, S., Haak, H., Jungclaus, J., Latif, M., and Roske, F.: The Max-Planck-Institute global ocean/sea ice model with orthogonal curvilinear coordinates, *Ocean Model.*, 5, 91–127, 2003.
- McGill, W. and Cole, C.: Comparative aspects of cycling of organic C, N, S, and P through soil organic matter, *Geoderma*, 26, 267–268, 1981.
- McGroddy, M., Daufresne, T., and Hedin, L.: Scaling of C : N : P stoichiometry in forests worldwide: Implications of terrestrial redfield-type ratios., *Ecology*, 85, 2390–2401, 2004.
- McKay, M., Beckman, R., and Conover, W.: A comparison of three methods for selecting values of input variables in the analysis of output from a computer code, *Technometrics*, 21, 239–245, 1979.
- Medlyn, B., Loustau, D., and Delzon, S.: Temperature response of parameters of a biochemically based model of photosynthesis. I. Seasonal changes in mature maritime pine (*Pinus pinaster* Ait.), *Plant cell and environment*, 25, 1155–1165, doi:10.1046/j.1365-3040.2002.00890.x, 2002.
- Meixner, T. and Bales, R.: Hydrochemical modeling of coupled C and N cycling in high-elevation catchments: Importance of snow cover, *Biogeochemistry*, 62, 289–308, doi:10.1023/A:1021118922787, 2003.
- Melillo, J. M., Butler, S., Johnson, J., Mohan, J., Steudler, P., Lux, H., Burrows, E., Bowles, F., Smith, R., Scott, L., Vario, C., Hill, T., Burton, A., Zhou, Y.-M., and Tang, J.: Soil warming, carbon-nitrogen interactions, and forest carbon budgets, *Proc. Natl. Acad. Sci. U. S. A.*, 108, 9508–9512, doi:10.1073/pnas.1018189108, 2011.
- Meybeck, M.: Carbon, nitrogen, and phosphorus transport by world rivers, *American Journal of Science*, 282, 401–450, URL <http://www.ajsonline.org/cgi/content/abstract/282/4/401>, 1982.
- Meziane, D. and Shipley, B.: Interacting determinants of specific leaf area in 22 herbaceous species: effects of irradiance and nutrient availability, *Plant Cell Environ.*, 22, 447–459, doi:10.1046/j.1365-3040.1999.00423.x, 1999.

- Morford, S. L., Houlton, B. Z., and Dahlgren, R. A.: Increased forest ecosystem carbon and nitrogen storage from nitrogen rich bedrock., *Nature*, 477, 78–81, URL http://www.nature.com/nature/journal/v477/n7362/full/nature10415.html?WT.ec%5C_i %5C%3B, 2011.
- Morin, X., Lechowicz, M., Augspurger, C., O' Keefe, J., Viner, D., and Chuine, I.: Leaf phenology in 22 North American tree species during the 21st century, *Glob. Change Biol.*, 15, 961–975, doi:10.1111/j.1365-2486.2008.01735.x, 2009.
- Niinemets, U.: Components of leaf dry mass per area - thickness and density - alter leaf photosynthetic capacity in reverse directions in woody plants, *New Phytol.*, 144, 35–47, doi:10.1046/j.1469-8137.1999.00466.x, 4th New Phytologist Symposium, MONTPELLIER, FRANCE, OCT 05-06, 1998, 1999.
- Niinemets, U.: Global-scale climatic controls of leaf dry mass per area, density, and thickness in trees and shrubs, *Ecology*, 82, 453–469, doi:10.2307/2679872, 2001.
- Norby, R., Warren, J., Iversen, C., Medlyn, B., and McMurtrie, R.: CO₂ enhancement of forest productivity constrained by limited nitrogen availability, *Proc. Natl. Acad. Sci. U. S. A.*, 107, 19 368–19 373, doi:10.1073/pnas.1006463107, 2010.
- Ogaya, R. and Penuelas, J.: Comparative field study of *Quercus ilex* and *Phillyrea latifolia*: photosynthetic response to experimental drought conditions, *Environ. Exp. Bot.*, 50, 137–148, doi: 10.1016/S0098-8472(03)00019-4, 2003.
- Ogaya, R. and Penuelas, J.: Contrasting foliar responses to drought in *Quercus ilex* and *Phillyrea latifolia*, *Biol. Plant.*, 50, 373–382, doi:10.1007/s10535-006-0052-y, 2006.
- Ogaya, R. and Penuelas, J.: Tree growth, mortality, and above-ground biomass accumulation in a holm oak forest under a five-year experimental field drought, *Plant Ecol.*, 189, 291–299, doi: 10.1007/s11258-006-9184-6, 2007.
- Ogaya, R. and Penuelas, J.: Changes in leaf $\delta(13)C$ and $\delta(15)N$ for three Mediterranean tree species in relation to soil water availability, *Acta Oecol.-Int. J. Ecol.*, 34, 331–338, doi: 10.1016/j.actao.2008.06.005, 2008.
- Olsson, P., Linder, S., Giesler, R., and Hogberg, P.: Fertilization of boreal forest reduces both autotrophic and heterotrophic soil respiration, *Glob. Change Biol.*, 11, 1745–1753, doi:10.1111/j.1365-2486.2005.001033.x, 2005.
- Onoda, Y., Hikosaka, K., and Hirose, T.: The balance between RuBP carboxylation and RuBP regeneration: a mechanism underlying the interspecific variation in acclimation of photosynthesis to seasonal change in temperature, *Functional plant biology*, 32, 903–910, doi: 10.1071/FP05024, 2005.
- Ordonez, J., van Bodegom, P., Witte, J.-P., Bartholomeus, R., van Dobben, H., and Aerts, R.: Leaf habit and woodiness regulate different leaf economy traits at a given nutrient supply, *Ecology*, 91, 3218–3228, doi:10.1890/09-1509.1, 2010a.

BIBLIOGRAPHY

- Ordonez, J. C., van Bodegom, P., Witte, J.-P., Bartholomeus, R., van Hal, J., and Aerts, R.: Plant Strategies in Relation to Resource Supply in Mesic to Wet Environments: Does Theory Mirror Nature?, *Am. Nat.*, 175, 225–239, doi:10.1086/649582, 2010b.
- Pagani, M., Caldeira, K., Berner, R., and Beerling, D. J.: The role of terrestrial plants in limiting atmospheric CO₂ decline over the past 24 million years., *Nature*, 460, 85–8, URL <http://www.ncbi.nlm.nih.gov/pubmed/19571882>, 2009.
- Pakeman, R., Garnier, E., Lavorel, S., Ansquer, P., Castro, H., Cruz, P., Dolezal, J., Eriksson, O., Freitas, H., Golodets, C., Kigel, J., Kleyer, M., Leps, J., Meier, T., Papadimitriou, M., Papanastasis, V., Quested, H., Quetier, F., Rusch, G., Sternberg, M., Theau, J.-P., Thebault, A., and Vile, D.: Impact of abundance weighting on the response of seed traits to climate and land use, *J. Ecol.*, 96, 355–366, doi:10.1111/j.1365-2745.2007.01336.x, 2008.
- Pakeman, R., Leps, J., Kleyer, M., Lavorel, S., Garnier, E., and Consortium, V.: Relative climatic, edaphic and management controls of plant functional trait signatures, *J. Veg. Sci.*, 20, 148–159, doi:10.1111/j.1654-1103.2009.05548.x, 2009.
- Pan, Y., Birdsey, R. A., Fang, J., Houghton, R., Kauppi, P. E., Kurz, W. A., Phillips, O. L., Shvidenko, A., Lewis, S. L., Canadell, J. G., Ciais, P., Jackson, R. B., Pacala, S., McGuire, A. D., Piao, S., Rautiainen, A., Sitch, S., and Hayes, D.: A large and persistent carbon sink in the world's forests, *Science*, doi:10.1126/science.1201609, URL <http://www.sciencemag.org/content/early/2011/07/13/science.1201609.abstract>, 2011.
- Parida, B.: The influence of plant nitrogen availability on the global carbon cycle and N₂O emissions, *Reports on Earth System Science*, URL http://www.mpimet.mpg.de/fileadmin/publikationen/Reports/WEB_BzE_92.pdf, 2010.
- Patino, S., Lloyd, J., Paiva, R., Baker, T., Quesada, C., Mercado, L., Schmerler, J., Schwarz, M., Santos, A. J., Aguilar, A., Czimczik, C., Gallo, J., Horna, V., Hoyos, E., Jimenez, E., Palomino, W., Peacock, J., Pena-Cruz, A., Sarmiento, C., Sota, A., Turriago, J., Villanueva, B., Vitzthum, P., Alvarez, E., Arroyo, L., Baraloto, C., Bonal, D., Chave, J., Costa, A., Herrera, R., Higuchi, N., Killeen, T., Leal, E., Luizao, F., Meir, P., Monteagudo, A., Neil, D., Nunez-Vargas, P., Penuela, M., Pitman, N., Priante Filho, N., Prieto, A., Panfil, S., Rudas, A., Salomao, R., Silva, N., Silveira, M., deAlmeida, S. S., Torres-Lezama, A., Vasquez-Martinez, R., Vieira, I., Malhi, Y., and Phillips, O.: Branch xylem density variations across the Amazon Basin, *Biogeosciences*, 6, 545–568, 2009.
- Perring, M., Hedin, L., Levin, S., McGroddy, M., and de Mazancourt, C.: Increased plant growth from nitrogen addition should conserve phosphorus in terrestrial ecosystems, *P. Natl. A. Sci. USA*, 105, 1971–1976, doi:10.1073/pnas.0711618105, 2008.
- Post, W., Emanuel, W., and Zinke, P.: Soil carbon pools and world life zones, *Nature*, 298, 156–159, 1982.

- Quasted, H., Cornelissen, J., Press, M., Callaghan, T., Aerts, R., Trosien, F., Riemann, P., Gwynn-Jones, D., Kondratchuk, A., and Jonasson, S.: Decomposition of sub-arctic plants with differing nitrogen economies: A functional role for hemiparasites, *Ecology*, 84, 12–9658, 2003.
- Raddatz, T. J., Reick, C. H., Knorr, W., Kattge, J., Roeckner, E., Schnur, R., Schnitzler, K.-G., Wetzell, P., and Jungclaus, J.: Will the tropical land biosphere dominate the climate-carbon cycle feedback during the twenty-first century?, *Climate dynamics*, 29, 565–574, doi:10.1007/s00382-007-0247-8, 2007.
- Raich, J. and Potter, C.: Global patterns of carbon-dioxide emissions from soils, *Global Biogeochem. Cy.*, 9, 23–36, 1995.
- Raymo, M. E., Ruddiman, W. F., and Froelich, P. N.: Influence of late Cenozoic mountain building on ocean geochemical cycles, *Geology*, pp. 649–653, 1988.
- Read, J. and Busby, J.: Comparative Responses to Temperature of the Major Canopy Species of Tasmanian Cool Temperate Rain-Forest and Their Ecological Significance .II. Net Photosynthesis and Climate Analysis, *Australian Journal of Botany*, 38, 185, doi:10.1071/BT9900185, URL http://www.publish.csiro.au/view/journals/dsp_journal_fulltext.cfm?nid=65&f=BT9900185, 1990.
- Redfield, A.: On the proportions of organic derivations in sea water and their relation to the composition of plankton, in: James Johnstone Memorial Volume, edited by Daniel, R., pp. 177–192, University Press of Liverpool, Liverpool, 1934.
- Reich, P.: The Carbon Dioxide Exchange, *Science*, 329, 774–775, doi:10.1126/science.1194353, 2010.
- Reich, P. and Oleksyn, J.: Global patterns of plant leaf N and P in relation to temperature and latitude, *P. Natl. A. Sci. USA*, 101, 11 001–11 006, doi:10.1073/pnas.0403588101, 2004.
- Reich, P., Hungate, B., and Luo, Y.: Carbon-nitrogen interactions in terrestrial ecosystems in response to rising atmospheric carbon dioxide, *Annu. Rev. Ecol. Evol. Syst.*, 37, 611–636, doi: 10.1146/annurev.ecolsys.37.091305.110039, 2006.
- Reich, P., Tjoelker, M., Pregitzer, K., Wright, I., Oleksyn, J., and Machado, J.-L.: Scaling of respiration to nitrogen in leaves, stems and roots of higher land plants, *col. Lett.*, 11, 793–801, doi:10.1111/j.1461-0248.2008.01185.x, 2008.
- Reich, P., Oleksyn, J., and Wright, I.: Leaf phosphorus influences the photosynthesis-nitrogen relation: a cross-biome analysis of 314 species, *Oecologia*, 160, 207–212, doi:10.1007/s00442-009-1291-3, 2009.
- Reichstein, M., Falge, E., Baldocchi, D., Papale, D., Aubinet, M., Berbigier, P., Bernhofer, C., Buchmann, N., Gilmanov, T., Granier, A., Grunwald, T., Havrankova, K., Ilvesniemi, H., Janous, D., Knohl, A., Laurila, T., Lohila, A., Loustau, D., Matteucci, G., Meyers, T., Miglietta, F., Ourcival, J.-M., Pumpanen, J., Rambal, S., Rotenberg, E., Sanz, M., Tenhunen, J.,

BIBLIOGRAPHY

- Seufert, G., Vaccari, F., Vesala, T., Yakir, D., and Valentini, R.: On the separation of net ecosystem exchange into assimilation and ecosystem respiration: review and improved algorithm, *Global Change Biology*, 11, 1424–1439, doi:10.1111/j.1365-2486.2005.001002.x, URL <http://doi.wiley.com/10.1111/j.1365-2486.2005.001002.x>, 2005.
- Reick, C. H., Raddatz, T., Pongratz, J., and Claussen, M.: Contribution of anthropogenic land cover change emissions to pre-industrial atmospheric CO₂, *Tellus B*, 62, 329–336, doi:10.1111/j.1600-0889.2010.00479.x, URL <http://www.tellusb.net/index.php/tellusb/article/view/16578>, 2010.
- Reth, S., Graf, W., Reichstein, M., and Munch, J. C.: Sustained stimulation of soil respiration after 10 years of experimental warming, *Environmental Research Letters*, 4, 024005, doi:10.1088/1748-9326/4/2/024005, URL <http://stacks.iop.org/1748-9326/4/i=2/a=024005?key=crossref.67e385e5e739574a48595e02df275a9e>, 2009.
- Roeckner, E., Brokopf, R., Esch, M., Giorgetta, M., Hagemann, S., Kornblueh, L., Manzini, E., Rhodin, A., Schlese, U., Schulzweida, U., and Tompkins, A.: The general circulation model ECHAM5. Part I: Model description, Tech. rep., Max-Planck-Institute for Meteorology, Hamburg, 2003.
- Roeckner, E., Giorgetta, M., Crueger, T., Esch, M., and Pongratz, J.: Historical and future anthropogenic emission pathways derived from coupled climate-carbon cycle simulations, *Climatic Change*, 105, 91–108, doi:10.1007/s10584-010-9886-6, 2011.
- Rustad, L. E. and Norby, R. J.: Temperature increase: Effects on terrestrial ecosystems, in: *Encyclopedia of Global Environmental Change*, vol. 2, *The Earth System: Biological and Ecological Dimensions of Global Environmental Change*, edited by Mooney, H. A. and Canadell, J. G., pp. 757–781, 2002.
- S., C. and J., R.: Comparison of temperate and tropical rainforest tree species: photosynthetic responses to growth temperature, *Oecologia*, 133, 112–119, doi:10.1007/s00442-002-1034-1, URL <http://www.springerlink.com/openurl.asp?genre=article&id=doi:10.1007/s00442-002-1034-1>, 2002.
- Sabine, C. L., Feely, R. A., Gruber, N., Key, R. M., Lee, K., Bullister, J. L., Wanninkhof, R., Wong, C. S., Wallace, D. W. R., Tilbrook, B., Millero, F. J., Peng, T.-H., Kozyr, A., Ono, T., and Rios, A. F.: The oceanic sink for anthropogenic CO₂, *Science (New York, N.Y.)*, 305, 367–71, URL <http://www.sciencemag.org/content/305/5682/367.abstract>, 2004.
- Sardans, J., Penuelas, J., and Ogaya, R.: Drought-induced changes in C and N stoichiometry in a *Quercus ilex* Mediterranean forest, *For. Sci.*, 54, 513–522, 2008a.
- Sardans, J., Penuelas, J., Prieto, P., and Estiarte, M.: Changes in Ca, Fe, Mg, Mo, Na, and S content in a Mediterranean shrubland under warming and drought, *J. Geophys. Res.-Biogeosci.*, 113, doi:10.1029/2008JG000795, 2008b.

- Saugier, B. and Roy, J.: Estimations of global terrestrial productivity: Converging towards a single number?, p. 573, *Global Terrestrial Productivity: Past, Present and Future*, Academic, San Diego, 2001.
- Scurlock, J., Johnson, K., and Olson, R.: Estimating net primary productivity from grassland biomass dynamics measurements, *Glob. Change Biol.*, 8, doi:10.1046/j.1365-2486.2002.00512.x, 2002.
- Seitzinger, S., Harrison, J., Dumont, E., Beusen, A., and Bouwman, A.: Sources and delivery of carbon, nitrogen, and phosphorus to the coastal zone: An overview of Global Nutrient Export from Watersheds (NEWS) models and their application, *Global Biogeochem. Cy.*, 19, doi:10.1029/2005GB002606, 2005.
- Shipley, B. and Lechowicz, M.: The functional co-ordination of leaf morphology, nitrogen concentration, and gas exchange in 40 wetland species, *Ecoscience*, 7, 183–194, 2000.
- Smil, V.: Phosphorus in the environment: Natural flows and human interferences, *Annual review of energy and the environment*, 25, 53–88, 2000.
- Sokolov, A., Kicklighter, D., Melillo, J., Felzer, B., Schlosser, C., and Cronin, T.: Consequences of considering carbon-nitrogen interactions on the feedbacks between climate and the terrestrial carbon cycle, *J. Climate*, 21, 3776–3796, doi:10.1175/2008JCLI2038.1, 2008.
- Solomon, S., Qin, M., Manning, M., Chen, Z., Marquis, M., Averyt, K., Tignor, M., and Miller, H., eds.: *Climate Change 2007: The Physical Science Basis. Contribution of Working Group I to the Fourth Assessment Report of the Intergovernmental Panel on Climate Change*, Cambridge University Press, Cambridge, United Kingdom and New York, NY, USA, 2007.
- Sprengel, C.: *Die Lehre vom Dünger oder Beschreibung aller bei der Landwirthschaft gebräuchlicher vegetabilischer, animalischer und mineralischer Düngermaterialien, nebst Erklärung ihrer Wirkungsart.*, Leipzig, 1838.
- Stallard, R. F. and Edmond, J. M.: Geochemistry of the Amazon 2. The influence of geology and weathering environment on the dissolved load, *Journal of Geophysical Research*, 88, 9671–9688, 1983.
- Stewart, J. and Tiessen, H.: Dynamics of soil organic phosphorus, *Biogeochemistry*, 4, 41–60, doi:10.1007/BF02187361, 1987.
- Stitt, M. and Hurry, V.: A plant for all seasons: alteration in photosynthetic carbon metabolism during cold acclimation in *Arabidopsis*, *Current Opinion in Plant Biology*, 5, 199–206, 2002.
- Swaine, E.: *Ecological and evolutionary drivers of plant community assembly in a Bornean rain forest.*, Ph.D. thesis, University of Aberdeen, Aberdeen, 2007.
- Thomas, R. Q., Canham, C. D., Weathers, K. C., and Goodale, C. L.: Increased tree carbon storage in response to nitrogen deposition in the US, *Nature Geoscience*, 3, 13–17, URL <http://dx.doi.org/10.1038/ngeo721>, 2009.

BIBLIOGRAPHY

- Thornton, P., Lamarque, J.-F., Rosenbloom, N., and Mahowald, N.: Influence of carbon-nitrogen cycle coupling on land model response to CO₂ fertilization and climate variability, *Global Biogeochem. Cy.*, 21, doi:10.1029/2006GB002868, 2007.
- Thum, T., Räisänen, P., Sevanto, S., Tuomi, M., Reick, C., Vesala, T., Raddatz, T., Aalto, T., Järvinen, H., Altimir, N., Pilegaard, K., Nagy, Z., Rambal, S., and Liski, J.: Soil carbon model alternatives for ECHAM5/JSBACH climate model: Evaluation and impacts on global carbon cycle estimates, *Journal of Geophysical Research*, 116, G02 028, doi:10.1029/2010JG001612, URL <http://www.agu.org/pubs/crossref/2011/2010JG001612.shtml>, 2011.
- Tjoelker, M., Oleksyn, J., and Reich, P.: Modelling respiration of vegetation: evidence for a general temperature-dependent Q(10), *Global change biology*, 7, 223–230, doi:10.1046/j.1365-2486.2001.00397.x, 2001.
- Tjoelker, M., Oleksyn, J., Lorenc-Plucinska, G., and Reich, P.: Acclimation of respiratory temperature responses in northern and southern populations of *Pinus banksiana*, *New Phytol.*, 181, 218–229, doi:10.1111/j.1469-8137.2008.02624.x, 2009.
- Townsend, A., Cleveland, C., Houlton, B., Alden, C., and White, J. W.: Multi-element regulation of the tropical forest carbon cycle, *Front. Ecol. Environ.*, 9, 9–17, doi:10.1890/100047, 2011.
- Valdespino, P., Romualdo, R., Cadenazzi, L., and Campo, J.: Phosphorus cycling in primary and secondary seasonally dry tropical forests in Mexico, *Ann. For. Sci.*, 66, doi:10.1051/forest:2008075, 2009.
- Veenendaal, E. M., Mantlana, K. B., Pammenter, N. W., Weber, P., Huntsman-mapila, P., and Lloyd, J. O. N.: Growth form and seasonal variation in leaf gas exchange of, pp. 417–424, 2008.
- Vitousek, P.: Litterfall, nutrient cycling, and nutrient limitation in tropical forests, *Ecology*, 65, 285–298, 1984.
- Vitousek, P. and Howarth, R.: Nitrogen limitation on land and in the sea - How can it occur, *Biogeochemistry*, 13, 87–115, 1991.
- Vitousek, P., Cassman, K., Cleveland, C., Crews, T., Field, C., Grimm, N., Howarth, R., Marino, R., Martinelli, L., Rastetter, E., and Sprent, J.: Towards an ecological understanding of biological nitrogen fixation, *Biogeochemistry*, 57, 1–45, 2002.
- Vitousek, P., Porder, S., Houlton, B., and Chadwick, O.: Terrestrial phosphorus limitation: mechanisms, implications, and nitrogen-phosphorus interactions, *Ecol. Appl.*, 20, 5–15, 2010.
- Walker, T. W. and Syers, J. K.: Fate of phosphorus during pedogenesis, *Geoderma*, 15, 1–19, 1976.
- Wang, Y.-P. and Houlton, B.: Nitrogen constraints on terrestrial carbon uptake: Implications for the global carbon-climate feedback, *Geophys. Res. Lett.*, 36, doi:10.1029/2009GL041009, 2009.

- Wang, Y.-P. and Houlton, B. Z.: Nitrogen constraints on terrestrial carbon uptake: Implications for the global carbon-climate feedback, *Geophysical Research Letters*, 36, L24 403, URL <http://www.agu.org/pubs/crossref/2009/2009GL041009.shtml>, 2009.
- Wang, Y.-P., Houlton, B., and Field, C.: A model of biogeochemical cycles of carbon, nitrogen, and phosphorus including symbiotic nitrogen fixation and phosphatase production., *Global Biogeochem. Cy.*, 21, 2007.
- Wang, Y.-P., Law, R., and Pak, B.: A global model of carbon, nitrogen and phosphorus cycles for the terrestrial biosphere, *Biogeosciences*, 7, 2261–2282, doi:10.5194/bg-7-2261-2010, 2010.
- Welp, L. R., Keeling, R. F., Meijer, H. A. J., Bollenbacher, A. F., Piper, S. C., Yoshimura, K., Francey, R. J., Allison, C. E., and Wahlen, M.: Interannual variability in the oxygen isotopes of atmospheric CO₂ driven by El Nino, *Nature*, 477, 579–582, doi:10.1038/nature10421, 2011.
- White, M., Running, S., and Thornton, P.: The impact of growing-season length variability on carbon assimilation and evapotranspiration over 88 years in the eastern US deciduous forest, *Int. J. Biometeorol.*, 42, 139–145, doi:10.1007/s004840050097, ISB Phenology Symposium, BOSTON, MASSACHUSETTS, MAR 26-27, 1998, 1999.
- White, M. A., Thornton, P. E., Running, S. W., and Nemani, R. R.: Parameterization and Sensitivity Analysis of the BIOME–BGC Terrestrial Ecosystem Model: Net Primary Production Controls, *Earth Interactions*, 4, 1–85, 2000.
- Willis, C., Halina, M., Lehman, C., Reich, P., Keen, A., McCarthy, S., and Cavender-Bares, J.: Phylogenetic community structure in Minnesota oak savanna is influenced by spatial extent and environmental variation, *Ecography*, 33, 565–577, doi:10.1111/j.1600-0587.2009.05975.x, 2010.
- Wolkovich, E. M., Cook, B. I., Allen, J. M., Crimmins, T. M., Betancourt, J. L., Travers, S. E., Pau, S., Regetz, J., Davies, T. J., Kraft, N. J. B., Ault, T. R., Bolmgren, K., Mazer, S. J., McCabe, G. J., McGill, B. J., Parmesan, C., Salamin, N., Schwartz, M. D., and Cleland, E. E.: Warming experiments underpredict plant phenological responses of climate change, *Nature*, doi:10.1038/nature11014, 2012.
- Wright, I., Reich, P., Westoby, M., Ackerly, D., Baruch, Z., Bongers, F., Cavender-Bares, J., Chapin, T., Cornelissen, J., Diemer, M., Flexas, J., Garnier, E., Groom, P., Gulias, J., Hikosaka, K., Lamont, B., Lee, T., Lee, W., Lusk, C., Midgley, J., Navas, M., Niinemets, U., Oleksyn, J., Osada, N., Poorter, H., Poot, P., Prior, L., Pyankov, V., Roumet, C., Thomas, S., Tjoelker, M., Veneklaas, E., and Villar, R.: The worldwide leaf economics spectrum, *Nature*, 428, 821–827, doi:10.1038/nature02403, 2004.
- Wright, I., Reich, P., Atkin, O., Lusk, C., Tjoelker, M., and Westoby, M.: Irradiance, temperature and rainfall influence leaf dark respiration in woody plants: evidence from comparisons across 20 sites, *New Phytol.*, 169, 309–319, doi:10.1111/j.1469-8137.2005.01590.x, 2006.

BIBLIOGRAPHY

- Wythers, K., Reich, P., Tjoelker, M., and Bolstad, P.: Foliar respiration acclimation to temperature and temperature variable $Q(10)$ alter ecosystem carbon balance, *Glob. Change Biol.*, 11, 435–449, doi:10.1111/j.1365-2486.2005.00922.x, 2005.
- Xu-Ri, C. and Prentice, I. C.: Terrestrial nitrogen cycle simulation with a dynamic global vegetation model, *Global Change Biology*, 14, 1745–1764, URL <http://doi.wiley.com/10.1111/j.1365-2486.2008.01625.x>, 2008.
- Yanai, R.: Phosphorus Budget of a 70-Year-Old Northern Hardwood Forest, *Biogeochemistry*, 17, pp. 1–22, URL <http://www.jstor.org/stable/1468740>, 1992.
- Yang, X. and Post, W.: Phosphorus transformations as a function of pedogenesis: a synthesis of soil phosphorus data using Hedley fractionation method, *Biogeosciences*, 8, 5907–5934, doi:10.5194/bgd-8-5907-2011, URL <http://www.biogeosciences-discuss.net/8/5907/2011>, 2011.
- Zaehle, S. and Dalmonech, D.: Carbon–nitrogen interactions on land at global scales: current understanding in modelling climate biosphere feedbacks, *Curr. Opin. Environ. Sustain.*, 3, 311–320, doi:10.1016/j.cosust.2011.08.008, 2011.
- Zaehle, S. and Friend, A.: Carbon and nitrogen cycle dynamics in the O-CN land surface model: 1. Model description, site-scale evaluation, and sensitivity to parameter estimates, *Global Biogeochem. Cy.*, 24, doi:10.1029/2009GB003521, 2010.
- Zaehle, S., Friedlingstein, P., and Friend, A.: Terrestrial nitrogen feedbacks may accelerate future climate change, *Geophys. Res. Lett.*, 37, doi:10.1029/2009GL041345, 2010a.
- Zaehle, S., Friend, A., Friedlingstein, P., Dentener, F., Peylin, P., and Schulz, M.: Carbon and nitrogen cycle dynamics in the O-CN land surface model: 2. Role of the nitrogen cycle in the historical terrestrial carbon balance, *Global Biogeochem. Cy.*, 24, doi:10.1029/2009GB003522, 2010b.
- Zhang, Q., Pitman, A., and Dai, Y.: Limitations of nitrogen and phosphorous on the terrestrial carbon uptake in the 20th century, *Geophys. Res. Lett.*, 38, doi:10.1029/2011GL049244, 2011.

Appendix A

Appendix of Chapter 2

A.1 Derivation of equations for labile P dynamics

The following derivation was adopted from the work of Wang et al. (2010). By assuming that P_l and P_{sr} are in equilibrium at a daily time scale, we model the changes in P_l and P_{sr} as

$$\begin{aligned} \frac{d(P_l + P_{sr})}{dt} = & F_M + F_D + F_W + F_{BC} + \epsilon\beta_l P_g \\ & - \gamma P_l R - \frac{1}{\tau_{sr}} P_{sr} - f_{\text{limit}}(D_{\text{veg}} + D_{\text{micr}}) \end{aligned} \quad (\text{A.1})$$

where F_M is mineralization, F_D is deposition, F_W is weathering, $f_{\text{limit}}(D_{\text{veg}} + D_{\text{micr}})$ is the uptake by biota, $\gamma P_l R$ is the rate of leaching, and $\frac{1}{\tau_{sr}}$ is the loss rate of strong sorption.

We also assume that P_{sr} at equilibrium can be described using a Michaelis-Menten equation. That is,

$$P_{sr} = \frac{S_{\text{max}} P_l}{K_s + P_l} \quad (\text{A.2})$$

where S_{max} is the maximum amount of sorbed phosphorus in the soil and K_s is an empirical constant. Differentiating Eq. (A.2), we have

$$\frac{dP_{sr}}{dt} = \frac{S_{\text{max}} K_s}{(K_s + P_l)^2} \frac{dP_l}{dt} \quad (\text{A.3})$$

Substituting Eq. (A.3) into Eq. (A.1), we have

$$\begin{aligned} \frac{dP_l}{dt} = & \frac{1}{1 + \frac{S_{\text{max}} K_s}{(P_l + K_s)^2}} (F_M + F_D + F_W + F_{BC} + \epsilon\beta_l P_g \\ & - \gamma_s P_l R - \frac{1}{\tau_{sr}} P_{sr} - f_{\text{limit}}(D_{\text{veg}} + D_{\text{micr}})) \end{aligned} \quad (\text{A.4})$$

A.2 Respiration fluxes

The respiration fluxes from litter decomposing heterotrophs $F_{la>A}^C$ and $F_{lw>A}^C$ are

$$F_{i>A}^C = \alpha_i d_i C_i \quad (\text{A.5})$$

where α_i is the fraction of mineralized C which is respired to the atmosphere, and d_i the decomposition rate of C_i . The decomposition rates d_i of the non-lignified litter pool ($i = la$), the woody litter pool ($i = lw$), and the slow pool ($i = s$) are computed using a Q_{10} model (Raich and Potter, 1995):

$$d_i = \frac{\zeta}{\tau_i} Q_{10}^{T_{\text{soil}}/10^\circ\text{C}} \quad (\text{A.6})$$

where ζ is soil humidity, T_{soil} the temperature of the uppermost soil layer in $^\circ\text{C}$. τ_i is the life time of pool i at 10°C and $\zeta = 1$ (Parida, 2010).

A.3 Sensitivity simulations on stoichiometry

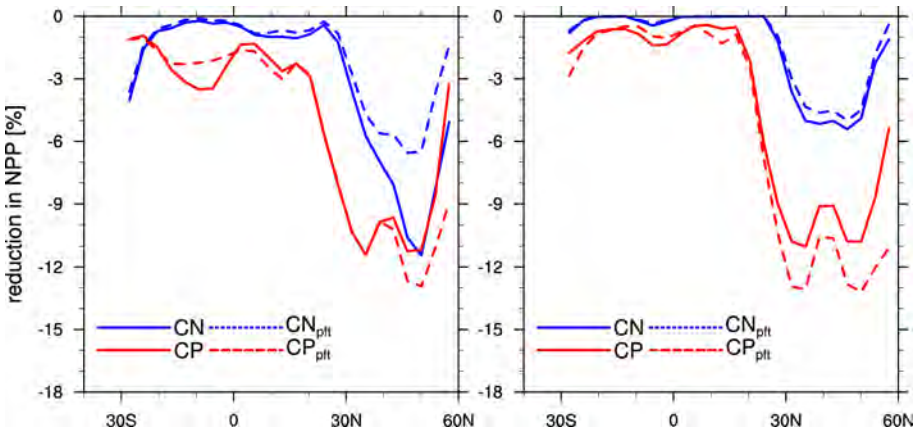


Figure A.1: Mean reduction of NPP [%] due to CNL (N or P) averaged over 30 yr (2070–2099 (left) and 2320–2349 (right)) as latitudinal means. Solid line are results from the CN and the CP simulation for N and P limitation, respectively. The dashed lines are results from the sensitivity experiments CP_{pft} and CN_{pft} .

Plants adjust their nutrient use efficiency by varying their C:nutrient ratio in response to environmental changes. The stoichiometry in JSBACH is rigid and therefore the model does not reflect observed flexibility in stoichiometry and nutrient use. To ensure that this strong simplification does not significantly affect our results, we did simulations in which vegetation is able to adjust drastically to nutrient scarcity. In these simulations, the C:N and C:P ratios of plant compartments is increased linearly up to 50% with nutrient limitation. The C:N and C:P ratio of shedded leaves is scaled similarly. As our model does not account for negative effects of lower leaf nutrient content on productivity, the effect of increasing nutrient use efficiency are maximized.

The differences in land C cycling between these simulations and the standard simulations are marginal (Fig. A.2), although the global means of the C:nutrient ratios of vegetation increase up

Table A.1: Ranges used to constrain the probability functions of the stoichiometric parameters in the LHS.

Parameter	molar ratios	Reference
CN active	25–85	White et al. (2000)
CN wood	125–217	Esser et al. (2011)
CN litter	45–120	White et al. (2000)
CN woody litter	500–730	White et al. (2000)
CN soil	13–15	Cleveland and Liptzin (2007)
NP active	20–48	McGroddy et al. (2004)
NP litter	21–68	McGroddy et al. (2004)

to 9% (not shown). Such a change in stoichiometry is high compared to the increase of about 1% in the C:N ratio of vegetation in a CN model with flexible stoichiometry (Esser et al., 2011). These results show that the assumption of rigid stoichiometry does not affect our results, especially because we neglect the negative effect of decreasing leaf nutrient content on photosynthesis.

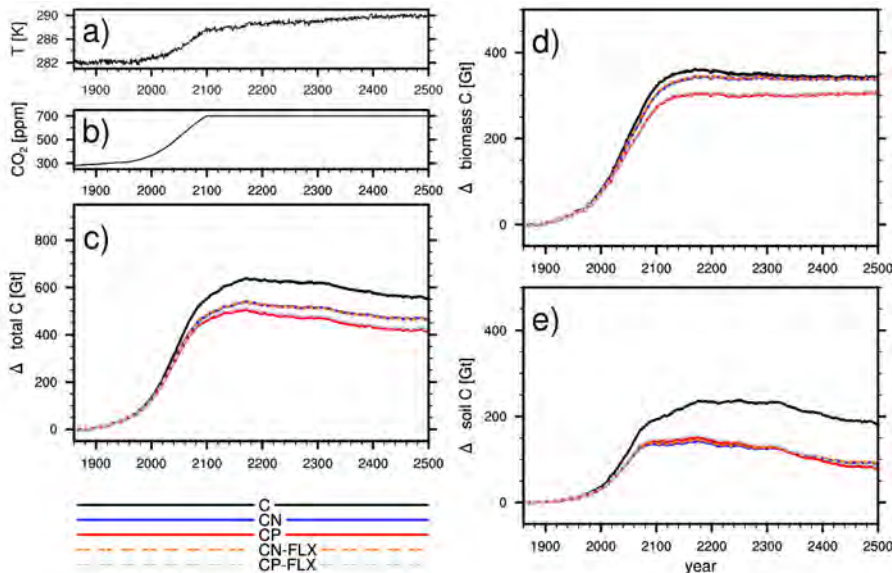


Figure A.2: The simulated change in land carbon storage under the SRES A1B scenario. Shown are the 10 yr mean of soil temperature (a), the CO₂ concentration as used in the forcing simulation (b), the resulting change in total land C storage (c), and the changes in the two main land compartments vegetation (d) and soil (e). CN-FLX and CP-FLX are the new simulations with flexible plant stoichiometry.

In addition, stoichiometric parameter perturbations were made using the Latin Hypercube Sampling (LHS) (McKay et al., 1979) procedure for testing the robustness of the modeling results against the uncertainty of the stoichiometric parameterization. The LHS procedure ensures an efficient sampling of the parameter distribution with a suitable amount of parameter samples thus avoiding impracticable computational efforts due to numerous model simulations. We sampled the C:N ratios of the active, wood and slow pool, as well as the N:P ratios of the active and the wood pool. The N:P ratio of the slow pool was excluded from sampling, because this parameter affects the calibration of the biochemical mineralization and the calibration procedure is compu-

tationally too demanding to be performed. The stoichiometric parameters of the litter pools were not sampled, but the fraction of nutrients retranslocated prior loss. This was done to avoid correlations between parameters, as the C:nutrient ratio of litter must be larger than the ratio of the corresponding vegetation pool. For all 7 parameters, the probability functions were assumed to be uniform and the ranges were constrained from literature (Table A.1). Due to the scarce data, we assumed that the ranges of N:P ratios for wood and woody litter is comparable to the range of N:P ratios for leaves and litter, respectively. The retranslocation fractions were chosen such that the resulting litter stoichiometry is in the range of observations (Table A.1) (0.45-0.55 for the active pool and 0.5 for the wood pool). A set of 140 simulations was performed for each of the three nutrient setups (more simulations were not possible due to the high computational effort). All simulations were performed in a similar manner as the standard simulations.

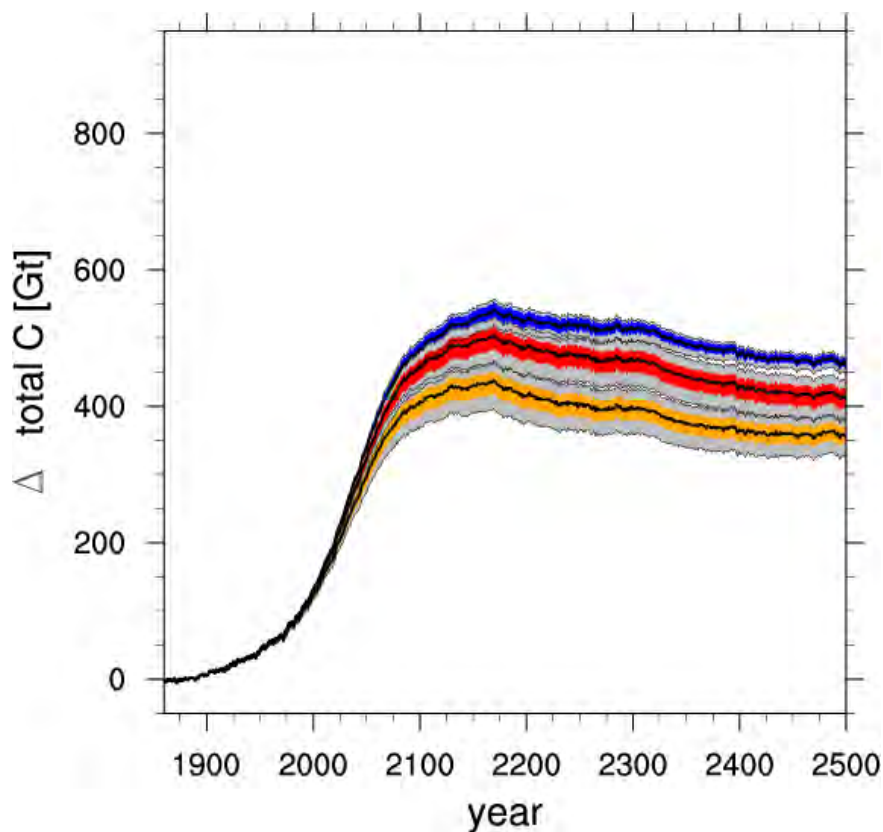


Figure A.3: The simulated change in land carbon storage in the parameter perturbation simulations. Shown are the median (bold black), the range between the 10th and 90th percentile (color) and the range between minimum and maximum of the each ensemble (grey).

The experiments showed that the overlaps between the CN, CP and CNP simulations are marginal (Fig. A.3). The ranges of simulations within the 10th and the 90th percentile do not overlap at all. In summary, the results support our conclusion that the reduction of land C uptake due to nutrient limitation is robust regarding the stoichiometric parameterization.

A.4 Additional figure and tables

Table A.2: PFT specific values of model parameters. See Parida (2010) for a detailed description.

PFT	α_a	ε
Tropical evergreen trees	0.85	0.0005
Tropical deciduous trees	0.85	0.0005
Temperate broadleaf evergreen trees	0.85	0.0005
Temperate broadleaf deciduous trees	0.85	0.0005
Coniferous evergreen trees	0.85	0.0005
Coniferous deciduous trees	0.85	0.0005
Raingreen shrubs	0.85	0.0005
Deciduous shrubs	0.85	0.0005
C ₃ grass	0.5	0.00125
C ₄ grass	0.5	0.00125
Tundra	0.5	0.0005

Table A.3: Soil order specific values of model parameters.

Soil	S_{\max}	K_s	F_W	M_{\min}	M_{\max}
Alfisols	134	75	0.01	0.4	0.8
Andisols	80	78	0.01	0.4	0.8
Aridisols	80	78	0.01	0.4	0.8
Entisols	50	64	0.05	0.4	0.8
Gelisols	77	65	0.05	0.4	0.8
Histosols	77	65	0.05	0.4	0.8
Inceptisols	77	65	0.05	0.4	0.8
Mollisols	74	54	0.01	0.4	0.8
Oxisols	145	10	0.003	2.0	4.0
Spodosols	134	75	0.01	2.0	4.0
Ultisols	133	64	0.005	2.0	4.0
Vertisols	32	32	0.01	0.4	0.8

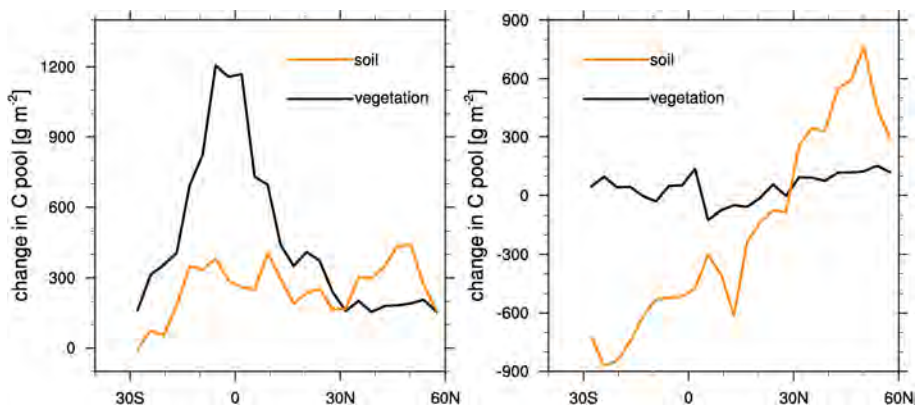


Figure A.4: The difference in C stored in vegetation (orange) and soil (black) in the C-only simulation as zonal means during the periods 1860–2100 (left) and 2100–2400 (right). Shown are is difference between the means of the years 1860–1889 (2070–2099) and 2070–2099 (2370–2399) for C in vegetation and soil. Soil includes C in litter and soil organic matter.

Appendix B

Acknowledgements

I would like to express my gratitude to my supervisor Dr. Victor Brovkin for his continuous support, for letting me freely find my way and for the guidance when I was about to lose the track. I thank Dr. Christian Reick and Dr. Thomas Raddatz for their scientific advices and their readiness to discuss whatever came into my mind. Further I thank Dr. Soenke Zaehle and Dr. Jens Kattge, for sharing their expertise, their constructive comments on my work, and for reminding me of the complexity of nature.

I thank Veronika Gayler and Reiner Schnur for the programming support and their endless willingness to help. I also want to thank the leader of the landveg group, Prof. Dr. Martin Claussen, and all members for making my stay at the Geomatikum very pleasant, especially my fellow sufferers: Freja, Helge, Robert, Sebastian, and Fabio.

I am glad to be a member of the International Max Planck Research School on Earth System Modelling (IMPRS-ESM). I thank Dr. Antje Weitz and Cornelia Kampmann for their tremendous efforts to solve all the non scientific problems so that I could fully concentrate on the science.

I thank Prof. Dr. Martin Claussen and Prof. Dr. Eva-Maria Pfeiffer for being responsible and motivating members of my advisory panel.

Last but not least, I thank my family and my friends—without them I wouldn't be who I am.

Die gesamten Veröffentlichungen in der Publikationsreihe des MPI-M
„Berichte zur Erdsystemforschung“,
„Reports on Earth System Science“,
ISSN 1614-1199

sind über die Internetseiten des Max-Planck-Instituts für Meteorologie
erhältlich:

<http://www.mpimet.mpg.de/wissenschaft/publikationen.html>

